國 立 交 通 大 學

電子工程學系 電子研究所碩士班

碩 士 論 文

考量閘極可靠度之
晶片上靜電放電防護電路設計

Design of On-Chip ESD Protection Circuits with Consideration of Gate-Oxide Reliability

研究生 ： 陳 穩 義

指導教授 ： 柯 明 道 教授

中華民國九十四年四月

考量閘極可靠度之晶片上靜電放電防護電路設計

Design of On-Chip ESD Protection Circuits with Consideration of Gate-Oxide Reliability

研 究 生：陳穩義　　Student：Wen-Yi Chen

指導教授：柯明道 教授　　Advisor：Ming-Dou Ker

國 立 交 通 大 學

電子工程學系　電子研究所碩士班

碩 士 論 文

A Thesis

Submitted to Institute of Electronics

College of Electrical Engineering and Computer Science

National Chiao-Tung University

in partial Fulfillment of the Requirements

for the Degree of

Master

in

Electronic Engineering

April 2004

Hsinchu, Taiwan, Republic of China

中華民國九十四年四月

考量閘極可靠度之晶片上靜電放電防護電路設計

學生: 陳穩義　　　　　　　　　　　　指導教授: 柯明道 教授

國立交通大學

電子工程學系　　電子研究所碩士班

摘 要

本論文旨在討論由於製程進步與電路結構改變，所造的靜電放電防護設計的問題，並進一步提出解決方案。設計宗旨爲不需額外光罩與製程步驟，僅利用電路上的設計來提升靜電放電防護能力。並可將本論文所提出的設計應用於不同製程上，不會侷限於某些特定製程才能達到效果，因此可廣泛地應用在不同晶片設計上。

第一個設計爲利用一閘極電壓鉗制電路，將 N 型金氧半導體的閘極電壓，在靜電放電發生的情況下，有效鉗制在一電位，避免過高的閘極電壓吸引過高的靜電放電電流，燒毀元件的氧化層，藉以有效克服閘極過度耦合效應的問題。本設計並可簡單調整靜電放電時的閘極耦合電壓大小，以應用於具有不同閘極厚度的製程設計。本設計實際驗證於 0.35-μm 互補式金氧半導體製程。於此驗證中，具有閘極電壓鉗制電路設計的 N 型金氧半導體，其機器放電模式的靜電放電防護能力獲得 30%的改善。

第二個設計爲一電源線間的靜電放電防護電路。本設計的特點在於可操作在 3.3-V 的高電源電壓下，但只使用 1-V/2.5-V 的低壓元件，且不會有閘極可靠度的問題。本應用特別適用於高/低壓共容輸出/入介面的設計上，並搭配內部電路的設計，無需使用較厚閘極氧化層的 3.3-V 元件而使用較薄閘極氧化層的 2.5-V 元件，使電路可應用在較高的操作頻率，縮短產品的市場導入時程，並可避免製程限制的窘境。本設計驗證於具 1-V/2.5-V 邏輯元件的 0.13-μm 互補式金氧半導體製程。實驗結果證明本設計在正常工作電壓下具有極小的漏電電流，對靜電放電事件具有極快的反應時間，並具有優異的靜電放電防護能力。

本論文之研究成果已發表於兩篇國際研討論會文，並已投稿至兩篇國際期刊。

Design of On-Chip ESD Protection Circuits with Consideration of Gate-Oxide Reliability

Student: Wen-Yi Chen Advisor: Ming-Dou Ker

Department of Electronics Engineering and Institute of Electronics

National Chiao-Tung University

ABSTRACT

The aim of this thesis is to propose solutions of ESD protection problems under the consideration of gate-oxide reliability. Objectives of the proposed designs are to achieve the desired ESD protection capabilities in circuit technique without modifying process steps or increasing mask layers. Therefore, the proposed designs are suitable to different CMOS processes and therefore can be widely applied to different circuit designs.

The first proposal is a gate-voltage-limited circuit that can clamp the coupled gate voltage of an gate-coupled NMOS device during ESD transition. The over-coupled gate voltage of an NMOS device draws over-huge ESD current in the channel region and burns out the gate oxide of the NMOS device. The gate-voltage-limited circuit can therefore prevent the gate-coupled devices from the over-gate-driven effect. This design was fabricated and verified in a 0.35-μm CMOS process. Experimental results show that a gate-coupled NMOS with the proposed gate-voltage-limited circuit can have a 30% improvement on its MM ESD protection level compared to a gate-coupled NMOS without the proposed circuit.

The second proposal is a power-rail ESD clamp circuit. The specialty of this proposed design is that it is designed with only 1-V and 2.5-V low voltage devices to be operated under the 3.3-V high power-supply voltage without the gate oxide reliability issue. This proposed design can collocate with mixed-voltage I/O designs to achieve a higher circuit operation frequency. This

proposed design was fabricated and verified in a 0.13-μm 1-V/2.5-V CMOS process. Experimental results show that the proposed design has extremely small standby leakage current under the normal circuit operating condition. This design also shows fast turn-on speed under ESD stresses and high ESD protection robustness.

Contents of this thesis have already been published on two international conferences and submitted to two international journals.

誌 謝

碩士班能順利畢業，第一個要感謝的是我的指導教授 柯明道博士，從大學部的專題到研究所，一路上的諄諄教誨以及辛勤督導，還有盡可能在研究資源上的幫助，讓我在碩士學位的路途上，得到許多的成長。 柯老師教導給我的不只在知識上，還有對自己應負責任的堅持，未來工作上應有的正面態度…等。回想現在的自己與大學剛畢業的我，從 柯老師身上學到的身教以及言教，實在太多太多。

其次，我要特別感謝已從本實驗室畢業的 徐國鈞博士，以及目前在聯詠科技的 張智毅先生。他們在我求學的路上對我所請教的問題不厭其煩地替我解說，引領我在短時間內進入碩士班的領域。並且三不五時被我拉去吃飯聊天，在生活的態度，以及人生路途的抉擇上讓我獲益良多。在這段路途上沒有二位，我也不能走得如此順遂，在此對兩位獻上特別的感謝。

另外，我要感謝在工研院以及華邦電子的學長、朋友們，有他們的支持與陪伴，讓我在學校以外還有另一塊生活圈，也有另一個知識的來源，也讓了解到學校以外的業界是怎麼樣的情形。工研院的莊哲豪學長，陳子平學長，林昆賢學長，彭政傑學長，世宏，項彬；以及在華邦電子的林奕成先生，曾仁洲先生…等。實驗室的學長朋友們也伴我良多，許勝福，陳榮昇，陳世倫，張瑋仁，鄧至剛，徐新智學長們，還有同學吳偉琳，陪我一起走過碩士班的路程，一起熬夜做實驗，在這裡一併獻上對你(妳)們的感激。

最後我要感謝的是自己的父母親 陳世霖先生與 林清珠女士。父母對我在生活上以及經濟上的支持，是讓我無後故之憂唸完碩士班的最大支柱。對父母該感謝的太多，不是三言兩語可用文字寫盡，在這裡誠心地對我偉大的父母親致上感謝。以及哥哥陳瑞宗，來自家人的關照還是最溫暖的來源。還有我的女朋友陳瑩柳小姐，從大學到研究所畢業，總是在背後替我打點瑣事，也在背後鼓勵我渡過每一個低潮，盡力給我協助。

其他該感謝的人還有很多，對一路上曾經幫助過我的各位，在此一併獻上感激之情。

陳穩義

94年3月

Content

ABSTRACT (CHINESE)……………..…………………………..…i

ABSTRACT (ENGLISH)………………..…………...…………ii

ACKNOWLEDGEMENT………………………………………...iv

CONTENTS…………………………………………......………v

TABLE CAPTIONS……………………………………..……viii

FIGURE CAPTIONS………………………………………...…..ix

Chapter 1 Introduction…………………………………………...1

1.1 MOTIVATION…………………………………………………..…1

1.2 THESIS ORGANIZATION…………………………………………..2

Chapter 2 Introduction to ESD and the Effects of Process Migration to ESD Protection Designs……………4

2.1 GENERAL INTRODUCTION TO ESD…………………………………4

2.1.1 Human Body Model (HBM)…………………………………...4

2.1.2 Machine Model (MM)………………………………………5

2.1.3 Charged Device Model (CDM)………………………………..5

2.2 ESD TEST METHODS…………………………………………..6

2.2.1 ESD Test on I/O Pins………………………………………...6

2.2.2 Pin to Pin ESD Test……………………………………………...6

2.2.3 VDD-to-VSS ESD Test……………………………..……7

2.3 ESD PROTECTION NETWORK……………………………………7

2.4 ESD PROTECTION DEVICES IN MODERN CMOS ICS………………………8

2.5 TRIGGERING TECHNIQUES TO ESD PROTECTION DEVICES…………………10
2.5.1 Gate-driven Technique……………………………………………...10
2.5.2 Substrate-triggered Technique………………………………………11
2.6 EFFECTS OF THE PROCESS MIGRATION TO ESD PROTECTION DESIGNS ……11
2.6.1 The Over-Gate-driven Effect………………………………………...12
2.6.2 High Voltage Tolerant ESD Protection Design…………………...12
Chapter 3 Circuit Solution to Overcome the Over-Gate-Driven Effect on ESD Protection Circuits in Deep-Submicron CMOS Processes……………………………………………18
3.1 INTRODUCTION………………………………………………………………18
3.2 THE OVER-GATE-DRIVEN EFFECT…………………………………………19
3.2.1 Non-uniform Turn-on Behavior……………………………………...19
3.2.2 Gate-coupled Technique………………………………………………20
3.2.3 Over-Gate-Driven Effect………………………………………………21
3.3 CIRCUIT SOLUTION TO OVERCOME THE OVER-GATE-DRIVEN EFFECT……23
3.3.1 Design Concept………………………………………………………...23
3.3.2 Gate Voltage Monitor Circuit…………………………………………...23
3.4 EXPERIMENTAL RESULTS……………………………………………………25
3.4.1 Clamping by NMOS String……………………………………………25
3.4.2 Clamping by Diode String……………………………………………29
3.5 CONCLUSION…………………………………………………………………30
Chapter 4 Design on Power-Rail ESD Clamp Circuit for 3.3-V I/O Interface By Using Only 1-V/2.5-V Low-Voltage Devices in a 130-nm CMOS Process………………………………44

4.1 INTRODUCTION..44
4.2 ESD PROTECTION SCHEME
FOR 1-V/3.3-V MIXED-VOLTAGE I/O INTERFACE..............................45
4.2.1 ESD Protection Scheme..45
4.2.2 Review on High Voltage Tolerant Power-Rail ESD Clamp Circuit...46
4.3 NOVEL POWER-RAIL ESD CLAMP CIRCUIT
FOR HIGH-VOLTAGE APPLICATIONS...48
4.3.1 Circuit Operation Under Normal Power-on Transition................49
4.3.2 Circuit Operation Under ESD Transition.....................................49
4.4 EXPERIMENTAL RESULTS..51
4.4.1 Standby Leakage Current...51
4.4.2 Turn-on Verification...52
4.4.3 ESD Robustness...54
4.4.4 Failure Analysis..55
4.4.5 Silicon Controlled Rectifier (SCR) as ESD Clamp Device...........55
4.5 CONCLUSION...56
Chapter 5 Conclusion and Future Work...................................68
5.1 CONCLUSION...68
5.2 FUTURE WORK...69
References...70
VITA...76

Table Captions

Table 4.1 Device Dimensions of the ESD Protection Circuit in this Work………………58

Table 4.2 Leakage Current of Prior Arts and the New Proposed Power-Rail ESD Clamp Circuit…………………………………………………………………………58

Table 4.3 ESD Robustness of STNMOS Devices with or without the New Proposed ESD Detection Circuit……………………………………………………………58

Figure Captions

Fig. 2-1 The equivalent circuit of the human body model ESD event……………………………13

Fig. 2-2 Definition of the HBM pulse decay time (td). ………………………………………13

Fig. 2-3 The equivalent circuit of the machine model ESD event…………………………14

Fig. 2-4 The current waveform of a 400-V MM ESD stress discharging through a short wire…14

Fig. 2-5 Comparison on waveforms of a 2-kV HBM ESD stress, 200-V MM ESD stress, and a 1-kV CDM ESD tress……………………………………………………………15

Fig. 2-6 (a) PS-mode, (b) NS-mode, (c) PD-mode, and (d) ND-mode, ESD test on I/O pins…15

Fig. 2-7 (a) Positive mode, (b) Negative-mode, pin-to-pin ESD test……………………………16

Fig. 2-8 (a) Positive mode, (b) Negative-mode, VDD-to-VSS ESD test………………………16

Fig. 2-9 The ESD current discharging paths (path 1 and path 2) during the pin-to-pin ESD stress condition……………………………………………………………………17

Fig. 2-10 Cross sectional view of a SCR device……………………………………………17

Fig. 3-1 The TLP-measured I-V characteristic of GGNMOS fabricated in a 0.35-µm CMOS Technology………………………………………31

Fig. 3-2 Two traditional circuit design methods to carry out the gate-coupled technique and to solve the non-uniform turn-on behavior in the ESD protection NMOS……………31

Fig. 3-3 The simulated current flow lines of NMOS with a bipolar trigger voltage of 5.7 V. Voltages applied to drain and gate electrodes are respectively ramped to 6.5 V and 2 V with simultaneous rise time of (a) 10 ns, and (b) 5 ns…………………………..…32

Fig. 3-4 MM ESD levels of NMOS (W/L= 600 µm/0.35 µm) under different gate voltages…33

Fig. 3-5 A novel circuit design concept which can overcome the over-gate-driven effect for ESD protection circuits with gate-coupled or gate-driven technique…………………33

Fig. 3-6 The gate voltage monitor circuit added on-chip can monitor Vg of GCNMOS during ESD transition without affecting the quantity of coupled voltage on GCNMOS……34

Fig. 3-7 The measured Vdet voltages when (a) 10-V, and (b) 15-V, voltage pulse with a rise time of 10 ns is applied to the GCNMOS without gate-voltage-limited circuit………..35

Fig. 3-8 Id-Vg curve of the gate voltage monitor circuit in a 0.35-µm CMOS process…………36

Fig. 3-9 The measured Vdet voltages when (a) 10-V, and (b) 20-V, voltage pulse with a rise time of 10 ns is applied to the GCNMOS with two stacked NMOS devices in the gate-voltage-limited circuit. Each stacked NMOS has a device dimension (W/L) of 50 µm/0.35 µm……………………………………………………………………37

Fig. 3-10 The measured Vdet voltages when the 20-V voltage pulse with a rise time of 10 ns is applied to GCNMOS with (a) three, and (b) five, stacked NMOS devices in the gate-voltage-limited circuit. Each stacked NMOS has a device dimension (W/L) of 50 µm/0.35 µm………………………………………..………………..…………38

Fig. 3-11 The measured Vdet voltages when 20-V voltage pulses with rise time of 10 ns are applied to GCNMOS with two different gate-voltage-limited circuits. One consists of three stacked NMOS devices with each device dimension (W/L) of 20 µm/0.35 µm, the other consists of three stacked NMOS devices with each device dimension of 50 µm/0.35 µm……………………………………………………………………39

Fig. 3-12 MM ESD levels of the GCNMOS with different numbers or different device dimensions of stacked NMOS devices in the gate-voltage-limited circuit……..………39

Fig. 3-13 SEM image of the GCNMOS with two stacked NMOS devices in the gate-voltage-limited circuit after 550-V MM ESD stress. Each stacked NMOS has device dimension (W/L) of 70 µm/0.35 µm…………………………………………40

Fig. 3-14 SEM image of (a) the GCNMOS with five stacked NMOS devices in the gate-voltage-limited circuit after 600-V MM ESD stress. Each stacked NMOS has device dimension (W/L) of 20 µm/0.35 µm. (b) The enlarged image of its ESD failure location……………………………………………………………………41

Fig. 3-15 SEM image of (a) the GCNMOS with five stacked NMOS devices in the gate-voltage-limited circuit after 650-V MM ESD stress. Each stacked NMOS has device dimension (W/L) of 70 µm/0.35 µm. (b) The enlarged image of its ESD failure location……………………………………………………………42

Fig. 3-16 MM ESD levels of the GCNMOS with different numbers or different device dimensions of stacked diodes in the gate-voltage-limited circuit……………………43

Fig. 4-1 ESD protection schemes for mixed-voltage I/O interfaces (a) with, and (b) without, the dummy supply line V_{ESD}……………………………………………………………59

Fig. 4-2 The cross-sectional view of a forward-biased stacked-diode string to show the parasitic p-n-p BJTs and its leakage current path. ……………………………………60

Fig. 4-3 The new proposed power-rail ESD clamp circuit with only 1-V and 2.5-V devices for operating under high-voltage VDD_h of 3.3V……………………………………60

Fig. 4-4 Hspice-simulated voltages on nodes of the ESD detection circuit under normal power-on transition with a rise time of 1ms…………………………………………61

Fig. 4-5 Hspice-simulated voltages on nodes of the ESD detection circuit and the current of Mp2 under 0-to-7V ESD-like transition…………………………………………61

Fig. 4-6 The snapback I-V characteristic curve of a stand-alone STNMOS device……………62

Fig. 4-7 The leakage currents of STNMOS with or without the ESD detection circuit under different temperatures……………………………………………………………62

Fig. 4-8 The clamped voltage waveforms by STNMOS with or without the ESD detection circuit under the voltage pulse stress with the pulse height of 20V and the rise time of 10ns……………………………………………………………………………63

Fig. 4-9 The measured substrate-triggered current generated by the ESD detection circuit under 0-to-7V voltage pulse with a rise time of 10ns on the VDD_h pin……………63

Fig. 4-10 TLP-measured I-V curves of STNMOS with ESD detection circuit under different device dimensions……………………………………………………………64

Fig. 4-11 The (a) OBIRCH, and (b) SEM, images of a 400μm/0.3μm STNMOS with ESD detection circuit after 325-V MM ESD stress……………………………………65
Fig. 4-12 SEM image of (a) a stand-alone 400μm/0.3μm STNMOS after 175-V MM ESD stress. (b) The enlarged image of its ESD failure location………………………………66
Fig. 4-13 SEM image of a stand-alone 400μm/0.3μm STNMOS after 1.5-kV HBM ESD stress……………………………………………………………67
Fig. 4-14 TLP-measured I-V characteristics of both SCR with and without ESD detection circuit……………………………………………………………………………67

Chapter 1

Introduction

1.1 MOTIVATION

ESD protection design has already been granted as one of the major challenges for deep-submicron CMOS technologies [1]. To reduce the power consumption and to increase the operating speed of IC chips, both the gate oxide thickness and the operating voltage of MOS devices keep scaling down. The progress is positive to the performance of IC chips but negative to the ESD protection because the on-chip devices are more and more fragile. Some problems are therefore comes into being with the progress of CMOS processes.

The gate-driven (or gate-coupled) technique has been widely used on ESD protection designs to shorten the turn-on time and to improve the turn-on uniformity of ESD protection devices for a long time [2]–[7]. However, with the constant shrinkage on gate-oxide thickness of MOSFET devices in deep-submicron CMOS processes, the gate-coupled technique has been found to adversely affect the ESD robustness of NMOS devices [8]-[10]. It has been also found that the thinner the gate oxide is, the severer degraded is the ESD robustness of NMOS devices [9]. In deep-submicron CMOS processes, the over-gate-driven effect is a problem in urgent. A new approach to overcoming the over-gate-driven-effect through the circuit structure is proposed in this thesis [11]. The proposed design is portable to different process technologies without modifying mask layers or process steps. With the proposed design, the gate-driven or gate-coupled technique can be devised more easily and properly.

In modern IC chips, though the power supply voltage of internal circuits keeps lowering to reduce the power consumption and the heat dissipation, their input/output interfaces are still

operated at higher voltage levels to cooperate with the peripheral components. For such mixed-voltage applications, special design through circuit structure or process modification is needed to avoid the gate-oxide reliability issue. Though the process technology can provide devices with different gate-oxide thickness to meet the requirement, it is not cost-effective and will lower the production yield in manufacturing. Devices with thicker gate-oxide also have worse device characteristics such as the inferior device driving capability, impeding the high speed system performance. A better solution to both overall system performance and cost is to propose a high-voltage tolerant circuit that can be operated under high power-supply voltage but is fabricated with only low-voltage devices. In this thesis, a substrate-triggered power-rail ESD protection circuit with only 1-V/2.5-V devices to sustain 3.3-V power supply voltage is proposed [12]. This substrate-triggered ESD clamp circuit is specially designed without suffering the gate-oxide reliability issue under the 3.3-V power supply voltage. The proposed ESD clamp circuit is fabricated and verified in a 130-nm 1-V/2.5-V CMOS process and shows extremely low standby leakage current, which is only 1/100 compared to the prior arts.

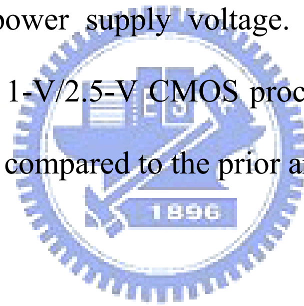

1.2 THESIS ORGANIZATION

The chapter 2 of this thesis introduces ESD events, ESD test methods, and general ESD protection techniques. The motivation of bringing up proposed designs, the gate-voltage limited circuit to overcome the over-gate-driven effect (in chapter 3), and the power-rail ESD protection circuit for 1-V/3.3-V mixed-voltage I/O interfaces (in chapter 4), is also concisely introduced in this chapter.

The chapter 3 of this thesis discusses the benefits and the problems of the gate-driven technique. This chapter includes methods to overcome the over-gate-driven effect, its design concept, measurement setup, and experimental results. This design is fabricated and verified in a 0.35-μm CMOS process. The usefulness of the gate-voltage limited circuit on protecting

gate-driven devices against the over-gate-driven effect is proven through the measured ESD protection levels and the failure analyses.

In the chapter 4, a power-rail ESD clamp circuit for 1-V/3.3-V I/O interfaces is proposed. The proposed power-rail ESD clamp circuit is designed with only 1-V/2.5-V low-voltage devices but can be safely operated under 1-V/3-3-V mixed-voltage environment without the gate-oxide reliability issue. The proposed clamp circuit has an on-chip ESD detection circuit that can provide substrate-triggered current to substantially improve the turn-on efficiency of ESD protection devices. This protection design is successfully verified in a 130-nm 1-V/2.5-V CMOS process. Experimental results of the proposed clamp circuit show high ESD protection capability with very low leakage current, which is one of the main concerns for portable designs. As a result, the proposed power-rail ESD clamp circuit is an excellent ESD solution especially to the portable electronic devices with mixed-voltage I/O interfaces.

In the end of this thesis, a short conclusion and future work are given in the chapter 5.

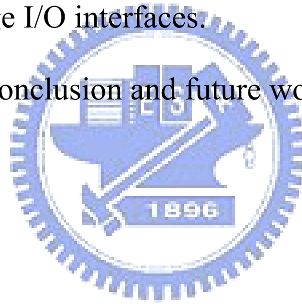

Chapter 2

Introduction to ESD and the Effects of Process Migration to ESD Protection Designs

2.1 GENERAL INTRODUCTION TO ESD

ESD is a phenomenon caused by the discharging of electrostatic charges on IC pins. It can be arose from events such as a physical contact of a human body and an IC products, touch of manufacturing machines and wafers, or discharge of secondhand induced electrical field on an IC chips. Because ESD can be brought about by different origins, it can be classified to human-body model (HBM), machine-model (MM), and charged-device model (CDM) according to different discharging methods and sources of electrostatic charges.

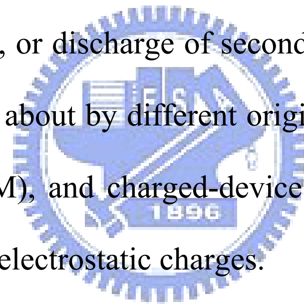

2.1.1 Human-Body Model (HBM)

HBM is a typical ESD event arose from the contact of an electrified human body and an IC product. The ESD static charges are initially stored in the human body and then transfer into the IC when the human body touches the IC. The equivalent circuit for HBM ESD event is shown in Fig. 2-1 [13], where the 1.5-kΩ resistor and the 100-pF capacitor represent the equivalent parasitic resistor and capacitor of a human body. The DUT in Fig. 2-1 represents the device under test. The HBM circuit is designed to eliminate the weak protection designs and susceptible devices of the DUT. Fig. 2-2 shows the specifications of a HBM ESD waveform generated by the ESD HBM tester to a short wire [13]. Generally, commercial ICs are requested to pass 2-kV HBM ESD stress at least, which can generate ESD current with a peak value of ~1.3Amp and a rise time of ~10ns.

2.1.2 Machine Model (MM)

The equivalent circuit diagram of MM ESD event is shown in Fig. 2-3 [14], where there is no equivalent resistor on the equivalent discharging path because the MM ESD stress is to replicate the ESD event arose from the contact of a machine and a semiconductor device. Fig. 2-4 shows the waveform of a 400-V MM ESD pulse generated by the MM ESD tester [14]. A commercial IC product is generally required to pass at least 200-V MM ESD stress, which can generate an ESD current with a peak value of ~3.5Amp and a rise time of ~10ns. The MM ESD level of a semiconductor device is generally 8~12 times smaller than its HBM ESD level for the faster rise time and voltage resonance of a MM ESD pulse.

2.1.3 Charged-Device Model (CDM)

The CDM ESD event is caused by the discharging of electrostatic charges initially stored in the body of a floating IC. Most of the CDM charges are stored in the body (the p-substrate) of a CMOS IC at first. When one or more pins of this charged IC is touched by an external grounded object, charges in the p-substrate will be discharged from the IC inside to the grounded pin outside. There is no standard equivalent parasitic capacitor for the CDM ESD stress because different dimension of chips, different form and size of packages result in different values of the parasitic capacitor of IC chips. A commercial IC is generally requested to pass at least 1-kV CDM ESD stress, which can generate an ESD current with peak current value as high as ~15A within a rise time less than 200ps [15]. Fig. 2-5 compares the waveforms of a 2-kV HBM ESD stress, a 200-V MM ESD stress, and a 1-kV CDM ESD stress which has 4-pF equivalent capacitor of the device under test.

2.2 ESD TEST METHODS

Since electrical charges in natural environment can be either positive or negative, ESD tests have positive and negative modes, too. Moreover, since ESD event can occur on input/output (I/O) pins, power pins, or between different I/O pins of an IC chip, ESD test methods have pin combinations as follows:

2.2.1 ESD Test on I/O Pins

For every I/O pin of an IC chip under the human-body model and the machine-mode ESD tests, there are four test modes as illustrated through Fig. 2-6(a) to 2-6(d) [16], [17]:

(1). PS mode

Positive ESD voltage applied to the tested I/O pin with VSS pins relatively grounded. VDD pins and all other pins are kept floating during the test, as shown in Fig. 2-6(a).

(2). NS mode

Negative ESD voltage applied to the tested I/O pin with VSS pins relatively grounded. VDD pins and all other pins are kept floating during the test Fig. 2-6(b).

(3). PD mode

Positive ESD voltage applied to the tested I/O pin with VDD pins relatively grounded. VSS pins and all other pins are kept floating during the test, Fig. 2-6(c).

(4). ND mode

Negative ESD voltage applied to the tested I/O pin with VDD pins relatively grounded. VSS pins and all other pins are kept floating during the test, Fig. 2-6(d).

2.2.2 Pin-to-Pin ESD Test

Besides the ESD test on I/O pins, ESD events can happen on one of the I/O pins with another I/O pin relatively grounded. If the two I/O pins are not correlated to each other in circuitry, ESD current will first be diverted from the stressed I/O pin to the VDD or VSS power line, and then be

discharged to the grounded I/O pin. Therefore, during the pin-to-pin ESD tests, power pins of the tested chip are kept floating. However, it could take a long testing period if every I/O pin of an IC chip is tested one by one. To shorten the testing period, positive or negative ESD voltage is applied on the tested I/O pin with all other I/O pins relatively grounded, as illustrated in Fig. 2-7(a) and Fig. 2-7(b).

2.2.3 ESD Test on Power Pins (VDD-to-VSS ESD Test)

The ESD test on power pins, or the VDD-to-VSS ESD stresses, simulate ESD events that happen between two power pins. A positive or a negative ESD voltage during the VDD-to-VSS ESD stress is applied to the VDD power pin of the device under test while the VSS power pin is relatively grounded, as shown in Fig. 2-8.

2.3 ESD PROTECTION NETWORK

The various ESD test methods suggest that ESD events can damage not only I/O circuits but also internal circuits, especially under the pin-to-pin and the VDD-to-VSS ESD stresses. These two ESD test modes often lead to some unexpected ESD current through the I/O ESD protection circuits and the power lines into the internal circuits and result in ESD damage on the internal circuits [18], [19]. Therefore, to effectively protect chips from the ESD damage, ESD protection designs are required on both I/O circuits and between the power lines. Fig. 2-9 illustrates the impact of the power-rail ESD clamp circuit to the discharging paths of ESD current (I_{ESD}) under the specified pin-to-pin ESD stress. When a positive ESD voltage is applied to some input pin (I/P) with some output pin (O/P) grounded and the VDD and VSS pins floating, some ESD current will be diverted from the input pin to the floating VDD power line and then to the internal circuits (path 1), if the power-rail ESD protection circuit is not designed in Fig. 2-9. The ESD protection circuits at the I/O pins are often designed strong enough to discharge the huge ESD current, but the internal

circuits are easily damaged to cause unexpected damages on internal circuits. If an effective ESD clamp circuit is added between the VDD and VSS power lines, the ESD current can be discharged through the power-rail ESD clamp circuit (path 2) instead of the internal circuits (path 1). Therefore, the internal circuits can be safely protected against such unexpected ESD damage. Moreover, the power-rail ESD clamp circuit can also protect the whole chip against the VDD-to-VSS ESD testing mode. Thus, an effective power-rail ESD clamp circuit between the VDD and VSS power lines is necessary for the whole-chip ESD protection [19].

Therefore, a whole-chip ESD protection network should include not only ESD protection circuits at the I/O pins but also power-rail ESD clamp circuits. The whole-chip ESD protection network, appropriate ESD protection devices, and effective techniques to trigger the ESD protection devices are the keys for IC products to carry off high ESD robustness.

2.4 ESD PROTECTION DEVICES IN MODERN CMOS ICS

To protect ICs from being damaged by ESD current, it is important to choose appropriate ESD protection device under different ESD protection networks and different system specifications. In modern CMOS ICs, ESD protection devices in common use include:

(1). P-N Junction Diode:

A diode device has low forward cut-in voltage (~ 0.6 V) and high reverse breakdown voltage, which can be higher than 10 V. Both forward diodes in series and a reverse diode can serve as the ESD protection circuit to protect internal circuits from being damaged by ESD current. When a reverse diode is used as an ESD protection device, its reverse breakdown voltage is required to be smaller than the gate oxide breakdown voltage of MOS devices so that ESD current can be discharged to ground through the reverse diode without damaging the gate oxide of internal circuits. A larger device dimension of the ESD protection diode is also required when it is operated

in reverse mode because the high reverse breakdown voltage generates huge heat to be dissipated during ESD stresses.

(2). MOS Device (NMOS or PMOS):

MOS devices are the most common ESD protection devices in CMOS ICs. The n+ drain junction, p-substrate and the n+ source junction of an NMOS device construct a parasitic n-p-n bipolar junction transistor. When the high ESD stress voltage occurs, the parasitic n–p-n bipolar junction transistor inherent in NMOS's device structure can be turned-on to carry the huge ESD current and to clamp down the ESD voltage to protect gate oxide of internal circuits. As a result, the I-V characteristic curve of an NMOS device under ESD stresses often has the snapback phenomenon due to the turn on of the parasitic n-p-n bipolar.

The p+ drain junction, n-well substrate and p+ source junction of PMOS device form a parasitic p-n-p bipolar junction transistor inherent in its device structure. PMOS devices in CMOS ICs can therefore serve as an ESD protection device. However, the beta gain of p-n-p bipolar junction transistor in CMOS process is much smaller than that of n-p-n bipolar junction transistor; I-V characteristic curves of PMOS under ESD stresses have no, or weak, snapback phenomenon.

(3). Field Oxide Device (FOD):

The field oxide device has similar device structure to that of NMOS device in CMOS process except the gate oxide of NMOS is replaced by the field oxide structure. The I-V characteristic curves of FOD under ESD stresses have larger turn-on resistance compared to that of NMOS because the depth of field oxide structure makes the ESD current discharging path of FOD longer than that of NMOS.

(4). Silicon Controlled Rectifier (SCR):

SCR device is a component with p-n-p-n structure, as shown in Fig. 2-10. A SCR device has a p-n-p and an n-p-n bipolar junction transistor with regenerative feedback to each other, so that SCR device can clamp the ESD voltage at a relatively low holding voltage (~1.2 V) compared to that of NMOS and FOD devices. Therefore, SCR device can achieve high ESD protection level

within small layout area due to its low holding voltage. However, a SCR device has drawbacks such as high turn-on voltage, low turn-on speed, and latch-up issue.

To sum up, different ESD protection devices have respective advantages and disadvantages. Therefore, it is important to pick the appropriate device as an ESD protection element according to different power-supply voltages, ESD protection networks, system specifications, and device characteristics.

2.5 TRIGGERING TECHNIQUES TO ESD PROTECTION DEVICES

In most applications, MOS devices are used as ESD protection elements in CMOS ICs. With the process scaling down, thickness of gate oxide of MOS devices in deep-submicron CMOS technologies keeps shrinking to achieve higher system operating frequency, lower power consumption and lower heat dissipation. As a result, the gate oxide breakdown voltages of MOS devices keep going down toward their junction breakdown voltages. Internal circuits protected by stand-alone ESD protection devices, which have no triggering techniques to increase their turn-on efficiencies, are therefore easily damaged under ESD stress. Moreover, it is also found that ESD levels of large-device-dimension NMOS devices are constrained by the non-uniform turn-on behavior [20]-[23], making it difficult for IC chips to have high ESD robustness. There are two popular measures that can be realized in circuitry to effectively increase the turn-on efficiency and uniformity of ESD protection devices: the gate-driven and the substrate-triggered techniques.

2.5.1 Gate-driven Technique

To prevent ESD protection devices from interacting with the signals in normal operation, the gate electrode of the ESD protection NMOS is grounded in most applications. This can also ensure that the NMOS has its minimum leakage under normal operation. However, a MOS device can be a more robustness ESD protection element if its gate is coupled high during ESD transition [2]-[7].

The gate-driven (or the gate-coupled) technique is to design a special ESD detection circuit that can drive the gate voltage of ESD protection NMOS high during ESD transition but keep the gate potential low to ensure the chip function during normal circuit operation. The gate-driven technique drives gate voltage of NMOS high to induce its channel current during ESD transition. The induced channel current can therefore help forward bias the base-emitter junction of parasitic n-p-n bipolar and increase its turn-on efficiency during ESD transition.

2.5.2 Substrate-Triggered Technique

The other method to improve the turn-on efficiency of ESD protection devices is the substrate-triggered technique. The basic concept of the substrate-triggered technique is to design an ESD detection circuit that can provide substrate-triggered current to the substrate of an ESD protection device during ESD transition. The trigger current can help forward bias the base-emitter junction of the parasitic bipolar junction transistor. As a result, the bipolar turn-on voltage, bipolar turn-on speed, and the ESD protection robustness of a substrate-triggered ESD protection device can be substantially improved. During normal circuit operation, the ESD detection circuit shall be kept off to ensure the regular function of internal circuits.

2.6 EFFECTS OF THE PROCESS MIGRATION TO ESD PROTECTION DESIGNS

In modern technologies, the power consumption of systems is pushing lower and lower so that the battery life time of handheld systems can stand longer, the operating frequency of CMOS processor can be driven faster, the complex circuit functions of multi-chips can be merged into a single SOC chip, etc. Therefore, the power supply voltages of internal circuits becomes smaller and smaller. The gate oxide thickness of MOS devices also keeps scaling down to attain the same, or better, device driving capability at a lower power supply voltage. With the migration from a

thicker gate oxide to a thinner one, some problems and demands on ESD protection designs are revealed.

2.6.1 The Over-Gate-Driven Effect

As mentioned in 2.5.1, the gate-driven technique can induce the channel current of an NMOS device to increase its ESD protection efficiency. However, the induced channel current also draws higher temperature beneath the gate oxide during ESD transition [22]. Therefore, the gate oxide of the ESD protection NMOS is more likely to be burned out during ESD stress. The gate-driven technique turns into a hazard to the ESD protection NMOS. This effect is so-called the "over-gate-driven effect", and it happens more often when the thickness of gate oxide keeps scaling down. Therefore, in this thesis, a solution to the over-gate-driven effect is proposed and canvassed in chapter 3.

2.6.2 High Voltage Tolerant ESD Protection Design

Though the power supply voltages keep lowering, voltages at I/O circuits are often higher than the internal circuits in order to cooperate with peripheral devices. For example, a standard PCI interface device has 3.3-V I/O voltage but its core voltage (power supply voltage of internal circuits) can be 1.2 V. Devices in the internal circuits are low voltage devices in order to minimize the chip size and to achieve better circuit performance. Devices in the I/O circuits are often designed with low voltage devices as well to increase the circuit performance, to meet the process limitation, or to fulfill the system specification. Therefore, the high voltage tolerant ESD protection design is required to collocate with the mixed-voltage applications. In chapter 4, a power-rail ESD clamp circuit that can be operated under 1-V/3.3-V mixed-voltage I/O interfaces is proposed. The proposed clamp circuit is specially designed with only 1-V/2.5-V devices. The proposed clamp circuit has an ESD detection circuit that can provide substrate-triggered current to the ESD protection device to substantially increase its ESD protection efficiency.

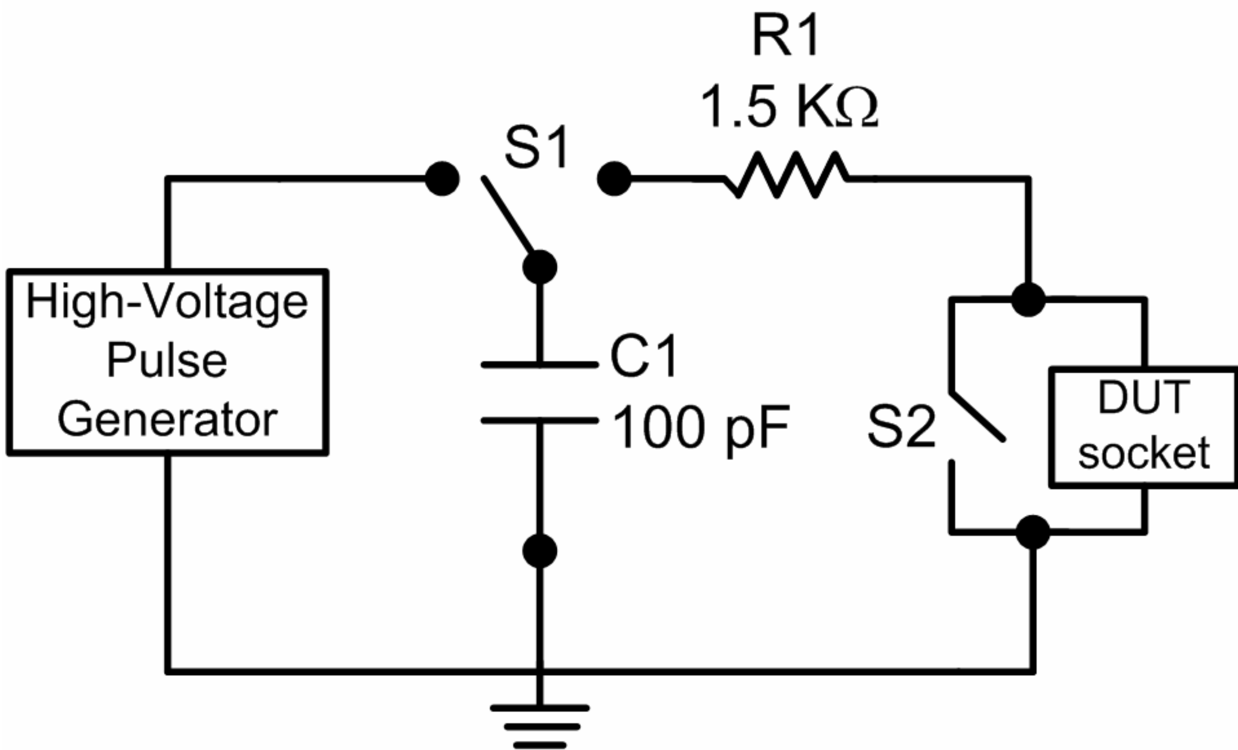

Fig. 2-1. The equivalent circuit of the human body model ESD event.

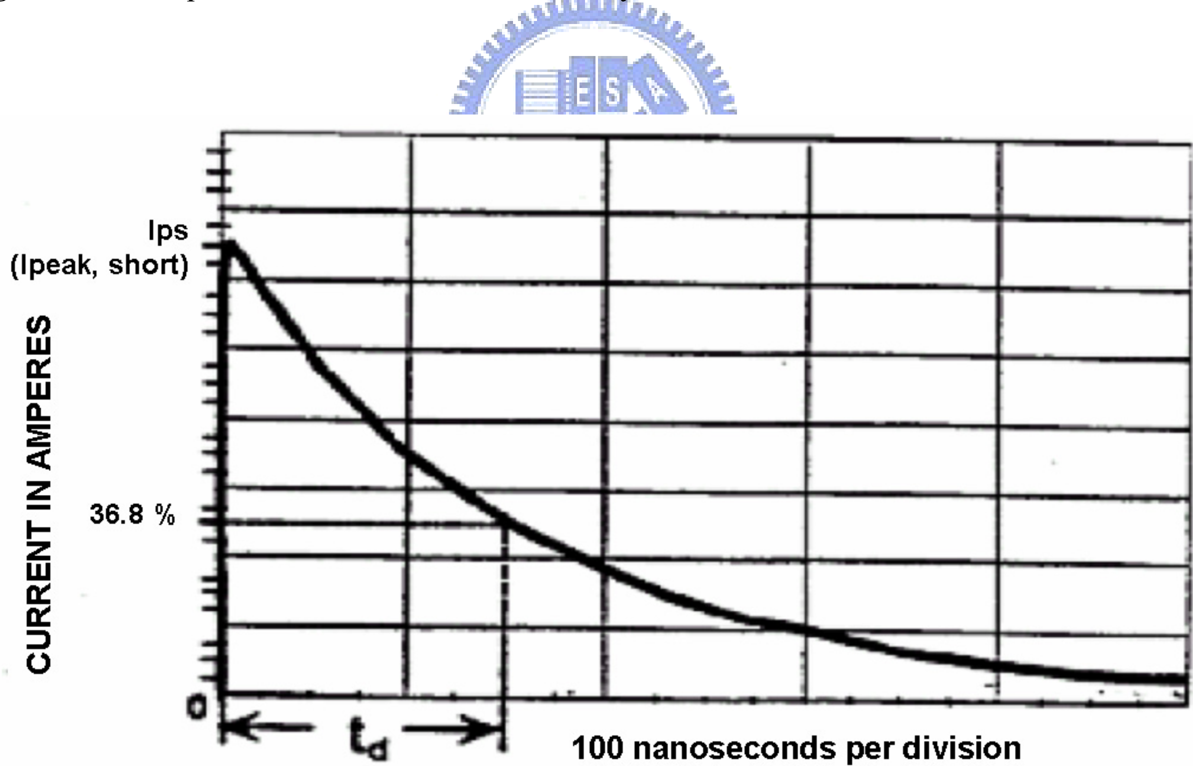

Fig. 2-2. Definition of the HBM pulse decay time (td).

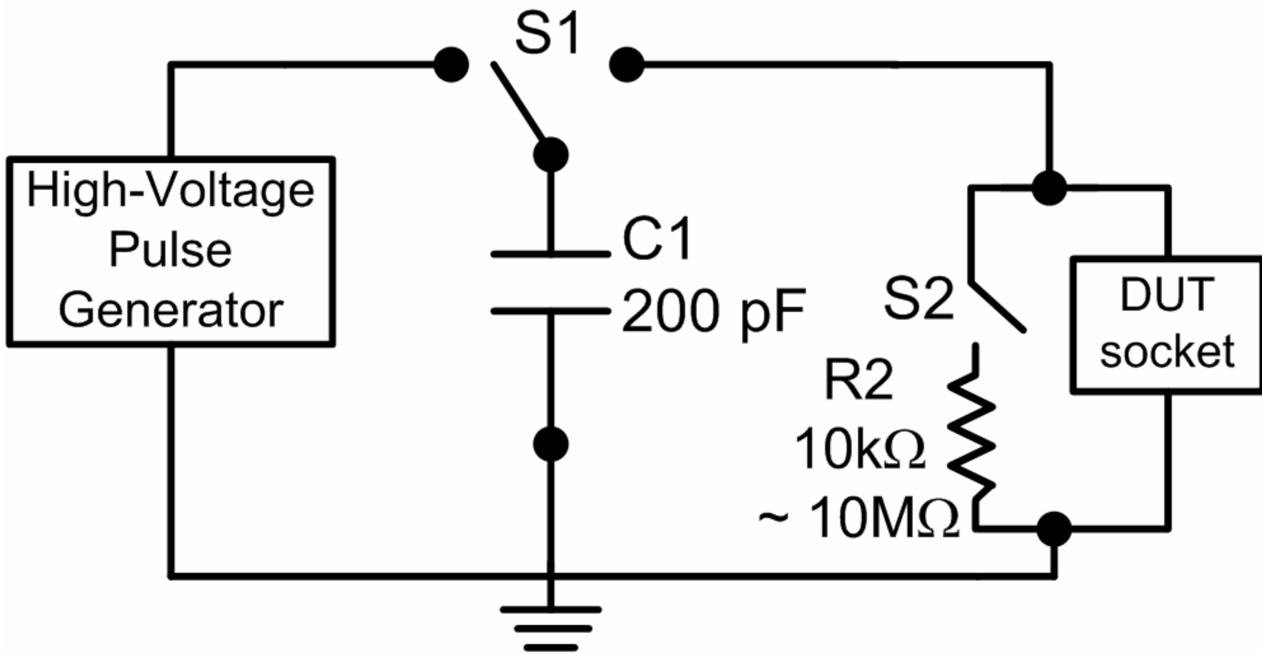

Fig. 2-3. The equivalent circuit of the machine model ESD event.

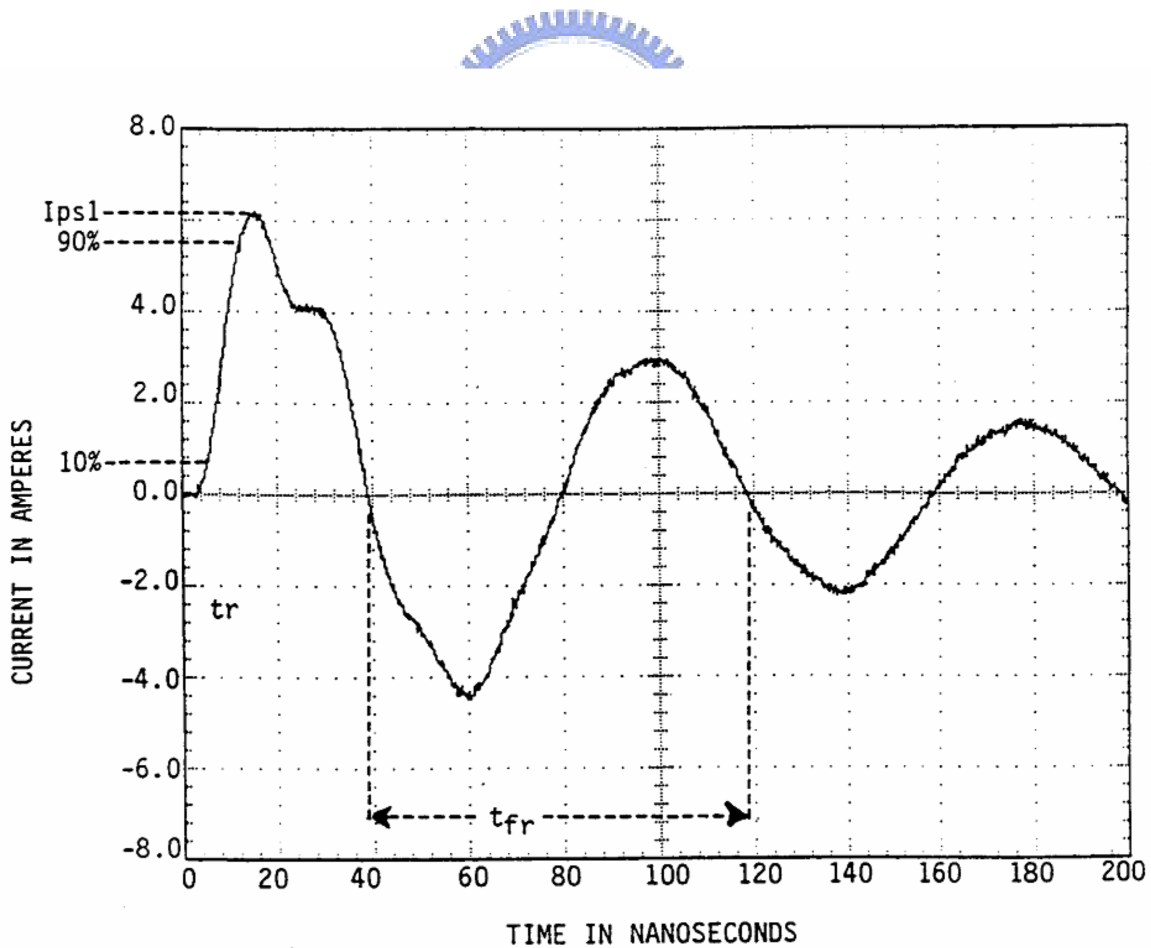

Fig. 2-4. The current waveform of a 400-V MM ESD stress discharging through a short wire.

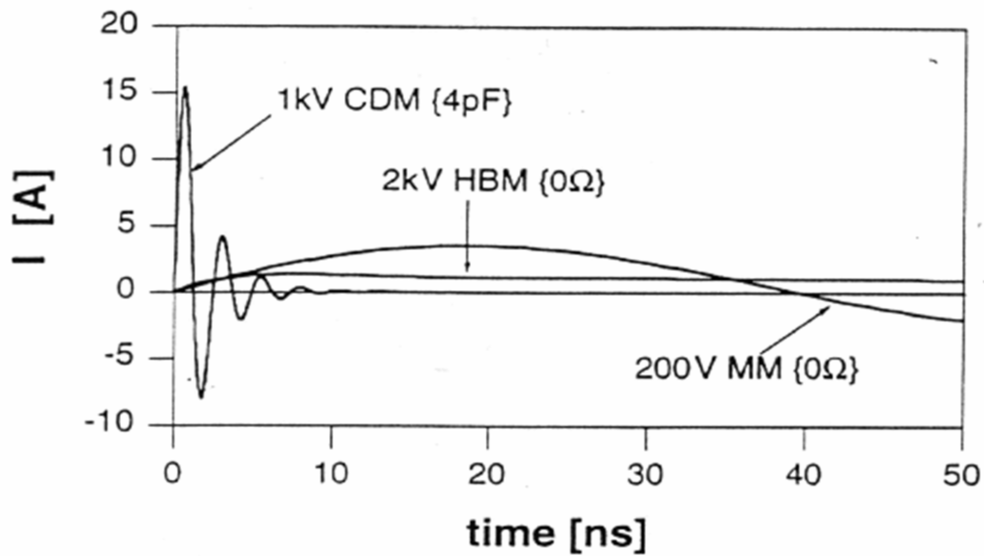

Fig. 2-5. Comparison on waveforms of a 2-kV HBM ESD stress, 200-V MM ESD stress, and a 1-kV CDM ESD stress.

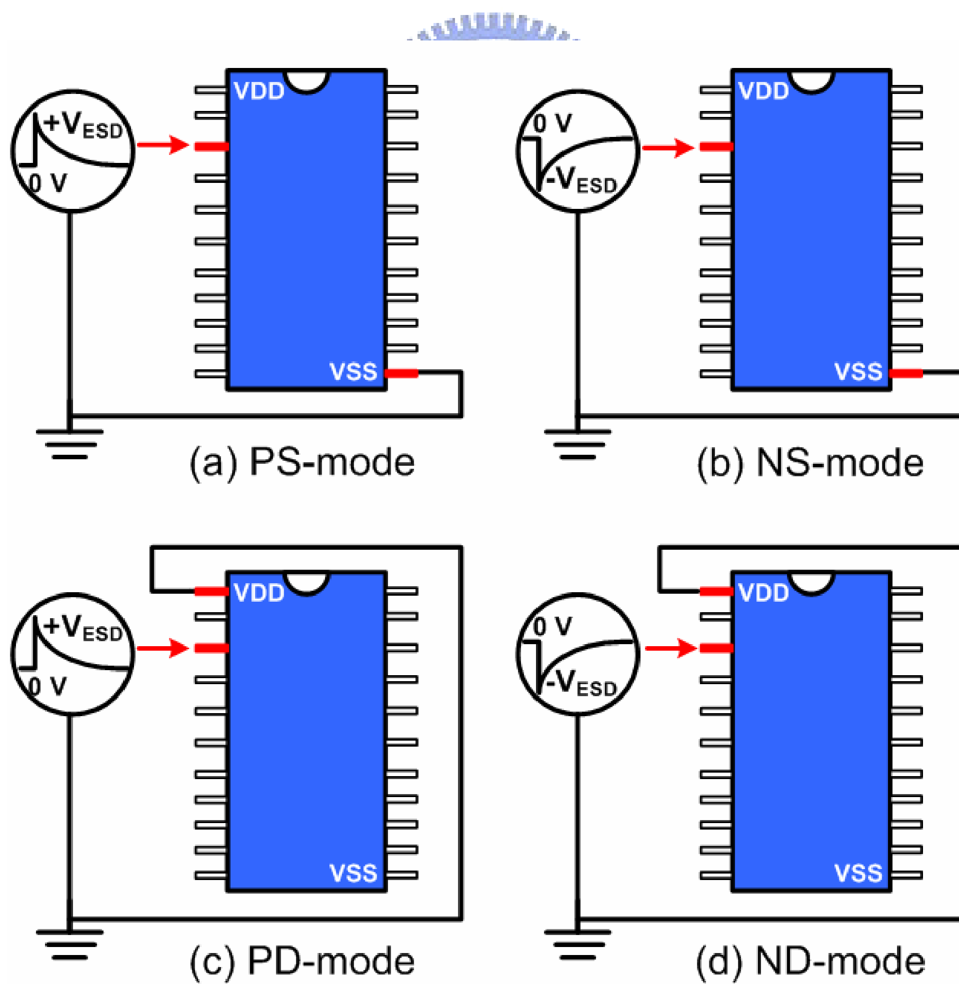

Fig. 2-6. (a) PS-mode, (b) NS-mode, (c) PD-mode, and (d) ND-mode, ESD test on I/O pins.

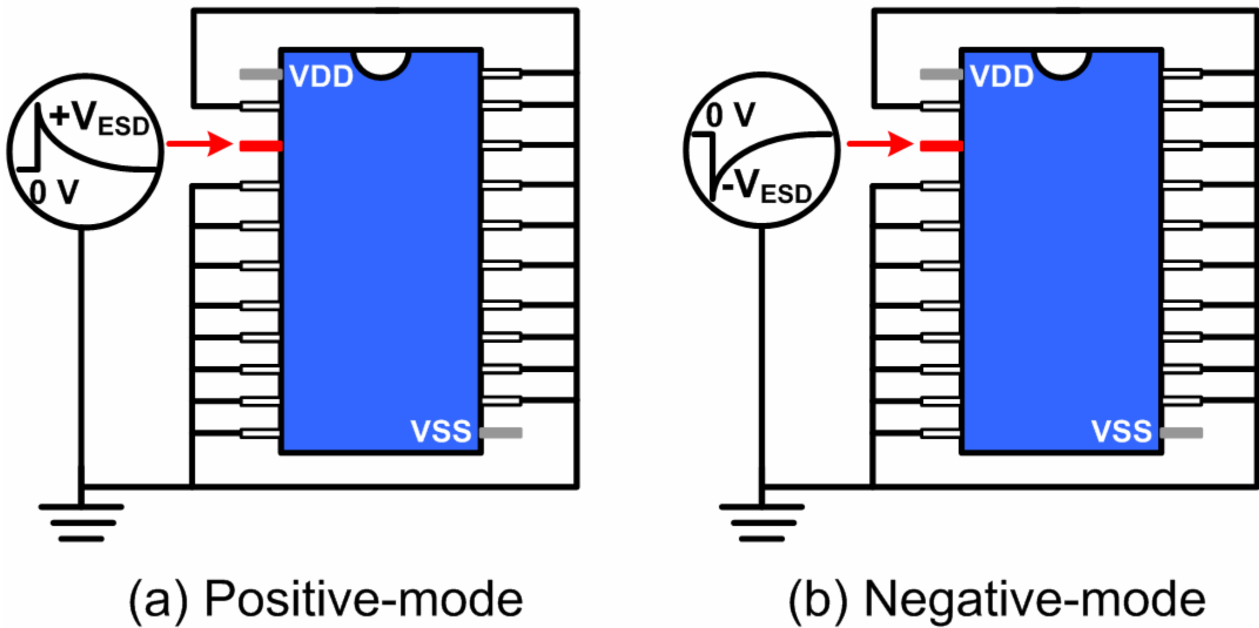

Fig. 2-7. (a) Positive mode, (b) Negative-mode, pin-to-pin ESD test.

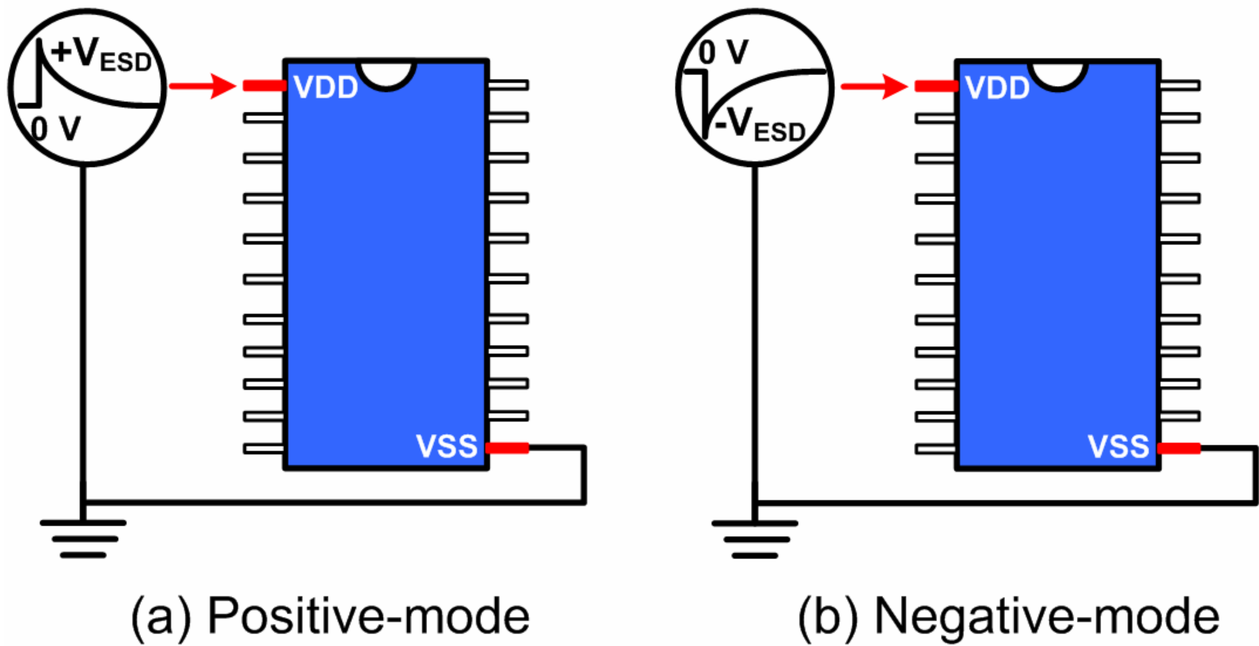

Fig. 2-8. (a) Positive mode, (b) Negative-mode, VDD-to-VSS ESD test.

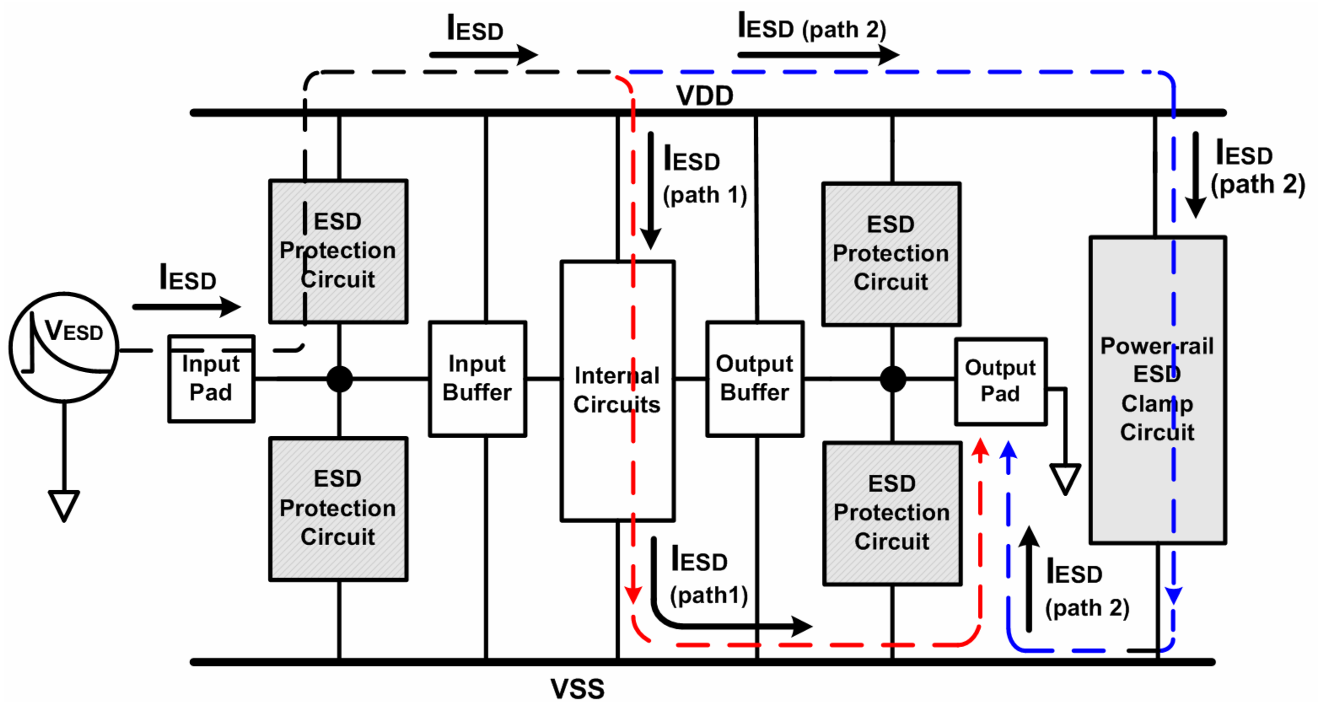

Fig. 2-9. The ESD current discharging paths (path 1 and path 2) during the pin-to-pin ESD stress condition.

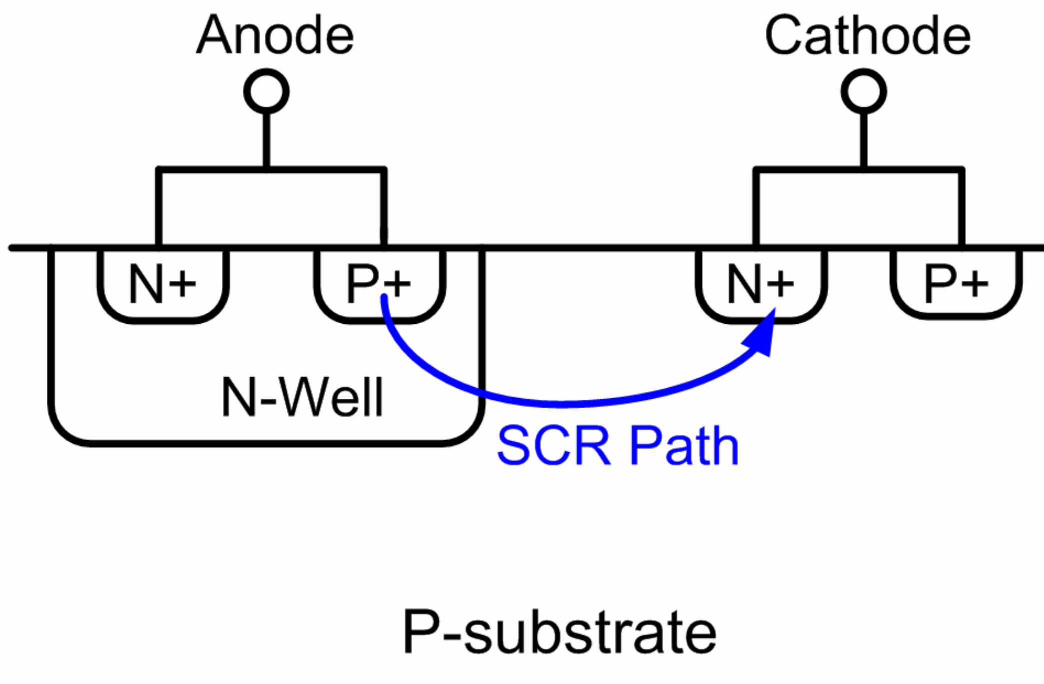

Fig. 2-10. Cross sectional view of a SCR device.

Chapter 3

Circuit Solution to Overcome the Over-Gate-Driven Effect on ESD Protection Circuits in Deep-Submicron CMOS Processes

---

3.1 INTRODUCTION

To sustain reasonable ESD robustness in deep-submicron CMOS ICs, on-chip ESD protection circuits must be added to the silicon chips. The typical ESD levels required by general commercial IC products are 2kV in human-body-model (HBM) ESD test and 200V in machine-model (MM) ESD test. To sustain the required ESD levels, ESD protection devices are often designed and drawn with large device dimensions, which are often realized in the multi-finger layout style to reduce the total occupied silicon area [24]. However, due to the non-uniform triggering among the multiple fingers of NMOS devices, the ESD robustness of NMOS devices are restricted and not linearly increased when the device dimension is increased [20]–[23]. To improve the turn-on uniformity of the ESD protection NMOS, the gate-driven (or gate-coupled) technique has been reported and widely used in CMOS technologies [2]–[7]. However, the ESD robustness of the gate-coupled NMOS has been found to be degraded dramatically due to the over-gate-driven effect [8]–[10]. It has been also found that the over-gate-driven effect occurs more easily when the thickness of gate oxide is shrunk with process migration [9]. When the CMOS technology is moving into the very deep sub-micron generation, the over-gate-driven effect could cause some difficulty in optimizing the gate-coupled ESD protection devices. The design margin for the gate-coupled NMOS devices to achieve high ESD robustness could be greatly reduced or even vanish in the very deep sub-micron CMOS technologies. Especially, the MM ESD robustness of NMOS devices in sub-quarter-micron CMOS process has been found to degrade seriously [25].

In this chapter, a new circuit design solution to overcome the over-gate-driven effect is proposed [11]. The proposed circuit design has been successfully verified in a 0.35-μm CMOS process with a great improvement on the machine-model ESD robustness. With the proposed circuit solution, the gate-driven or gate-coupled technique for ESD protection can be optimized more easily and properly.

3.2. THE OVER-GATE-DRIVEN EFFECT

3.2.1 Non-uniform Turn-on Behavior

The snapback I-V curve of a gate-grounded NMOS (GGNMOS) fabricated in a 0.35-μm CMOS process is measured by the transmission-line-pulse (TLP) system with the pulse width of 100 ns [26], [27], and the result is shown in Fig. 3-1. The device dimension of the measured GGNMOS is 600 μm/0.35 μm with each finger width of 30 μm. Under the ESD stress condition, the drain-substrate junction of the NMOS device begins to avalanche due to the high overstress ESD voltage, and some electron-hole pairs are generated. The electrons are swept into the drain while the holes drift to the source of NMOS. These electron-hole pairs serve as the base current of the parasitic lateral n-p-n bipolar junction transistor (BJT) inherent in NMOS device structure. Once the source-substrate junction of NMOS becomes forward biased, the lateral n-p-n BJT is triggered on to discharge ESD current.

For this lateral BJT to carry amperes of ESD current, the device width of ESD protection NMOS is often drawn over several hundred micrometers. The multi-finger layout structure is often used to realize such large-dimension NMOS device to save the occupied silicon area [24]. A P+ guardring in the P-type substrate is often surrounding the whole NMOS device to provide the substrate bias at ground. Therefore, the central fingers of the multi-finger NMOS is relatively farther from the substrate guardring. The lateral BJTs inherent in these central fingers equivalently have larger base resistance to the grounded P+ guardring. During ESD stress, these BJTs inherent

in the central fingers are often triggered on earlier than those in the sided regions of the multi-finger NMOS structure. The NMOS device is hence driven into snapback region, and the ESD transient voltage is clamped down to the holding voltage of the NMOS device, as shown in Fig 3-1. The ESD current is discharged through the earlier-turned-on fingers to cause the non-uniform turn-on behavior among the fingers of ESD protection NMOS device. If the secondary breakdown voltage (Vt2) of NMOS is smaller than its trigger voltage (Vt1), those BJTs inherent in the sided fingers of NMOS cannot be turned on. This non-uniform turn-on effect suppresses ESD robustness of NMOS, even if it is drawn with a large device dimension. Consequently, ESD robustness of NMOS cannot be linearly increased when the device dimension is increased.

3.2.2 Gate-Coupled Technique

Since the non-uniform turn-on effect results from the fact that the Vt2 of ESD protection NMOS is smaller than its Vt1, this effect can be diminished by increasing the Vt2 value or by decreasing the Vt1 value. The Vt2 can be increased by introducing the back-end-ballasting [28] or N-Well extension resistor [29] into NMOS device structure. The Vt1 can be lowered by the gate-driven (or gate-coupled) technique [2]-[7]. The gate-coupled technique realized with simple RC circuit has been used to ensure uniform turn-on behavior among all fingers of NMOS during ESD stress. Two traditional gate-coupled circuit implementations are shown in Figs. 3-2(a) and 3-2(b). The capacitor C of the gate-coupled structure is used to couple ESD-transient voltage to the gate of ESD protection NMOS. As long as the gate voltage (Vg) of the gate-coupled NMOS (GCNMOS) is coupled higher than its threshold voltage (Vt), the channel current is induced and helps to forward bias the source-substrate junction of GCNMOS. Therefore, the parasitic BJT can be triggered on earlier, and the Vt1 of GCNMOS can be lowered. If the Vt1 value is lowered and smaller than the Vt2 value, the lateral BJT inherent in the sided fingers of NMOS can be further turned on to shunt the huge ESD current before the earlier-turned-on fingers are unrecoverably

thermally damaged. With all fingers being triggered on during ESD stresses, the ESD robustness of NMOS with the gate-coupled technique can be significantly improved [5].

Under normal circuit operating conditions, the ESD protection circuits are kept off to avoid interacting with the input/output signals. To achieve the correct RC time constant in the gate-coupled design, the resistor used in Fig. 3-2(a) is usually required in the order of several ten thousand ohms [5], which takes a large layout area in silicon chips. To save silicon area, another gate-coupled design is shown in Fig. 3-2(b), where the resistor is realized by an NMOS transistor Mr1 with its gate being connected to Vdd. Both methods shown in Figs. 3-2(a) and 3-2(b) have been widely used today for application to the input/output pin and even to the power-rail ESD clamp circuits. In this work, the structure shown in Fig. 3-2(b) is chosen to carry out the GCNMOS for further study.

3.2.3 Over-Gate-Driven Effect

Though the gate-coupled technique is useful for solving the non-uniform turn-on behavior in NMOS devices, the over-gate-driven effect [9] will turn this beneficial technique into a hazard. The gate-coupled technique enables the ESD current to be initially discharged through the surface channel of GCNMOS. With higher gate voltage on NMOS during ESD stress, the ESD current will generate higher temperature beneath the gate oxide [10], [22]. If the gate voltage of GCNMOS is over coupled during ESD stress, in deep-submicron CMOS technologies with the ultra thin gate-oxide thickness, the surface channel or the gate oxide of NMOS is easily burned out by the localized ESD current. As a result, the over-gate-driven effect could reversely affect the effectiveness of gate-coupled technique and dramatically decrease the device capability for ESD protection.

For ESD transient voltage with faster rise time, the over-gate-driven effect is found to affect NMOS more easily and critically. Figs. 3-3(a) and 3-3(b) show the transient simulation results of an NMOS device with 0.5-µm gate length when 6.5-V voltage pulses with different rise time are

applied on it. The simulated NMOS has a bipolar trigger voltage of 5.7 V when its gate is biased at 2 V. Fig. 3-3(a) shows the current flow lines along the NMOS when the 6.5-V voltage pulse with a rise time of 10 ns is applied to the drain electrode. Meanwhile, the gate voltage of NMOS is simultaneously ramped to 2 V. Under this condition, the current flow lines distribute a depth of 1.5 μm into the substrate. When the rise time of the applied transient voltage pulses on both drain and gate electrodes are further shortened to 5 ns, a large number of current flow lines are drawn beneath the gate oxide, as shown in Fig. 3-3(b), and the total current distributes only a depth of 1 μm into the substrate. So, ESD transient voltage with faster rise time will result in larger peak current under the gate oxide of NMOS, which in turn easily burns out the device. The MM ESD stress without series resistance in its discharging path has a faster rise time than that of HBM ESD stress. The GCNMOS during MM ESD stress will suffer more serious over-gate-driven effect.

To practically investigate the over-gate-driven effect, the MM ESD levels of NMOS fabricated in a 0.35-μm CMOS process with gate-oxide thickness of ~75Å are tested under different gate voltages. The failure criteria of tested devices are judged by the leakage current over 1 μA under 3.3 V drain bias. The tested NMOS devices have device dimension of 600 μm/0.35 μm with each finger width of 30 μm. As shown in Fig. 3-4, when the gate voltage is 0 V (namely the GGNMOS), the non-uniform turn-on behavior causes a lower MM ESD level. With the increase of gate voltage up to 2 V, the non-uniform turn-on behavior can be diminished, and therefore the MM ESD level increases because more fingers of NMOS can be turned on to shunt ESD current. When the gate voltage is larger than 2 V, the trend of increase on MM ESD level is limited because all fingers have been fully triggered into snapback during ESD stress. When the gate bias voltage is over 8 V, the MM ESD level is dropped down dramatically due to the over-gate-driven effect in this 0.35-μm CMOS process.

3.3. CIRCUIT SOLUTION TO OVERCOME THE OVER-GATE-DRIVEN EFFECT

3.3.1 Design Concept

Since the over-gate-driven effect results from the over-coupled transient voltage at the gate of GCNMOS during ESD stress, this unwanted effect can be successfully overcome by a gate-voltage-limited circuit, which is added between the gate and the source of GCNMOS, to clamp the coupled gate voltage to a desired voltage level during ESD stress. In this work, the diodes or NMOS connected in series are used to realize the gate-voltage-limited circuit, as shown in Fig. 3-5. The coupled gate voltage on the GCNMOS during ESD stress can be controlled by varying the number and the device dimension of stacked diodes (or NMOS). Ideally, with the gate-voltage-limited diode (or NMOS) string, the coupled gate voltage (Vg) of GCNMOS during ESD stress can be clamped at Vt × n, where n and Vt are the number and the threshold voltage of the clamping device, respectively.

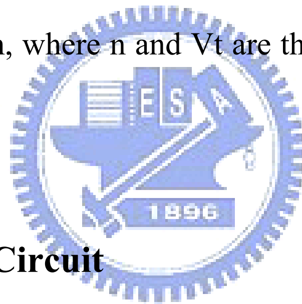

3.3.2 Gate Voltage Monitor Circuit

To verify the effectiveness of the proposed gate-voltage-limited circuit, a special on-chip gate voltage monitor circuit is added onto GCNMOS to monitor the coupled gate voltage (Vg) of GCNMOS during ESD stress. To monitor the gate voltage of GCNMOS under different transient voltages, the parasitic capacitance in the measurement setup should be minimized. The gate of GCNMOS cannot be directly connected to a bond pad or a voltage probe because the parasitic capacitance of the bond pad and the measurement instrument will affect the quantity of the coupled gate voltage on GCNMOS during ESD transition to cause the monitored gate voltage different from the practical cases. The special gate voltage monitor circuit is made up of an on-chip NMOS Mn2 and an external resistor R_{ext}, as shown in Fig. 3-6. The device dimension (W/L) of Mn2 is 10 μm/1 μm and the resistance of R_{ext} is 1 kΩ. The gate of Mn2 and the gate of GCNMOS (Mn1) are connected together, and the drain of Mn2 is biased at 3 V through R_{ext}. By

using this gate voltage monitor circuit, the parasitic capacitance from Mn2 that affects the quantity of coupled gate voltage on GCNMOS is small enough to be negligible.

With the gate voltage monitor circuit, the coupled gate voltage of GCNMOS can be monitored through the drain voltage of Mn2 (indicated as V_{det} in Fig. 3-6). When a voltage pulse is applied to the pad, the gate voltage of GCNMOS is coupled high through the capacitor C. If the gate voltage of GCNMOS, which is the same potential of the gate voltage of Mn2, is not lifted greater than the threshold voltage of Mn2 (Vt_{Mn2}), Mn2 is kept off and V_{det} voltage is biased at 3 V through R_{ext}. When the gate voltage of GCNMOS is coupled higher than Vt_{Mn2}, Mn2 is turned on to drop the potential on V_{det} from 3 V to (3 V – I_{Mn2} × 1 kΩ), where I_{Mn2} is the current flowing through Mn2. Vg can be figured out with the help of HSPICE simulation because the gate voltage of an NMOS device is a function of its drain current. Therefore, the gate voltage of GCNMOS can be estimated from the V_{det} voltage of the gate voltage monitor circuit and the HSPICE simulation.

Figs. 3-7(a) and 3-7(b) show the measured results of the gate voltage monitor circuit on a GCNMOS without the gate-voltage-limited circuit. As shown in Fig. 3-7(a), when a 10-V voltage pulse was applied to the pad, the coupled Vg turned on Mn2 and the voltage on V_{det} dropped from 3 V to 1.9 V. I_{Mn2} can be calculated from (3 V－V_{det})/R_{ext} as 1.1 mA. When a 15-V voltage pulse was applied, because there was no gate-voltage-limited circuit added to the GCNMOS, the coupled gate voltage of GCNMOS was higher than that when a 10-V voltage pulse was applied. Therefore, V_{det} voltage dropped from 3 V to a lower value, 1.2 V, as shown in Fig. 3-7(b), whereas the I_{Mn2} is calculated as 1.8 mA. From the HSPICE-simulated Id-Vg curve of the gate voltage monitor circuit, as shown in Fig. 8, GCNMOS without gate-voltage-limited circuit under 10-V and 15-V voltage pulses has the peak voltages of 1.85 V and 2.45 V, respectively. If no gate-voltage-limited circuit is added to GCNMOS, the larger ESD voltage pulse results in the higher coupled gate voltage on GCNMOS to suffer the over-gate-driven effect.

3.4. EXPERIMENTAL RESULTS

In this work, the gate-voltage-limited circuit is realized by the stacked diode string or the stacked NMOS string with different numbers or different dimensions. Every NMOS (diode) in the stacked NMOS (diode) string has the same device dimension. The GCNMOS is realized with a 3-pF coupling capacitor and an NMOS device (W/L) of 30 μm/1.5 μm, whose gate is connected to Vdd. The gate voltage monitor circuit is added to every GCNMOS for further exploring the effectiveness of the gate-voltage-limited circuit. ESD levels of GCNMOS were measured by ZapMaster and the tested devices were stressed by three continuous ESD zaps at every ESD test level under positive-to-VSS mode. The failure criteria of tested devices were judged by the leakage current over 1 μA under 3.3-V drain bias.

3.4.1. Clamping by NMOS String

To verify the effectiveness of the gate-voltage-limited circuit, voltage pulses with different pulse heights were applied to GCNMOS with the stacked NMOS string, which consists of two stacked 50 μm/0.35 μm NMOS. When a 10-V voltage pulse with a rise time of 10 ns was applied to GCNMOS, the V_{det} voltage dropped from 3 V to 2.3 V with a ΔV_{det} of 0.7 V, as shown in Fig. 3-9(a). When the applied voltage pulse was increased to 20 V, the maximum ΔV_{det} was still 0.7 V, as shown in Fig. 3-9(b). The applied voltage pulse with a larger pulse height results in a larger overshooting peak voltage coupled to the gate of GCNMOS. More charges are expected to be coupled to the gate of GCNMOS when a 20-V voltage pulse was applied on the GCNMOS. However, the measured ΔV_{det} between Figs. 3-9(a) and 3-9(b) do not increase when the applied voltage pulse has the larger pulse height. Moreover, the ΔV_{det} of 0.7 V represents the I_{Mn2} of 0.7 mA and the Vg voltage of 1.5 V, which is smaller than the Vg voltage of 2.45 V when a 15-V voltage pulse was applied on the GCNMOS without gate-voltage-limited circuit. Thus, the gate voltage of GCNMOS is successfully clamped by the gate-voltage-limited circuit.

For the GCNMOS with gate-voltage-limited circuit, the voltage coupled on its gate during ESD stress can be easily modulated by varying the number of stacked NMOS devices (or diodes). When the gate-voltage-limited circuits consist of more stacked NMOS devices, it is expected that a higher coupled voltage will stay on the gate of GCNMOS during ESD stress. Voltage pulses with 20-V pulse height and rise time of 10 ns were applied on GCNMOS with three or five stacked NMOS devices to measure the clamping voltage across the NMOS strings. When the GCNMOS has three (five) stacked NMOS devices in the gate-voltage-limited circuit, the measured ΔV_{det} is 1.4 V (2 V), as shown in Fig. 3-10(a) (Fig. 3-10(b)). From the voltage waveforms shown in Figs. 3-9(b), 3-10(a), and 3-10(b), the gate voltages of GCNMOS with two, three, and five stacked NMOS devices can be clamped to 1.5 V, 2.1 V, and 2.9 V, respectively, under the stress of a 20-V voltage pulse.

Since the gate voltage on GCNMOS can be modulated by varying the stacked NMOS devices (or diodes) in the gate-voltage-limited circuit, when a process has devices with thinner gate oxide, the number of stacked NMOS devices should be decreased to avoid the over-gate-driven effect. Therefore, the gate-voltage-limited circuit is portable between different CMOS technologies without modifying process steps or mask layers. Moreover, with a limited gate voltage on the GCNMOS during ESD stress, the optimization of gate-coupled design for GCNMOS becomes simpler.

Ideally, during ESD stress, the gate-voltage-limited circuit can clamp the gate voltage of GCNMOS at its total cut-in voltage, $Vt \times n$, where n is the number and Vt is the threshold voltage of NMOS (diode). However, the equation of $Vt \times n$ should be modified to $[(Vt \times n) + (I_{ON} \times R_{ON})]$, where I_{ON} is the current flowing through the gate-voltage-limited circuit and R_{ON} is the turn-on resistance of the NMOS string.

Voltage pulses with 20-V pulse height and rise time of 10 ns were applied on two GCNMOS with different sizes of stacked NMOS devices in the gate-voltage-limited circuits. Both of the GCNMOS have three stacked NMOS devices in their gate-voltage-limited circuit. However, one

of the gate-voltage-limited circuits consists of NMOS string where each NMOS device has device dimension of 50 μm/0.35 μm. The other consists of NMOS string where each NMOS device has device dimension of 20 μm/0.35 μm. When 20-V voltage pulses were applied to the two GCNMOS, the measured V_{det} waveforms are shown in Fig. 3-11, where difference of 0.2 V is found between the V_{det} voltages. The gate-voltage-limited circuit which consists of NMOS devices with smaller device dimension results in the lower V_{det} voltage, and therefore has the larger I_{Mn2} and the higher gate voltage of GCNMOS during ESD stress. This result is owing to the larger turn-on resistance of smaller NMOS device dimension in the gate-voltage-limited circuit. From the Id-Vg curve shown in Fig. 3-8, the 0.2 V voltage difference on V_{det} represents a voltage difference of 0.15 V on the gate voltage of GCNMOS. In nano-scale CMOS technologies, to limit the gate voltage of GCNMOS within the small design window, where the over-gate-driven effect is minimized or nullified during ESD stress, can be easily achieved by varying the device dimension and the device number of stacked NMOS (diode) devices in the gate-voltage-limited circuit.

Comparing the MM and HBM ESD stresses, the MM ESD stress with fast transition is more sensitive to suffer the over-gate-driven effect. The MM ESD levels per square micrometer of GCNMOS with different NMOS strings are shown in Fig. 3-12. For GCNMOS without the NMOS string, it has the lowest MM ESD level of 490 V. This lowest MM ESD level apparently does not result from the non-uniform turn-on behavior but the over-gate-driven effect, because the gate-coupled technique has been applied on the GCNMOS. With the NMOS string, a 30% increase on the MM ESD level of GCNMOS has been achieved. As shown in Fig. 3-12, the highest MM ESD level of GCNMOS is increased from 490 V to 645 V.

Comparing the MM ESD levels of GCNMOS with different numbers or different sizes of stacked NMOS devices, the trend of these curves is consistent with the characteristics of the gate-voltage-limited circuit. The more number of stacked NMOS devices in the gate-voltage-limited circuit results in the higher MM ESD level because the higher clamped gate voltage can further trigger on more fingers of GCNMOS during ESD stress. For the smaller

NMOS device dimension in the gate-voltage-limited circuit, it has larger turn-on resistance, resulting in the higher gate voltage to trigger on more fingers of GCNMOS during ESD stress. Therefore, under the same number of stacked NMOS devices, the NMOS devices with smaller device dimension in the gate-voltage-limited circuit result in the higher MM ESD level.

When the gate-voltage-limited circuit is composed of five stacked NMOS devices, the clamped gate voltage of GCNMOS during ESD stress is too high to overcome the over-gate-driven effect. Therefore, the MM ESD levels degrade again, except for the gate-voltage-limited circuit with the largest NMOS device dimension of 70 μm/0.35 μm. The gate-voltage-limited circuit with five stacked NMOS devices of 70 μm/0.35 μm can still protect GCNMOS from the over-gate-driven effect due to its lowest turn-on resistance to limit the over-coupled gate voltage on GCNMOS during ESD stress. For GCNMOS under HBM ESD stress which has slow ESD transition due to the 1.5-kΩ resistor in its discharging path, every GCNMOS (both with and without the gate-voltage-limited circuit) can pass 8-kV HBM ESD stress because the multiple fingers of GCNMOS with a large device dimension of 600 μm/0.35 μm can be uniformly triggered on by the gate-coupled design.

To further support the effectiveness of the gate-voltage-limited circuit on MM ESD levels shown in Fig. 3-12, failure analyses on these failed GCNMOS were carried out through the scanning electron microscope (SEM) images. Fig. 3-13 shows the ESD failure location of GCNMOS with gate-voltage-limited circuit, which consists of two stacked NMOS devices with each device dimension of 70 μm/0.35 μm. Because the over-gate-driven effect is overcome by the gate-voltage-limited circuit, the drain-substrate junction of the GCNMOS was damaged by MM ESD stress but its gate oxide is still intact.

When GCNMOS has five stacked NMOS devices with each device dimension of 20 μm/0.35 μm, its MM ESD level is degraded, as shown in Fig. 3-12. The SEM image shown in Fig. 3-14(a) indicates that the gate of this GCNMOS was damaged by the ESD current, supporting the interpretation that the over-gate-driven effect causes such ESD failure on this GCNMOS. The

image of its ESD failure location on the gate is enlarged in Fig. 3-14(b).

For GCNMOS with five stacked NMOS devices with each device dimension of 70 μm/0.35 μm, its MM ESD level is still increased, as shown in Fig. 3-12. The ESD failure on this GCNMOS has been found at the drain-substrate junction instead of its gate oxide, indicating that the over-gate-driven effect can still be overcome due to the lowest turn-on resistance of the NMOS string with larger device size. Fig. 3-15(b) shows the enlarged image of its ESD failure location on the drain contacts. From these visual evidences, the effectiveness of the gate-voltage-limited circuit has been strongly confirmed.

3.4.2 Clamping by Diode String

The other implementation of the gate-voltage-limited circuit in this work is with the diode string, composed of stacked diodes with different numbers and different device dimensions. The diode string has similar characteristics to that of the clamping NMOS string. The larger number of stacked diodes in the gate-voltage-limited circuit will cause the higher clamped gate voltage on GCNMOS during ESD stress. Turn-on resistance of the stacked diodes should be also finely tuned to control the gate voltage of GCNMOS during ESD stress.

The MM ESD levels of GCNMOS with different numbers or different device dimensions of stacked diodes are shown in Fig. 3-16. The larger number and the smaller device dimension of the stacked diodes in the diode string result in the higher MM ESD level, which has a higher coupled gate voltage to help the turn-on uniformity of GCNMOS. With the diode string, the highest MM ESD level of GCNMOS is 645 V, which is a 30% increase compared with that of GCNMOS without the gate-voltage-limited circuit. When the number of stacked diodes with device dimension of 25×25 μm^2 in the gate-voltage-limited circuit is increased up to 3, the MM ESD level becomes saturated, as shown in Fig. 3-16. This implies that somewhat over-gate-driven effect was initiated in the GCNMOS. If the diode device dimension is enlarged, the MM ESD level becomes increased again. So, the over-gate-driven effect can be successfully overcome by circuit

design technique without involving the process modification. The ESD robustness of GCNMOS can be optimized in different CMOS processes by the proposed circuit design technique.

3.5 CONCLUSION

The effectiveness and the characteristics of the proposed gate-voltage-limited circuit have been successfully verified. The new proposed ESD design method with the gate-voltage-limited circuit can successfully prevent the over-gate-driven effect and continually improve the ESD level of ESD protection circuits with the gate-coupled or gate-driven technique in the sub-quarter-micron CMOS processes. From the experimental results in a 0.35-μm CMOS process, a 30% increase of MM ESD robustness of GCNMOS has been achieved by adding the gate-voltage-limited circuit to the GCNMOS. The new proposed portable design method provides a high flexibility to realize the gate-voltage-limited circuit in different CMOS processes without process modification to save the fabrication cost of IC products.

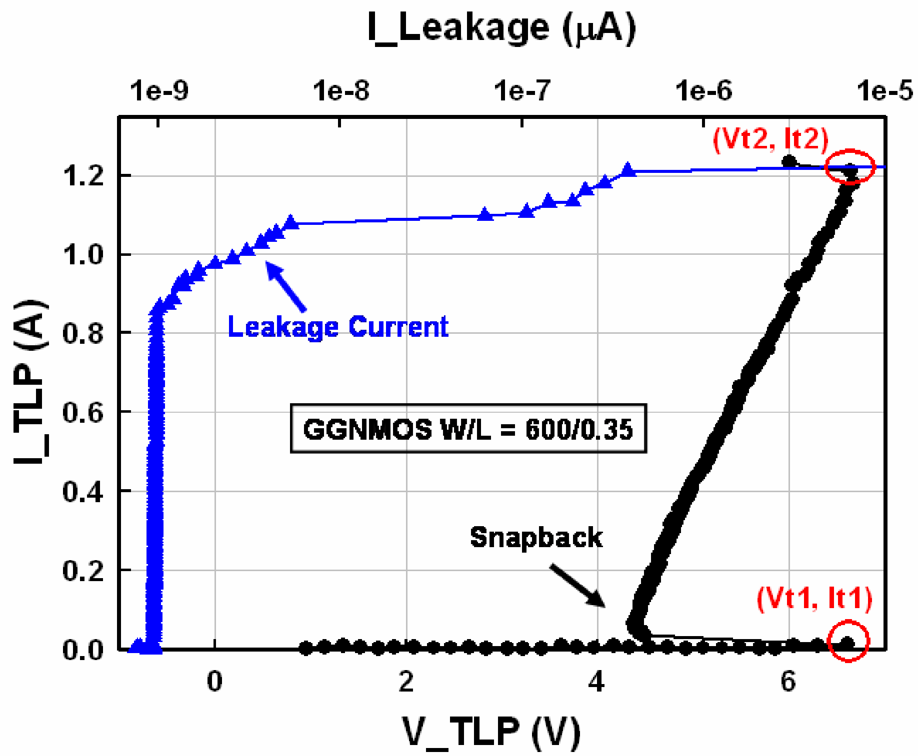

Fig. 3-1. The TLP-measured I-V characteristic of GGNMOS fabricated in a 0.35-μm CMOS technology.

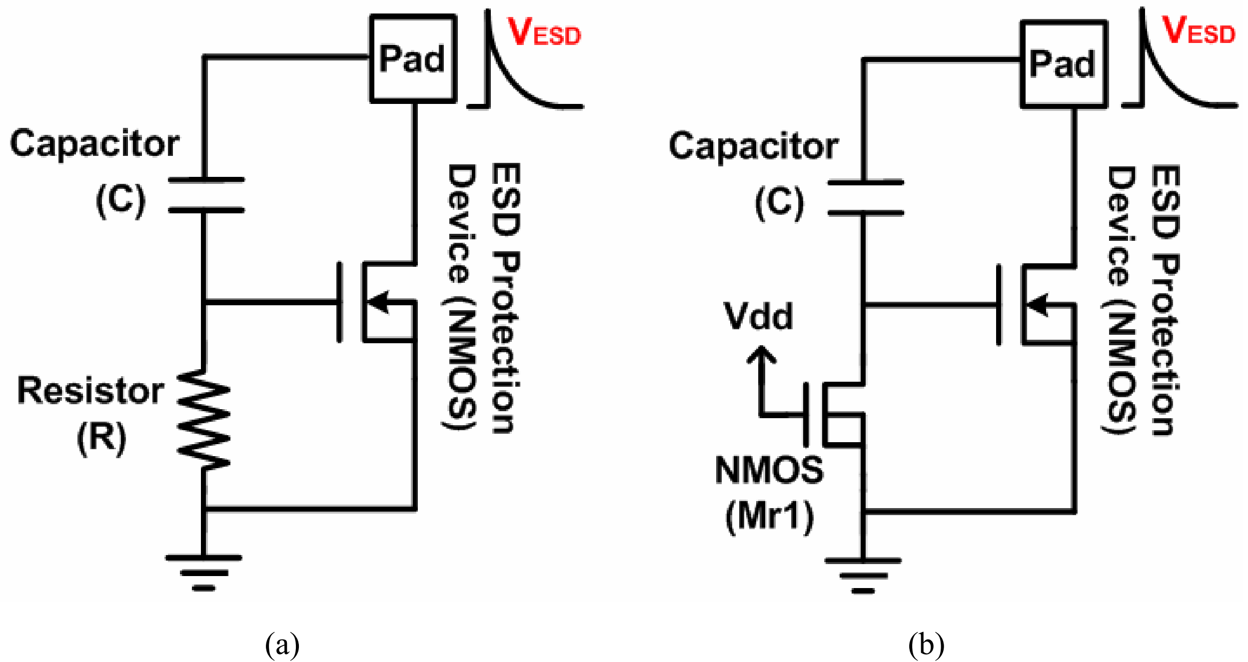

(a) (b)

Fig. 3-2. Two traditional circuit design methods to carry out the gate-coupled technique and to solve the non-uniform turn-on behavior in the ESD protection NMOS.

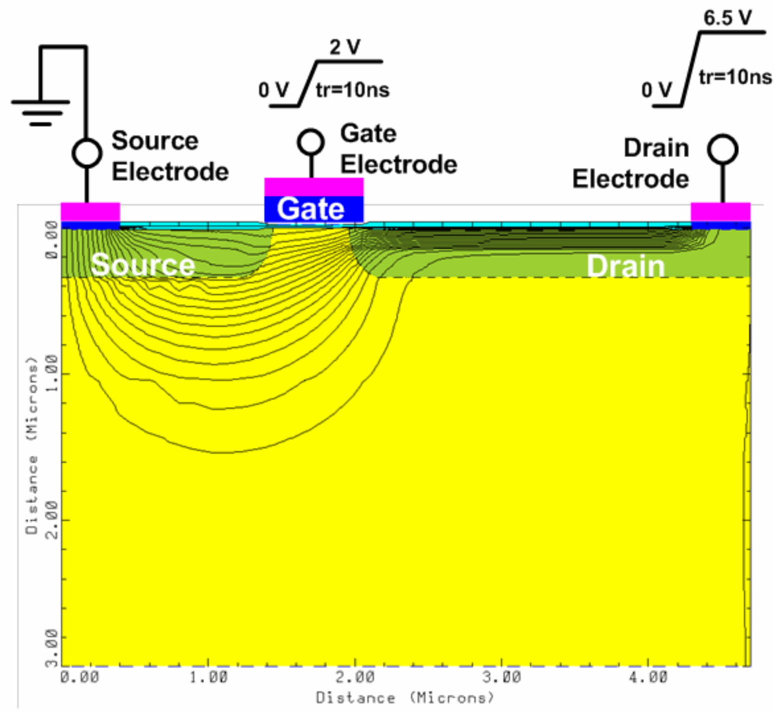

(a)

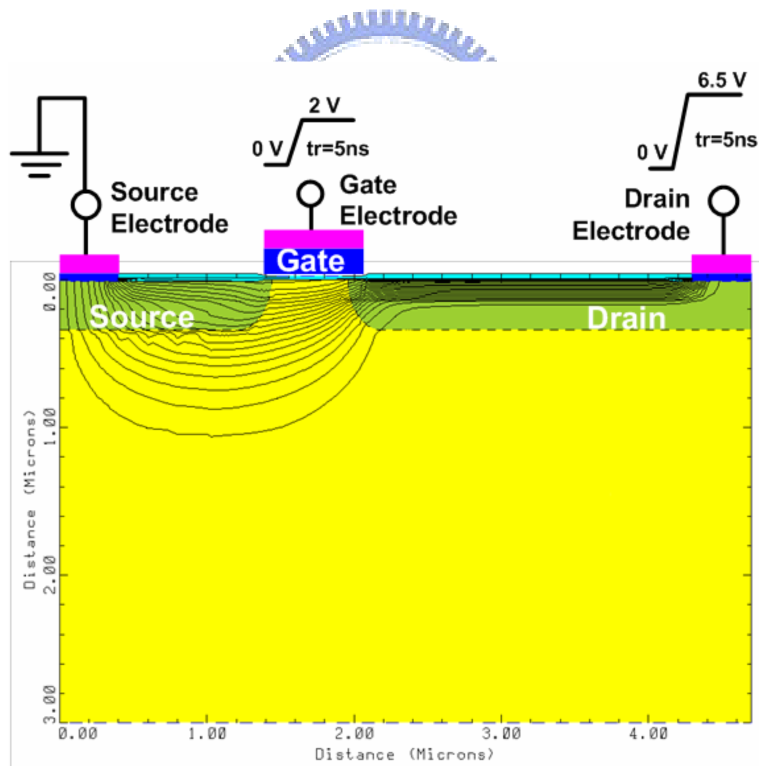

(b)

Fig. 3-3. The simulated current flow lines of NMOS with a bipolar trigger voltage of 5.7 V. Voltages applied to drain and gate electrodes are respectively ramped to 6.5 V and 2 V with simultaneous rise time of (a) 10 ns, and (b) 5 ns.

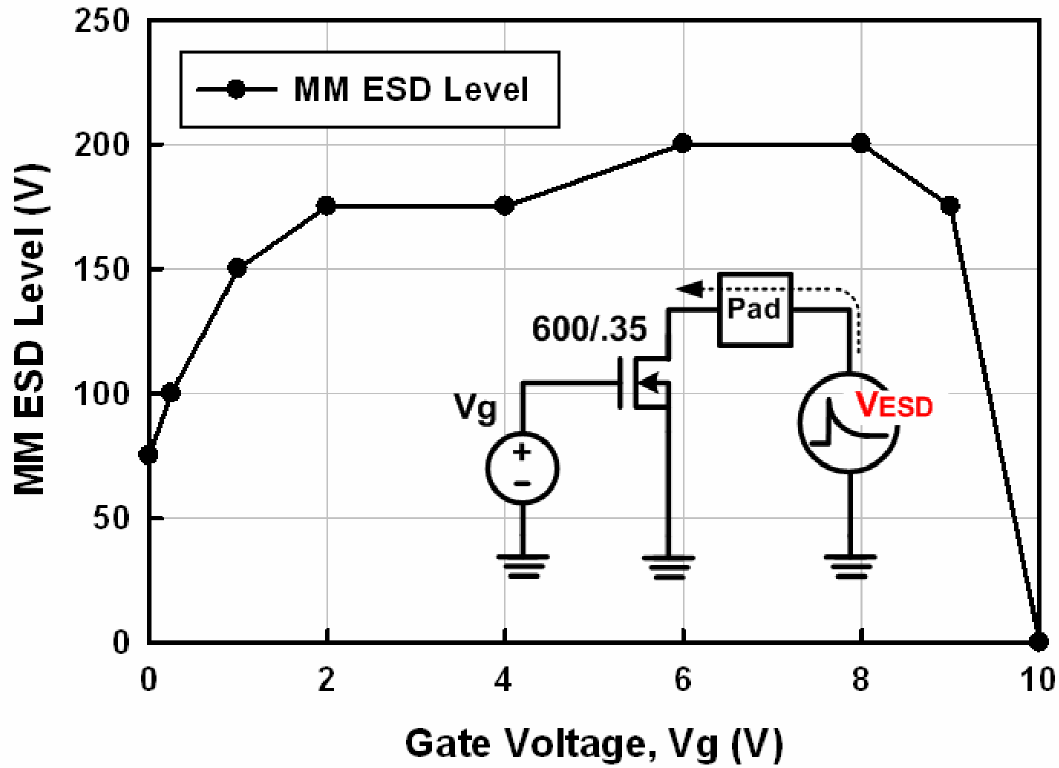

Fig. 3-4. MM ESD levels of NMOS (W/L= 600 μm/0.35 μm) under different gate voltages.

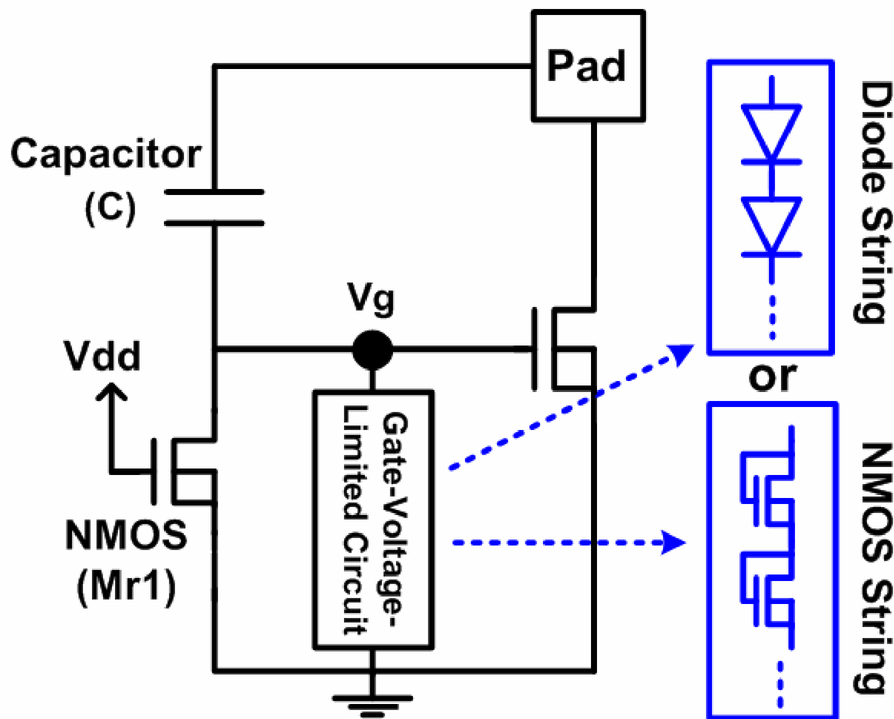

Fig. 3-5. A novel circuit design concept which can overcome the over-gate-driven effect for ESD protection circuits with gate-coupled or gate-driven technique.

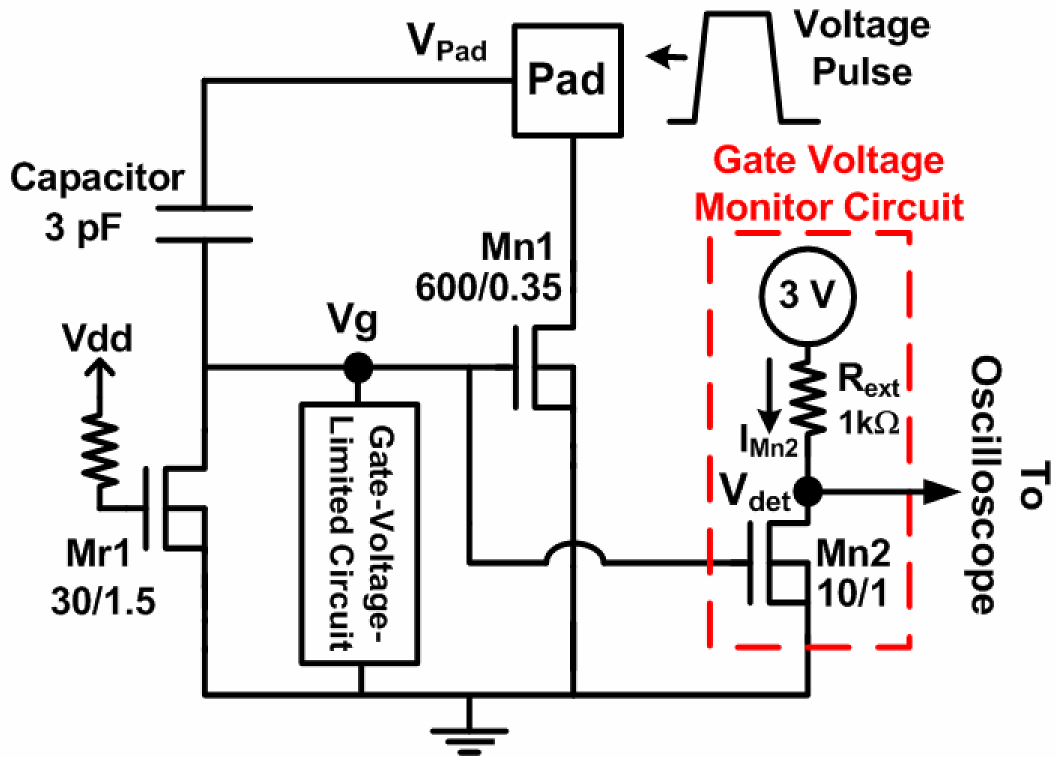

Fig. 3-6. The gate voltage monitor circuit added on-chip can monitor Vg of GCNMOS during ESD transition without affecting the quantity of coupled voltage on GCNMOS.

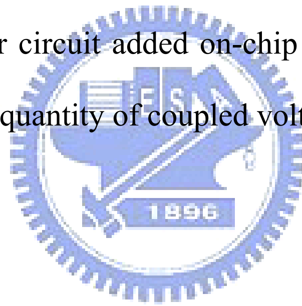

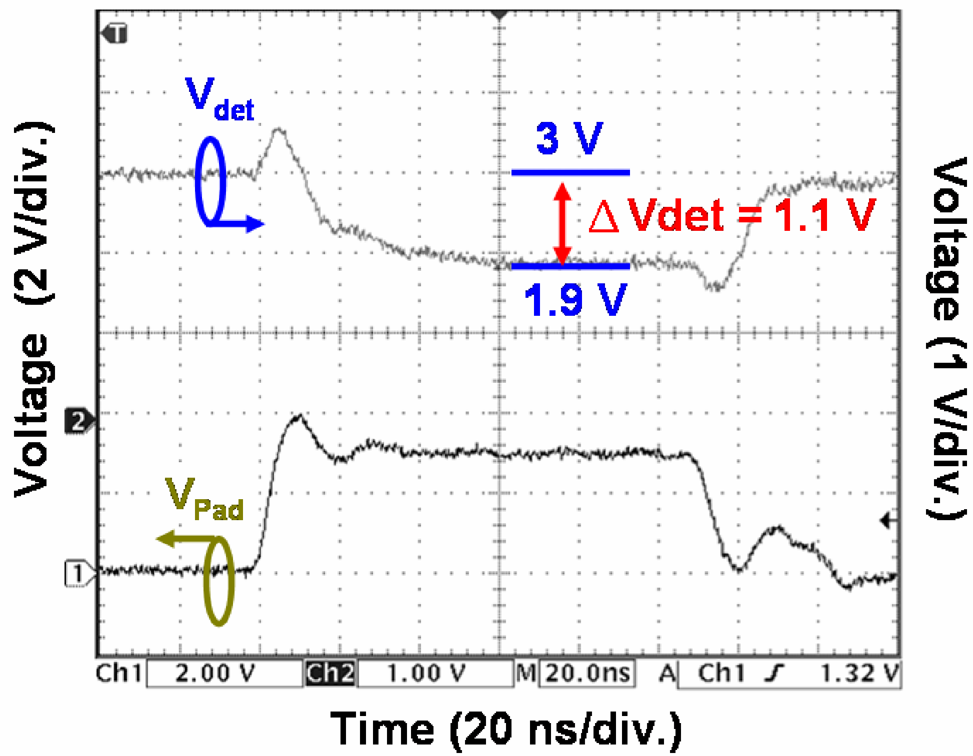

(a)

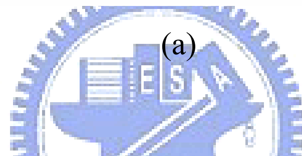

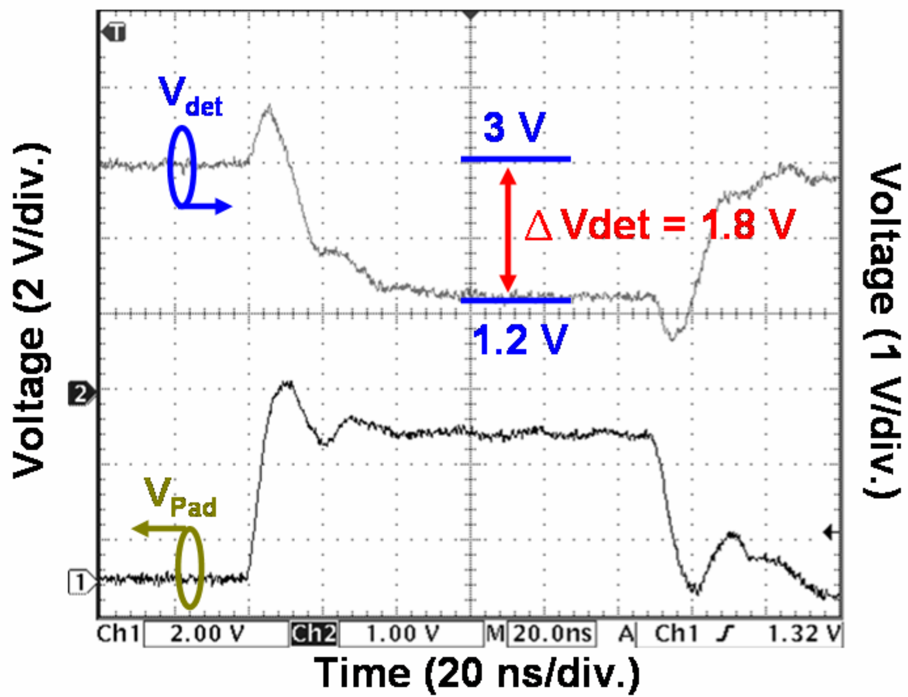

(b)

Fig. 3-7. The measured V_{det} voltages when (a) 10-V, and (b) 15-V, voltage pulse with a rise time of 10 ns is applied to the GCNMOS without gate-voltage-limited circuit.

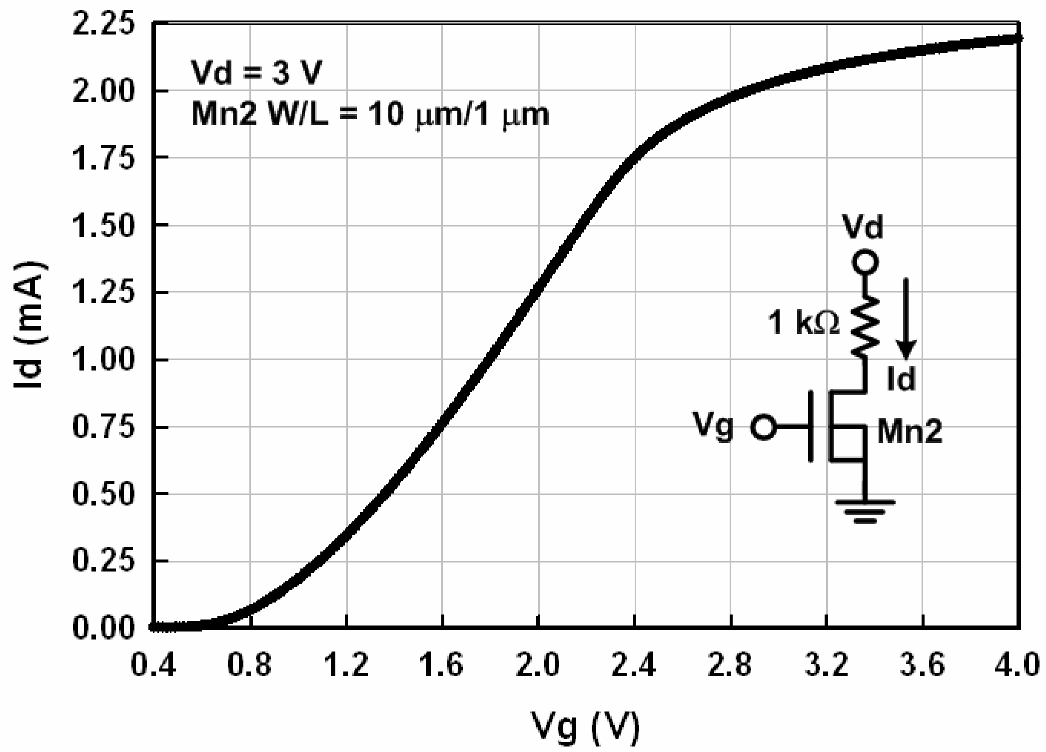

Fig. 3-8. Id-Vg curve of the gate voltage monitor circuit in a 0.35-μm CMOS process.

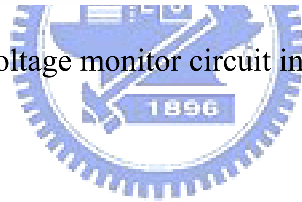

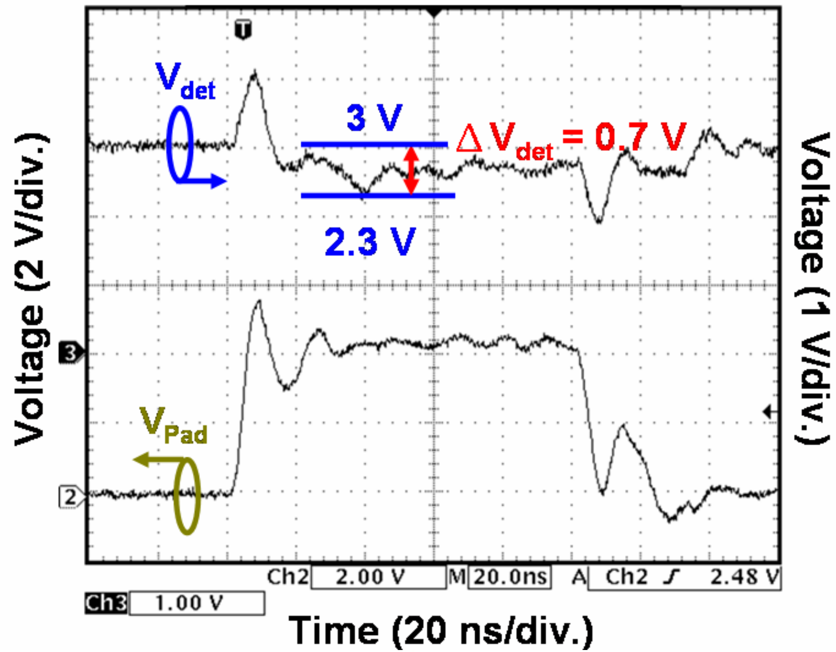

(a)

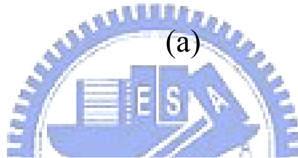

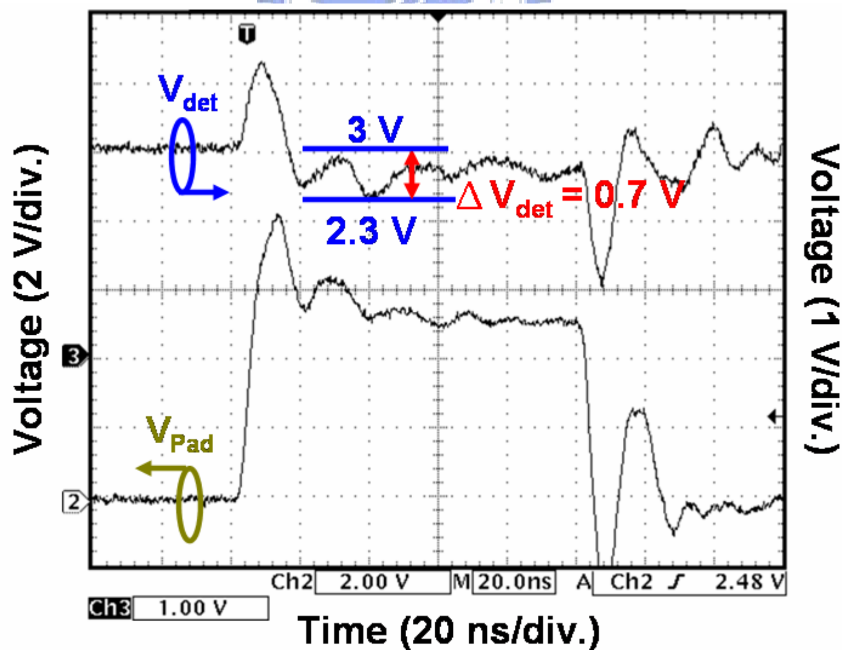

(b)

Fig. 3-9. The measured V_{det} voltages when (a) 10-V, and (b) 20-V, voltage pulse with a rise time of 10 ns is applied to the GCNMOS with two stacked NMOS devices in the gate-voltage-limited circuit. Each stacked NMOS has a device dimension (W/L) of 50 μm/0.35 μm.

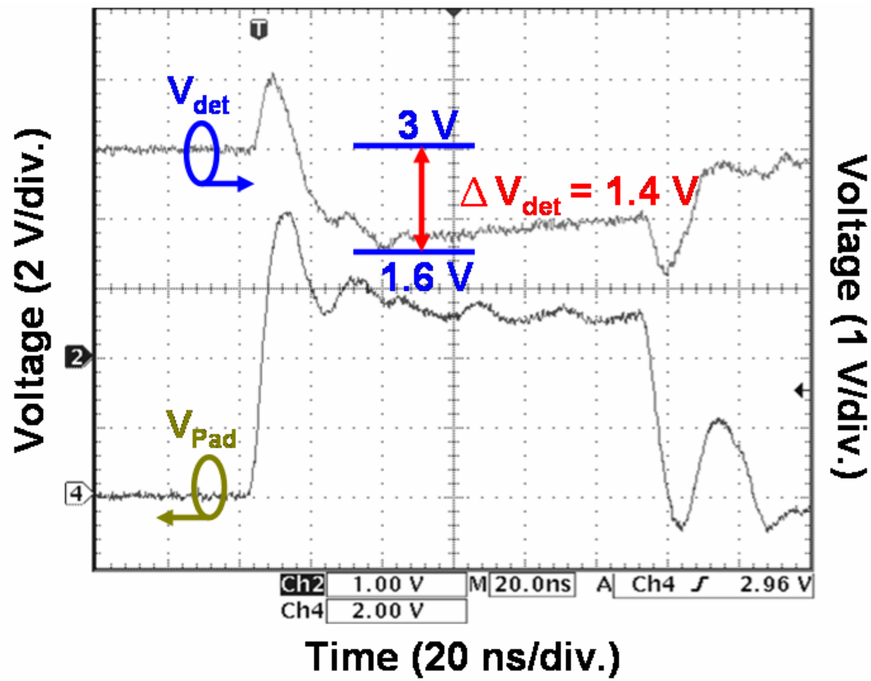

(a)

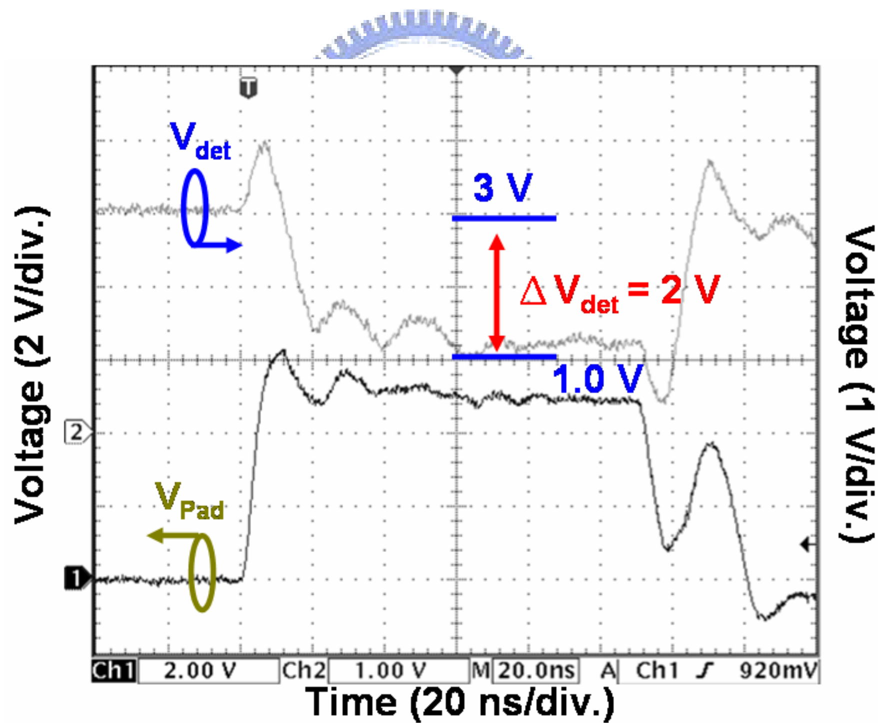

(b)

Fig. 3-10. The measured V_{det} voltages when the 20-V voltage pulse with a rise time of 10 ns is applied to GCNMOS with (a) three, and (b) five, stacked NMOS devices in the gate-voltage-limited circuit. Each stacked NMOS has a device dimension (W/L) of 50 μm/0.35 μm.

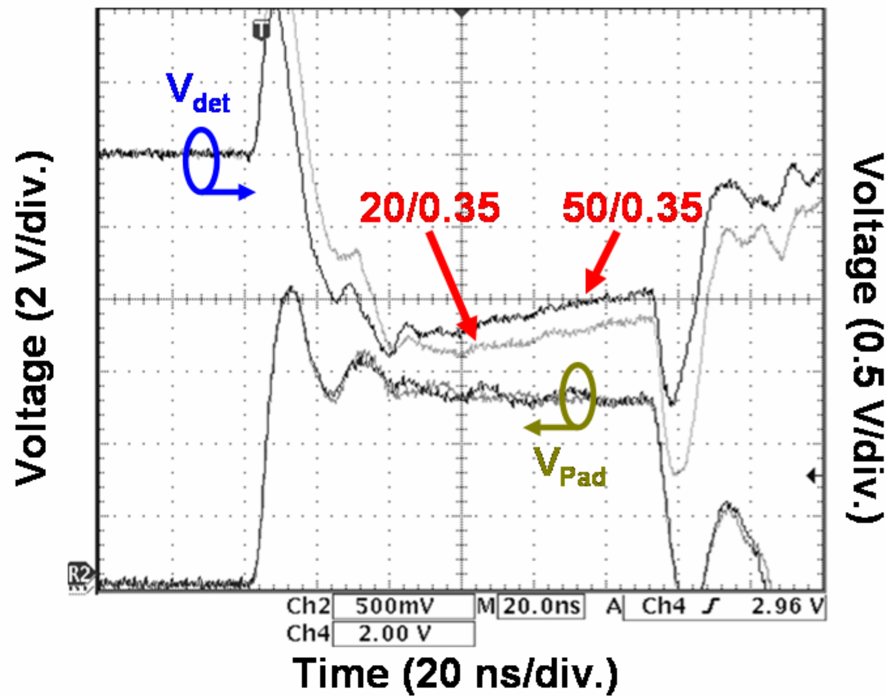

Fig. 3-11. The measured V_{det} voltages when 20-V voltage pulses with rise time of 10 ns are applied to GCNMOS with two different gate-voltage-limited circuits. One consists of three stacked NMOS devices with each device dimension (W/L) of 20 μm/0.35 μm, the other consists of three stacked NMOS devices with each device dimension of 50 μm/0.35 μm.

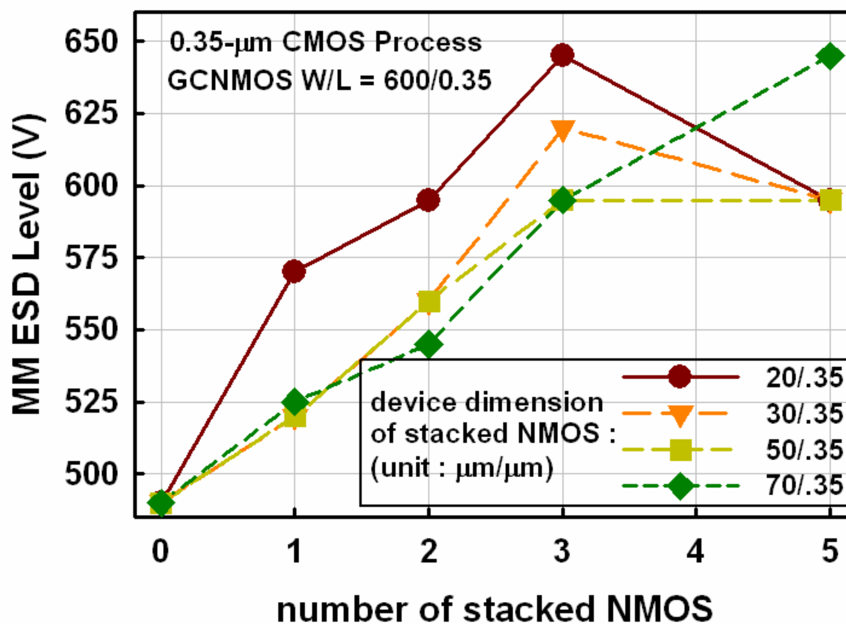

Fig. 3-12. MM ESD levels of the GCNMOS with different numbers or different device dimensions of stacked NMOS devices in the gate-voltage-limited circuit.

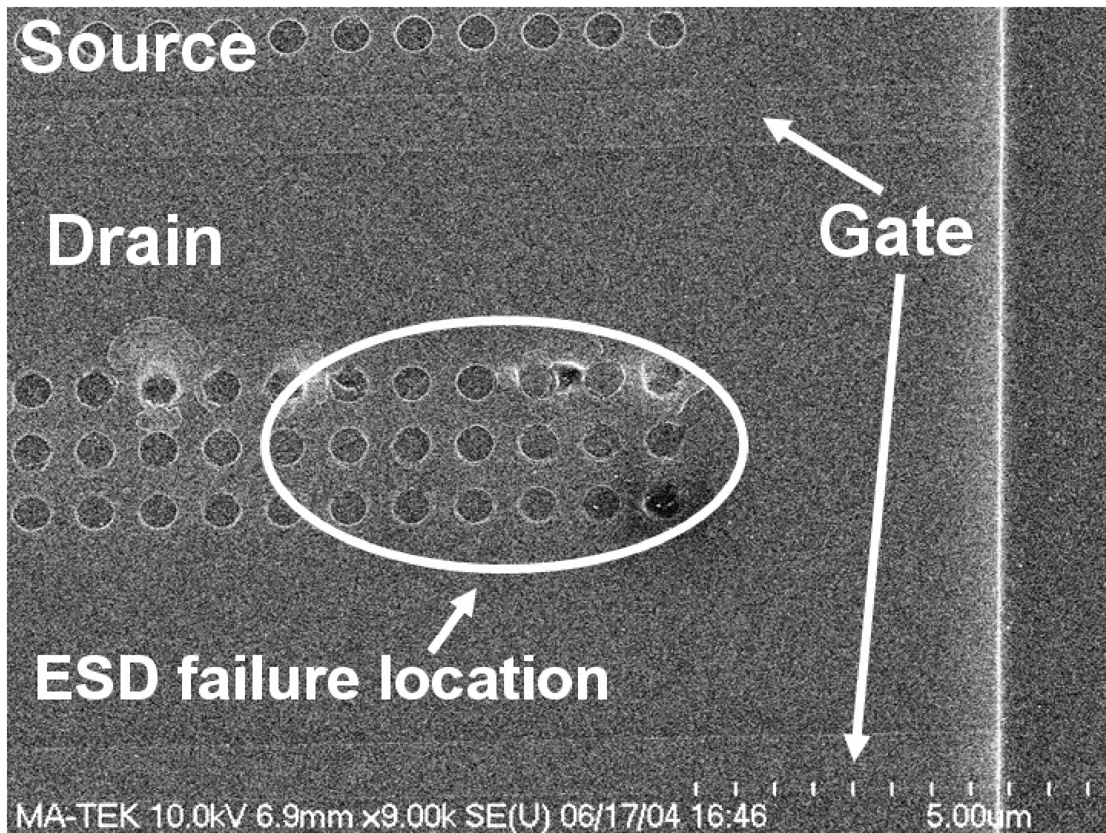

Fig. 3-13. SEM image of the GCNMOS with two stacked NMOS devices in the gate-voltage-limited circuit after 550-V MM ESD stress. Each stacked NMOS has device dimension (W/L) of 70 μm/0.35 μm.

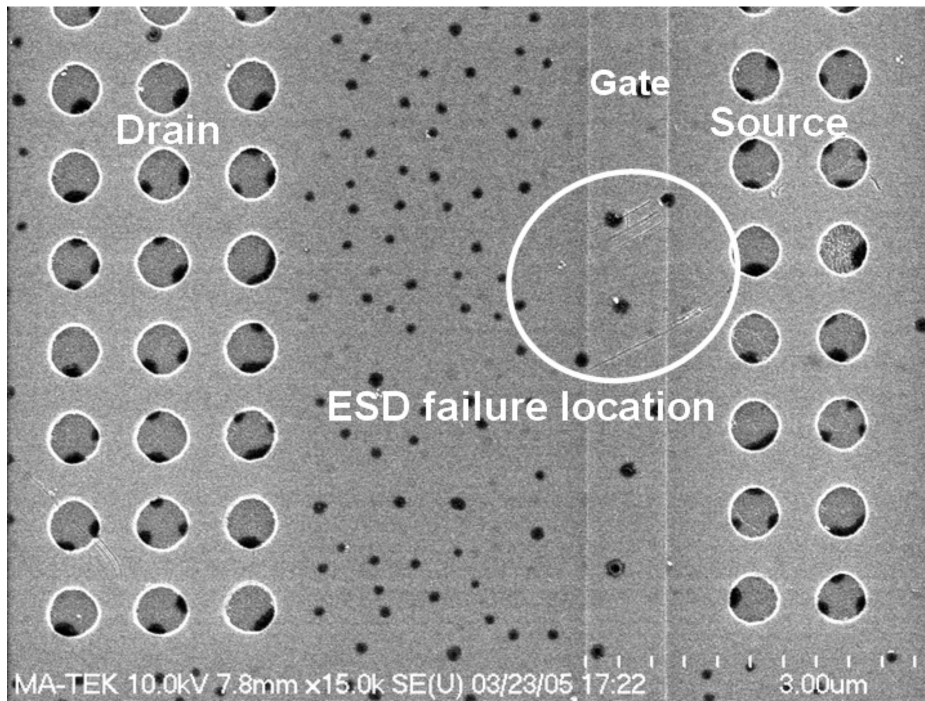

(a)

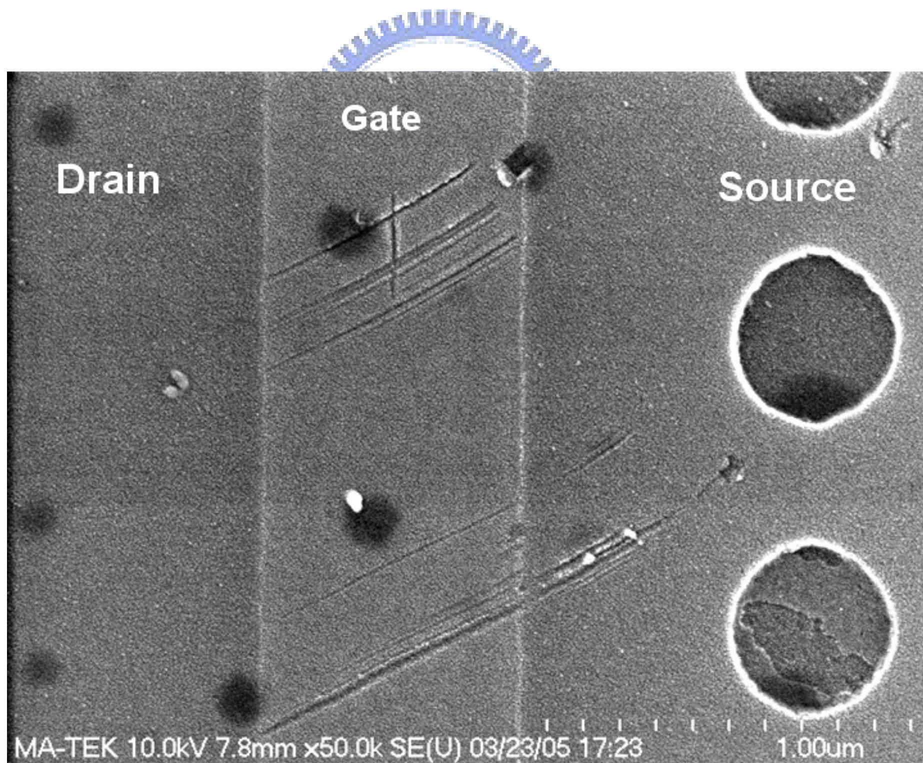

(b)

Fig. 3-14. SEM image of (a) the GCNMOS with five stacked NMOS devices in the gate-voltage-limited circuit after 600-V MM ESD stress. Each stacked NMOS has device dimension (W/L) of 20 μm/0.35 μm. (b) The enlarged image of its ESD failure location.

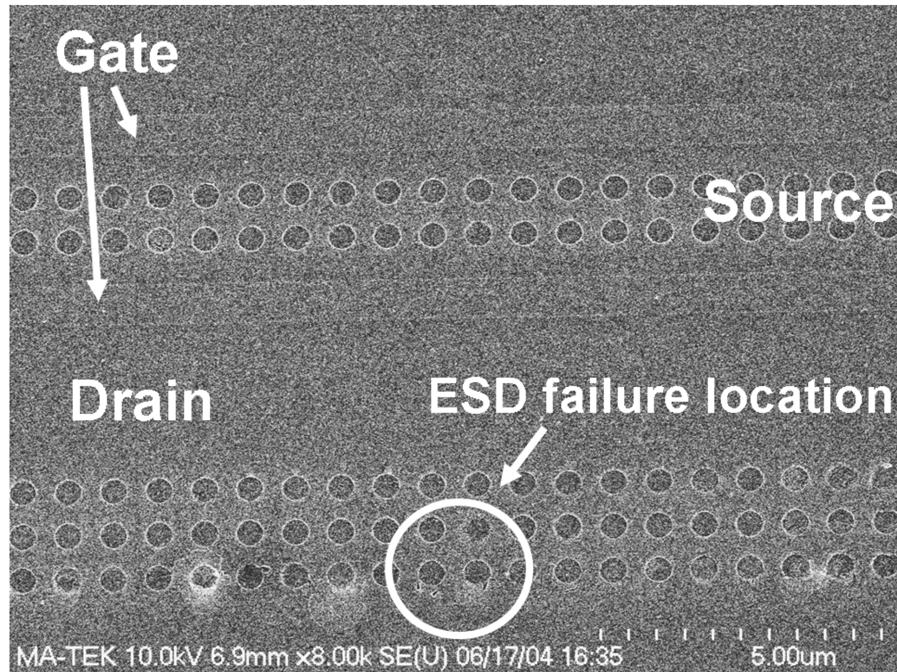

(a)

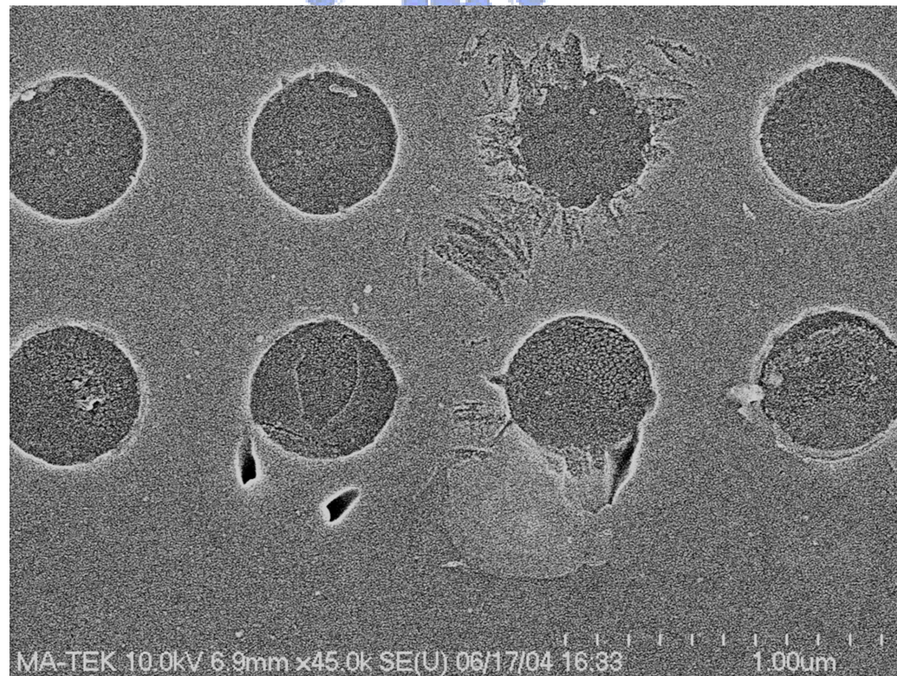

(b)

Fig. 3-15. SEM image of (a) the GCNMOS with five stacked NMOS devices in the gate-voltage-limited circuit after 650-V MM ESD stress. Each stacked NMOS has device dimension (W/L) of 70 μm/0.35 μm. (b) The enlarged image of its ESD failure location.

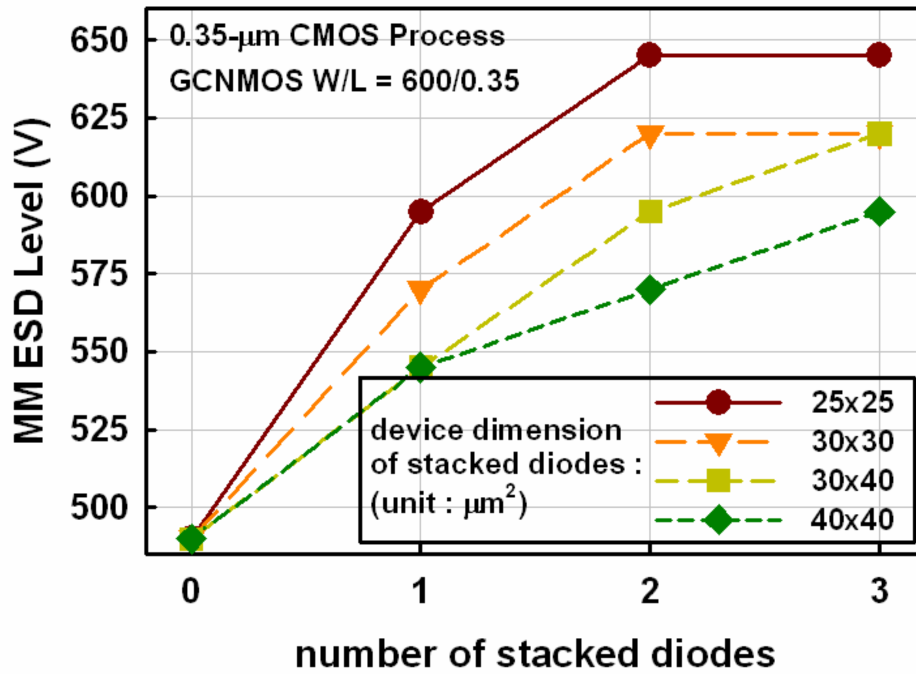

Fig. 3-16. MM ESD levels of the GCNMOS with different numbers or different device dimensions of stacked diodes in the gate-voltage-limited circuit.

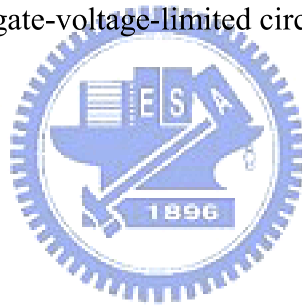

Chapter 4

Design on Power-Rail ESD Clamp Circuit for 3.3-V I/O Interface By Using Only 1-V/2.5-V Low-Voltage Devices in a 130-nm CMOS Process

4.1 INTRODUCTION

When CMOS technologies are scaled down toward nanometer generation, the power supply voltage is also decreased as well to reduce the power consumption. However, some peripheral components or other ICs on the system board are still operated with the higher voltage levels such as 3.3V to meet the system specification. Therefore, the mixed-voltage I/O design is needed for the interface of semiconductor chips or sub-systems with different power-supply voltages [30]-[32]. In such mixed-voltage I/O interfaces, the ESD protection circuits are requested to be designed with only low-voltage devices of a given technology without suffering the gate-oxide reliability issue [33], [34]. To achieve a good whole-chip ESD protection scheme for the mixed-voltage I/O applications, it is required to design the power-rail ESD clamp circuit with only low-voltage devices that can sustain the high power-supply voltage without suffering the gate-oxide reliability issue [35]. Besides the gate-oxide reliability issue, the standby leakage current of the power-rail ESD clamp circuit during normal circuit operating conditions is another concern [36], especially for the portable electronic products. Thus, how to design a turn-on-efficient power-rail ESD clamp circuit with only low-voltage devices to sustain the high-voltage input signals or the high power-supply voltages becomes a quite significant challenge to the nano-scale mixed-voltage CMOS ICs.

In this work, a novel power-rail ESD clamp circuit implemented with only 1-V/2.5-V NMOS/PMOS devices is proposed for application in the 3.3-V I/O interfaces without suffering the

gate-oxide reliability issue [12]. This new power-rail ESD clamp circuit has an efficient ESD detection circuit to trigger on the ESD clamp device, so that the turn-on efficiency of the power-rail ESD clamp device can be substantially increased. The proposed power-rail ESD clamp circuit has been successfully verified in a 130-nm 1-V/2.5-V CMOS process with excellent ESD protection capability and extremely low standby leakage current.

4.2 ESD PROTECTION SCHEME FOR 1-V/3.3-V MIXED-VOLTAGE I/O INTERFACE

4.2.1 ESD Protection Scheme

For the mixed-voltage I/O applications, there are separated power lines with different power supply voltages. So, the internal circuits of mixed-voltage ICs are more easily damaged under the pin-to-pin ESD stress. As a result of different power supply voltages, some ESD protection techniques for ICs with separated power lines, such as the bi-directional back-to-back diodes [37], are not applicable. Therefore, the dummy supply ESD bus has been proposed [38], which is an effective method to quickly discharge the ESD current away from the internal circuits, especially under the pin-to-pin ESD stress.

Two modified successful whole-chip ESD protection schemes for 1-V/3.3-V mixed-voltage I/O interfaces are shown in Figs. 4-1(a) and 4-1(b) [39]-[41]. In Fig. 4-1(a), an extra dummy supply line (marked as V_{ESD}) is added into the chip for cooperation with the power-rail ESD clamp circuit to achieve ESD protection in the I/O pad with 3.3-V input signals. The ESD current at I/O pads under positive-to-VSS (PS-mode) ESD stress is discharged through the diode D1 and the power-rail ESD clamp circuit between V_{ESD} and VSS power lines. For positive-to-VDD (PD-mode) ESD stress on I/O pads, the ESD current can be discharged through the diode D1, the power-rail ESD clamp circuit between V_{ESD} and VSS power lines, and then the parasitic diode of the power-rail ESD clamp circuit between the VDD_h and the VSS power lines (the active clamp between VDD_l and VSS) to the

grounded VDD_h (VDD_l). For VDD_h-to-VDD_l ESD stress, the ESD current is discharged through the diode D4, the power-rail ESD clamp circuit between the V_{ESD} and the VSS power lines, and then the parasitic diode of the active clamp between VDD_l and VSS power lines.

The whole-chip ESD protection scheme shown in Fig. 4-1(a) can be applied to the ICs with power-down mode circuit operation [41], which is an important power-saving technology in nowadays SOC or portable devices. The diode D4 between the VDD_h power line and the V_{ESD} dummy supply line can prevent the circuit, which has entered the power-down mode, being awakened by the input signal at I/O pads. For generic ICs without specific circuit functions such as the power-down mode operation, the whole-chip ESD protection scheme shown in Fig. 4-1(a) can be further simplified to Fig. 4-1(b). In Fig. 4-1(b), the extra bond pad for external 3.3-V power supply (marked as VDD_h) is optional, depending on the system specification and the circuit requirement. For circuits without external 3.3-V power supply pins, the VDD_h line shown in Fig. 4-1(b) can be treated as a dummy supply line and the extra bond pad is dispensable.

In these successful designs, the power-rail ESD clamp circuits must sustain the high-voltage (3.3-V) stress in the mixed-voltage I/O interfaces during normal circuit operating conditions without the gate-oxide reliability issue. About the active clamp for the internal circuits shown in Figs. 4-1(a) and 4-1(b), it can be realized by the traditional RC-based ESD detection circuits with 1-V devices [18].

4.2.2 Review on High-Voltage-Tolerant Power-Rail ESD Clamp Circuit

With the increasing demand for the mixed-voltage I/O interface circuits, several prior arts about the high-voltage-tolerant power-rail ESD clamp circuits had been reported, such as the diode string, the stacked-PMOS clamp with voltage divider, and the stacked-NMOS configuration [33]-[35], [42]-[45]. Because the forward-biased p-n junction diode can sustain quite high ESD current without the gate oxide reliability issue, the diode string with multiple stacked diodes had been developed to protect the mixed-voltage I/O [45], or as the power-rail ESD clamp circuit [42]-[44].

However, the main disadvantage of using the forward-biased stacked diodes as the power-rail ESD clamp circuit is the huge standby leakage current. Fig. 4-2 shows the leakage current path of a forward-biased diode string in a common p-type substrate. Each diode structure and the grounded p-substrate form a parasitic p-n-p bipolar junction transistor (BJT). Although the total cut-in voltage of the diode string can be increased by increasing the number of stacked diodes, these parasitic p-n-p BJTs still provide a leakage current path I_{LEAK} under normal circuit operating conditions. The Darlington beta gain makes the leakage current of the parasitic BJTs increase dramatically at high operating temperature [46]. To reduce the leakage current of the diode string, especially for ICs operating under the high temperature condition, some modified designs, such as the Cladded diode string, Boosted diode string, and Cantilever diode string, were reported in [43]. An improved design by using SCR device to stop the leakage current through the diode string was also reported to achieve an ultra low leakage level in the high temperature condition [46].

Since the gate-oxide reliability issue results from the over-induced electric field across the gate-drain, gate-source, and gate-bulk terminals of MOSFET devices, the voltage divider that divides the high power-supply voltage (Vcc) to be 1/3Vcc or 2/3Vcc is incorporated to some of the ESD protection circuits to reduce the voltage across the gate-drain, gate-source, and gate-bulk terminals [35]. The voltage divider is useful to avoid the gate-oxide reliability issue but the divider itself provides a standby current path from the power supply to ground, causing leakage current in the order of several micron-amps. In [35], the leakage current of the stacked-PMOS ESD protection circuit under 25°C (125°C) and 3.3-V power supply voltage is roughly 0.8μA (8μA), which could be still too large for most portable microelectronic products and low-power IC products.

Another well-known and widely used high-voltage-tolerant structure is the stacked-NMOS configuration [33], where the top gate of the stacked-NMOS is biased at a relatively low voltage to drop the drain voltage of the bottom NMOS and to safely meet the reliability limitation during normal circuit operating conditions. Unfortunately, the stacked-NMOS has been found to have

some disadvantages of ESD protection capability, including the non-uniform turn-on behaviors, slower turn-on speed, and the lower ESD robustness. Therefore, to uniformly and quickly turn on the stacked-NMOS in the mixed-voltage I/O buffers under ESD stress conditions, some ESD detection circuits are therefore developed to trigger the stacked-NMOS [47], [48]. In this work, a novel low-leakage power-rail ESD clamp circuit, which contains a high-voltage tolerant ESD detection circuit to substantially increase the ESD protection efficiency of stacked-NMOS, is proposed.

4.3 Novel Power-Rail ESD Clamp Circuit for High-Voltage Applications

The novel power-rail ESD clamp circuit which contains ESD clamp device and ESD detection circuit is shown in Fig. 4-3, where the ESD clamp device is realized by a substrate-triggered stacked-NMOS (STNMOS). The new proposed power-rail ESD clamp circuit is realized with only 1-V and 2.5-V devices to operate at 3.3-V I/O interface without the risk of gate oxide reliability. Under normal circuit operating conditions, the ESD detection circuit is inactive and doesn't interfere with the functions of internal circuits. But, it is active to provide the substrate-triggered current to quickly trigger on the STNMOS device under ESD stress conditions. The STNMOS is formed by two stacked NMOS transistors with 2.5-V gate oxide in the 130-nm 1-V/2.5-V CMOS process. The gate of the top NMOS transistor of STNMOS is biased at VDD_l of 1V through a resistor, and that of the bottom NMOS transistor is directly connected to VSS. The voltage level at the shared N+ diffusion region between the top and bottom NMOS transistors of STNMOS device will be kept at VDD-Vth during normal circuit operating conditions, where Vth is the threshold voltage of the 2.5-V NMOS transistor. Therefore, the STNMOS is free from the gate-oxide reliability issue under high power-supply voltage VDD_h of 3.3V. The ESD detection circuit is formed by Mp1, Mp2, and C of 2.5-V PMOS devices, Mn1 of 1-V NMOS device, Mn2 of 2.5-V NMOS device, an N-Well

resistor R1, and a poly resistor R2. The selected device dimensions of the proposed ESD detection circuit in this work is listed in Table 4.1.

4.3.1 Circuit Operation under Normal Power-on Transition

When the 3.3-V VDD_h and 1-V VDD_l have been powered on, the gate of Mp1 (node 1 in Fig. 4-3) is biased at 3.3V through the resistor R1, and the gate of Mp2 is biased at 1V through the resistor R2 of 1kΩ. With a gate-to-source bias of 0V, the Mp1 should be kept off. With a gate-to-source bias of 1V, the Mn1 is turned on. So, no trigger current will be generated from the ESD detection circuit into the trigger node (node 3 in Fig. 4-3) of the STNMOS. The turned-on Mn1 can guarantee the off-state of STNMOS during normal circuit operating conditions. Because the gate of Mp2 is biased at VDD_l through the resistor R2, the drain voltage of Mp1 (node 2 in Fig. 4-3) is kept at (1V+|Vtp|), where Vtp is the threshold voltage of the 2.5-V PMOS transistor. By such arrangement, all low-voltage devices in the new proposed power-rail ESD clamp circuit are free from the gate-oxide reliability issue under normal circuit operating conditions with VDD_h of 3.3V in the mixed-voltage I/O interfaces. Fig. 4-4 shows the Hspice-simulated voltages on nodes of the ESD detection circuit. In this simulation, the VDD_h and VDD_l are respectively powered-on to 3.3V and 1V with a simultaneous rise time of 1ms. The Hspice-simulated results show that the voltages across the gate-drain, gate-source, and gate-bulk terminals of every device do not exceed the process limitation. Moreover, the gate voltage of PMOS Mp1 in the ESD detection circuit with the selected R1-C value can follow up the power-on transition of VDD_h to turn off the PMOS Mp1.

4.3.2 Circuit Operation under ESD Transition

When ESD transient voltage is applied to VDD_h with VSS relatively grounded, the gate of Mp1 (node 1 in Fig. 4-3) is initially kept at a low voltage level (around 0V) due to the RC delay of R1 and C in the ESD detection circuit. The VDD_l node is initially floating with an initial voltage level of

0V, before the ESD voltage is applied across VDD_h and VSS. Some ESD transient voltage would be coupled to VDD_l through the parasitic capacitance when ESD stress is zapped on VDD_h, but the R2 and the parasitic capacitance at the gates of Mn1 and Mp2 will keep the gate of Mp2 at 0V for a long time period. So, Mp1 and Mp2 with initial gate voltages at ~0V can be quickly turned on by the ESD energy to generate the trigger current into the trigger node (node 3 in Fig. 4-3) of STNMOS. As long as the base-emitter voltage of the lateral n-p-n BJT inherent in the STNMOS device is greater than its cut-in voltage of ~0.7V, the STNMOS can be triggered on to discharge ESD current from VDD_h to grounded VSS. Fig. 4-5 shows the Hspice-simulated voltages and current of the ESD detection circuit under ESD transition. A 0-to-7V ESD-like voltage pulse with rise time of 10ns is applied to the VDD_h to simulate the ESD transition before junction breakdown on the devices. The Hspice-simulated results show that the gate voltage of Mp1 is kept low due to the time delay of R1 and C. The PMOS Mp1 and Mp2 can provide the substrate-triggered current larger than 60mA within 10ns when the 0-to-7V transient voltage is applied to VDD_h. By selecting the device dimensions, the substrate-triggered current can be designed to meet different applications or specifications. The time constant of R1 and C should be designed around the order of ~ 1μs to distinguish the power-on transition (with a rise time of several milliseconds) from the ESD transition (with a rise time of several nanoseconds) [18].

If Mn1 is turned on during ESD transition by unexpected coupling effect to its gate through the parasitic capacitance in the layout, the base voltage of the lateral BJT could be pulled down to zero to turn off the lateral BJT in the STNMOS device. To avoid such possible condition during ESD transition, the Mn2 is added in the ESD detection circuit to keep the gate of Mn1 and Mp2 at 0V, when the base voltage of lateral BJT in the STNMOS device is charged up by the current flowing through Mp1 and Mp2.

4.4 EXPERIMENTAL RESULTS

The proposed power-rail ESD clamp circuit has been designed and fabricated in a 130-nm 1-V/2.5-V CMOS process. The stand-alone STNMOS with the same device dimension and layout has been also fabricated in the same chip for reference. In the test structures, all the STNMOS devices are salicide-blocked whereas all the ESD detection circuits are fully salicided. The snapback I-V characteristic curve of a stand-alone STNMOS device with 2.5-V gate oxide is measured by Tek370 curve tracer and shown in Fig. 4-6. The measured 2.5-V STNMOS has a bipolar trigger voltage (Vt1) of 11.7V and a holding voltage larger than the high power-supply voltage (3.3V). Therefore, the stand-alone STNMOS is not a good power-rail ESD clamp device due to its high bipolar trigger voltage. In this section, the experimental results will show that the new proposed ESD detection circuit can effectively lower the Vt1 and substantially increase the ESD robustness of STNMOS. Moreover, the experimental results also show that the proposed ESD detection circuit can successfully distinguish the normal power-on transition and the ESD transition. Therefore, ICs with the new proposed high-voltage-tolerant power-rail ESD clamp circuit have no risk of latch-up issue.

1896

4.4.1 Standby Leakage Current

To save the power consumption of portable devices or low-power applications, especially chips that are driven by small batteries, the standby leakage current becomes one of major concerns [36]. The measured leakage currents of the fabricated power-rail ESD clamp circuit under different temperatures are shown in Fig. 4-7, where the STNMOS is drawn with a device dimension (W/L) of 300μm/0.3μm. Under normal circuit operating conditions with VDD_l of 1V and temperature of 25°C, the leakage current of the power-rail ESD clamp circuit at VDD_h of 3.3V is 283pA, whereas the leakage current of the stand-alone STNMOS is 153pA. If the temperature is increased to 125°C, the leakage current of the power-rail ESD clamp circuit (the stand-alone STNMOS) is

increased to 19.8nA (11.3nA) under VDD_h of 3.3V. With a leakage current of ~20 nA under the temperature of 125°C, it is quite small as comparing to those of the prior arts. Table 4.2 summarizes the comparison on the leakage current between the new proposed power-rail ESD clamp circuit and the prior arts [35], [46]. In [35], the ESD clamp device, stacked-PMOS, has a total device width of 4000μm to get a high ESD robustness at the cost of ~8μA standby leakage current and larger silicon area. From the viewpoint of leakage current per silicon area of ESD clamp devices, the new proposed design of this work is superior to those of the prior arts in the aspect of standby leakage current. In [43], diode strings were fabricated on p-substrate with epitaxial layer, which can suppress the beta gain of parasitic BJT and therefore reduce the overall leakage current of diode strings. However, epitaxy is a quite costly process step, so that most consumer IC products are not fabricated on epitaxial substrate if they have to compromise with their costs. Therefore, diode strings fabricated on a 0.35-μm CMOS process without epitaxial layer in [46] is compared with the proposed design of this work instead of diode strings in [43]. Comparing to the prior arts, this new proposed power-rail ESD clamp circuit has no standby current path in the voltage divider circuits from high-voltage power supply to ground, so that it has very small leakage current in the order of ~nA under high temperature condition.

4.4.2 Turn-on Verification

One of the main benefits of the new proposed power-rail ESD clamp circuit is to enhance the turn-on speed of ESD clamp device (STNMOS) during ESD stress conditions. The turn-on speed of the STNMOS device with or without ESD detection circuit is measured in Fig. 4-8, where a voltage pulse with pulse height of 20V and rise time of 10ns is applied to the VDD_h. The time to clamp the 20-V voltage pulse to the holding voltage level (~5.8V) by the stand-alone STNMOS device is about ~20ns, as shown in Fig. 4-8. Moreover, the overshooting peak voltage of the stand-alone STNMOS in Fig. 4-8 is about ~13V, which could be higher than the gate-oxide breakdown voltage of the low-voltage devices in the internal circuits. On the contrary, the 20-V

voltage pulse can be quickly clamped by the STNMOS with ESD detection circuit to a low voltage level without overshooting. This result verifies that the turn-on speed of the STNMOS can be indeed improved by the proposed ESD detection circuit. The clamped voltage level will be limited by the snapback holding voltage of the STNMOS device, after the lateral n-p-n BJT in the STNMOS device is triggered on by the ESD detection circuit. From the measured voltage waveforms in Fig. 4-8, the excellent turn-on efficiency of the new proposed power-rail ESD clamp circuit has been successfully verified. Therefore, the internal circuits can be effectively protected by the new proposed power-rail ESD clamp circuit in cooperation with the whole-chip ESD protection schemes shown in Fig. 4-1.

To verify the effectiveness of the ESD detection circuit in the proposed power-rail ESD clamp circuit, a measurement setup is shown in the inset of Fig. 4-9 to observe the substrate-triggered current. In the specially drawn testchip, the output node of a stand-alone ESD detection circuit is also connected to another pad. The substrate trigger node of a stand-alone STNMOS is connected to a pad. In the circuit board, the output node of a stand-alone ESD detection circuit is connected to the substrate trigger node of a stand-alone STNMOS by a wired line. A current probe is used to measure the transient current flowing through this wired line. With such measurement setup, the measured substrate-triggered current generated by the ESD detection circuit under 0-to-7V voltage pulse with a rise time of 10ns on the VDD_h pin is shown in Fig. 4-9. The substrate-triggered current almost simultaneously appears with a peak current of ~43mA, when the 0-to-7V voltage pulse is applied to VDD_h pin. So, the STNMOS with ESD detection circuit can be quickly triggered on to clamp the overstress ESD voltage, as the clamped voltage waveform shown in Fig. 4-8. After 800ns, the voltage at the gate of the PMOS Mp1 follows up the given 0-to-7V voltage transient. Therefore, the ESD detection circuit is turned-off and the measured trigger current drops to zero. The timing for the gate voltage of Mp1 to follow up the transient voltage applied to VDD_h pin can be controlled by changing the R1 and C values and is designed to distinguish between the power-on transition and the ESD transition.

4.4.3 ESD Robustness

The TLP-measured I-V curves of the STNMOS with the proposed ESD detection circuit under different device dimensions are shown in Fig. 4-10. These I-V curves have no snapback phenomenon, as that is often seen in the gate-grounded NMOS. Because the ESD detection circuit can provide large enough substrate-triggered current, as shown in Fig. 4-9, the STNMOS can be directly triggered into its holding region without snapback switching. So, the turn-on speed of the proposed power-rail ESD clamp circuit can be significantly improved to effectively protect the internal circuits with low-voltage devices and thin gate oxide [49]. In addition to the improvement on turn-on speed, the substrate-triggered technique can also improve the turn-on uniformity to enhance ESD robustness of the ESD protection devices. The ESD current can be distributed into deeper substrate region of the STNMOS device for better heat dissipation by the substrate-triggered technique [9]. As comparing to the stand-alone STNMOS, the secondary breakdown current (It2) of STNMOS under device dimensions (W/L) of 300μm/0.3μm and 400μm/0.3μm can be increased from 2.8A to 3.1A and from 3.7A to 4.3A, respectively, by the new proposed ESD detection circuit. Moreover, because the STNMOS is uniformly turned on, the larger device dimension of STNMOS results in a smaller turn-on resistance and a better pulsed I-V response. Therefore, to have a smaller clamped voltage under the same ESD current, the STNMOS with larger device dimension should be chosen when the internal circuits are implemented with the low-voltage devices [49].

The human-body-model (HBM) [15] ESD robustness and the machine-model (MM) [16] ESD robustness of the STNMOS devices with the ESD detection circuit are also greatly increased as compared with that of the stand-alone STNMOS devices. The HBM and MM ESD levels are measured by KeyTek ZapMaster and the devices are judged ESD failure if their I-V characteristic curves shift over 20% after three continuous ESD zaps at every ESD test level. The TLP-measured It2 value, the HBM and MM ESD levels of the STNMOS with and without the ESD detection circuit are compared in Table 4.3.

4.4.4 Failure Analysis

The experimental results have shown that the ESD robustness of STNMOS can be substantially increased by the proposed ESD detection circuit. Failure analyses carried out by OBIRCH [50] and SEM images provide the visual evidence for the proposed ESD detection circuit to uniformly trigger on the ESD clamp device, STNMOS.

Fig. 4-11 shows the ESD failure location of a STNMOS (400μm/0.3μm) with ESD detection circuit after 325-V MM ESD stress. When ESD transient events occur, the ESD detection circuit conducts the initial ESD current to trigger the STNMOS. After the STNMOS device is turned on, it provides a path with low resistance to conduct ESD current to ground, so that most of ESD current is discharged through the STNMOS. Therefore, the ESD damage of the STNMOS with ESD detection circuit locates on the STNMOS device instead of the ESD detection circuit, as the OBIRCH image shown in Fig. 4-11(a). The SEM image of this ESD-damaged STNMOS with ESD detection circuit is shown in Fig. 4-11(b), indicating that the STNMOS is uniformly turned on with the help of the ESD detection circuit. About the stand-alone STNMOS (400μm/0.3μm) after 175-V MM ESD stress, the SEM image indicates that it is not uniformly turned on among the fingers of the STNMOS, as shown in Fig. 4-12(a). The ESD damage of this stand-alone STNMOS only locates within some region of one finger. Fig. 4-12(b) shows the enlarged image of the ESD failure location indicated in Fig. 4-12(a).

The STNMOS devices (400μm/0.3μm) zapped by HBM ESD stress have similar failure results to those zapped by MM ESD stress. Fig. 4-13 reveals the localized ESD damage of the stand-alone STNMOS due to non-uniform turn-on behavior after 1.5-kV HBM ESD stress.

4.4.5 Silicon-Controlled-Rectifier (SCR) as ESD Clamp Device

The silicon-controlled-rectified (SCR), which is composed of cross-coupled n-p-n and p-n-p BJTs with regenerative feedback, has been found to play an important role for ESD protection in very deep sub-micron CMOS technologies. However, main concerns of the SCR device as ESD

clamp device are the slow turn-on speed and the higher switching voltage (Vt1). The substrate-triggered technique has been reported as an effective method to lower the Vt1 and to increase the turn-on speed of SCR devices [51]. Therefore, as another choice of high-voltage tolerant ESD clamp device, the ESD detection circuit in this work was applied on triggering the substrate of SCR devices. The SCR devices, both stand-alone and substrate-triggered, are in series with three diodes to increase its overall holding voltage to 3.8V to avoid the latch-up issue. The TLP measured I-V curves of SCR with or without the proposed ESD detection circuit are shown in Fig. 4-14. In Fig. 4-14, the stand-alone SCR has a Vt1 as high as 15.9V, which is unqualified for protecting internal circuits during ESD transition. With the proposed ESD detection circuit, the Vt1 can be greatly lowered to 5.6V. When the substrate-triggered SCR is 30μm in width, the measured It2 is ~ 3.4A. It is increased to be greater than 6A when the substrate-triggered SCR is 90μm in width. As a result of the lowered Vt1 and the increased turn-on speed, SCR device with the proposed ESD detection circuit is also an useful power-rail ESD clamp circuit to the 3.3-V mixed-voltage I/O interfaces.

4.5 CONCLUSION

A new power-rail ESD clamp circuit realized with low-voltage devices for 1-V/3.3-V mixed-voltage I/O interface has been successfully verified in a 130-nm 1-V/2.5-V CMOS process. As comparing to the stand-alone STNMOS, the turn-on speed of the STNMOS can be effectively improved by the proposed ESD detection circuit. As well as, its HBM (MM) ESD level can be improved from 1kV (150V) to 3.75kV (250V) for the STNMOS with a device dimension (W/L) of 300μm/0.3μm. The ESD detection circuit has also shown significant help on lowering the Vt1 of SCR devices. This new proposed power-rail ESD clamp circuit with the advantages of very low leakage current, fast turn-on speed, higher ESD robustness, and no gate-oxide reliability issue is an

excellent ESD protection solution to the mixed-voltage I/O interface with high-voltage input/output signals.

TABLE 4.1

DEVICE DIMENSIONS OF THE ESD PROTECTION CIRCUIT IN THIS WORK

	Device parameter (each finger)	Number of fingers
Mp1	30 μm/0.28 μm	4
Mp2	30 μm/0.28 μm	4
Mn1	20 μm/0.28 μm	1
Mn2	10 μm/0.28 μm	1
C	20 μm/3.5 μm	4
R1	50 kΩ	
R2	1 kΩ	

TABLE 4.2

LEAKAGE CURRENT OF PRIOR ARTS AND THE NEW PROPOSED POWER-RAIL ESD CLAMP CIRCUIT

	Temperature		Number of diodes	Operating voltage
	25°C	125°C		
pure diode string	12.45 μA	3.45 mA	6	3.3 V
Cladded diode string	3.5 μA	3.33 mA	6	3.3 V
Boosted diode string	44.03 μA	0.61 mA	8	3.3 V
Cantilever diode string	4.96 μA	1.25 mA	6	3.3 V
stacked-PMOS clamp	~ 0.8 μA	~ 8 μA		3.3 V
this work	283 pA	19.8 nA		3.3 V

TABLE 4.3

ESD ROBUSTNESS OF STNMOS DEVICES

WITH OR WITHOUT THE NEW PROPOSED ESD DETECTION CIRCUIT

STNMOS W/L (μm/μm)	HBM ESD Level (kV)		MM ESD Level (V)		It2 Level (A)	
	without detection circuit	with detection circuit	without detection circuit	with detection circuit	without detection circuit	with detection circuit
300/0.3	1	3.75	150	250	2.8	3.1
400/0.3	1.5	5	175	325	3.7	4.3
600/0.3		6.5		375		5.2

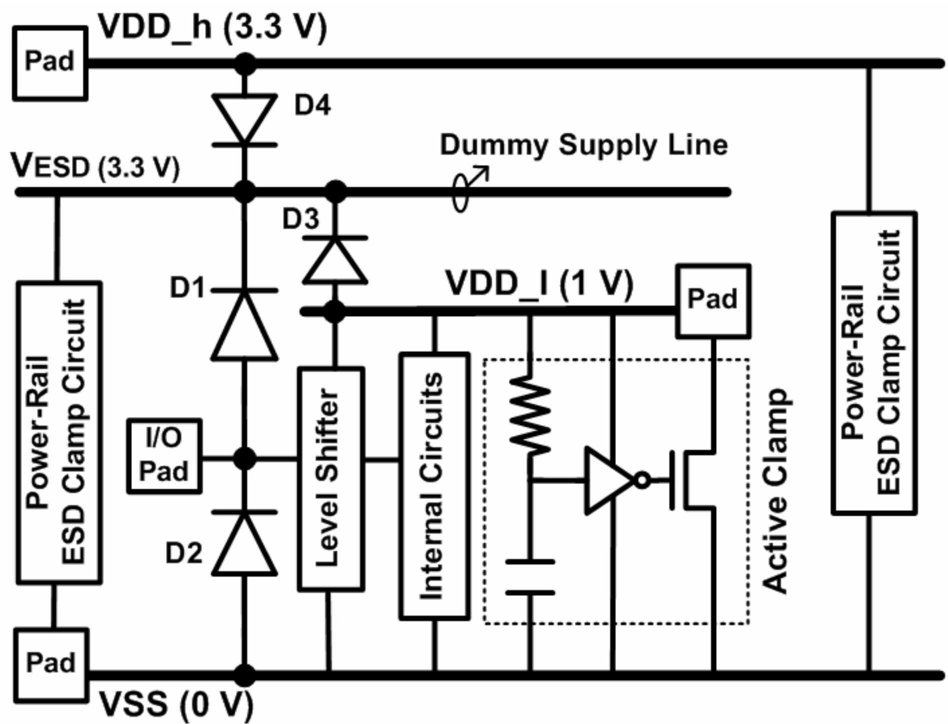

(a)

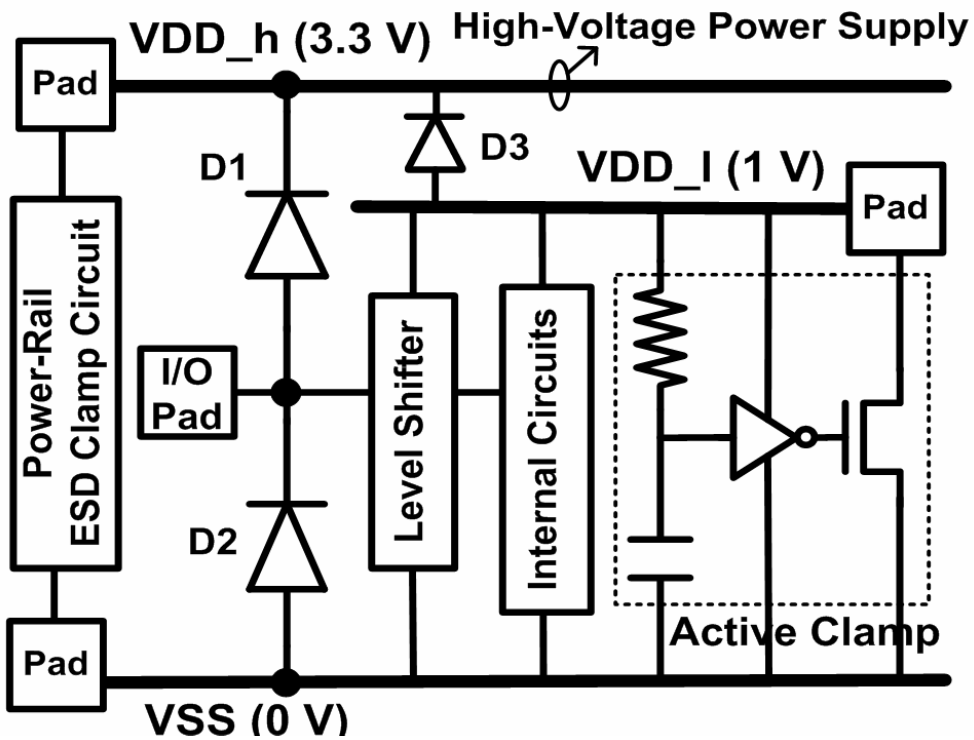

(b)

Fig. 4-1. ESD protection schemes for mixed-voltage I/O interfaces (a) with, and (b) without, the dummy supply line V_{ESD}.

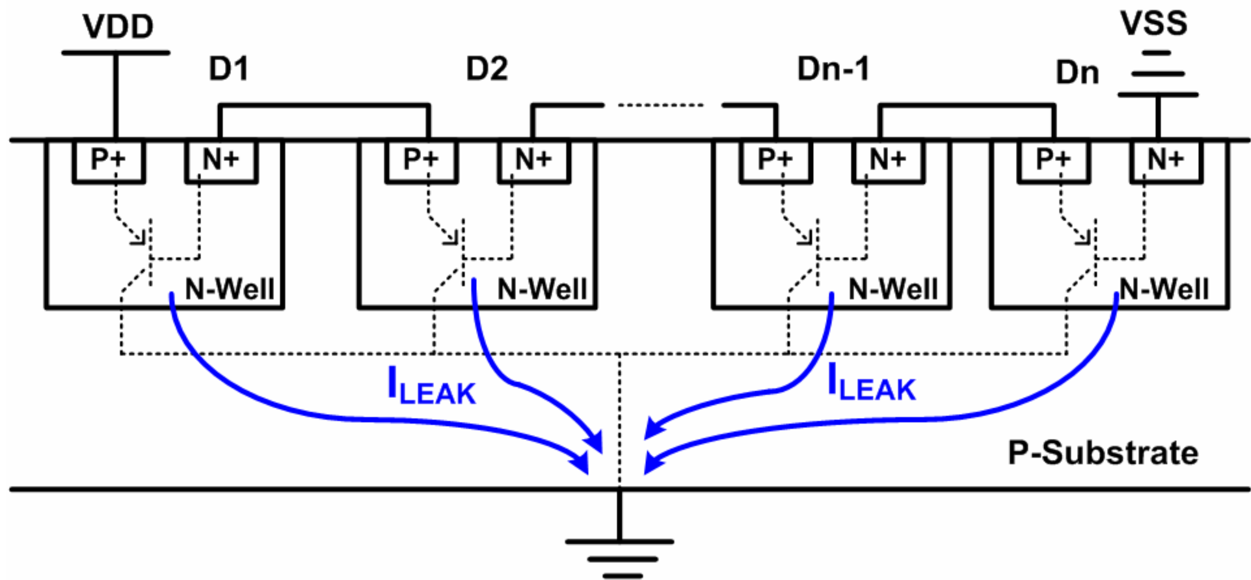

Fig. 4-2. The cross-sectional view of a forward-biased stacked-diode string to show the parasitic p-n-p BJTs and its leakage current path.

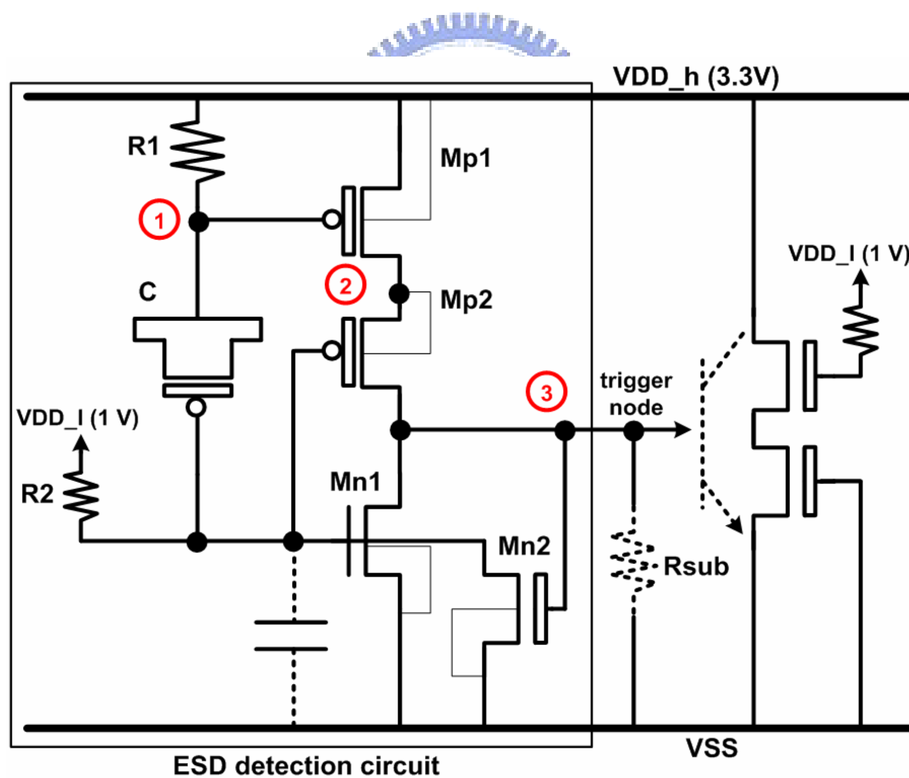

Fig. 4-3. The new proposed power-rail ESD clamp circuit with only 1-V and 2.5-V devices for operating under high-voltage VDD_h of 3.3V.

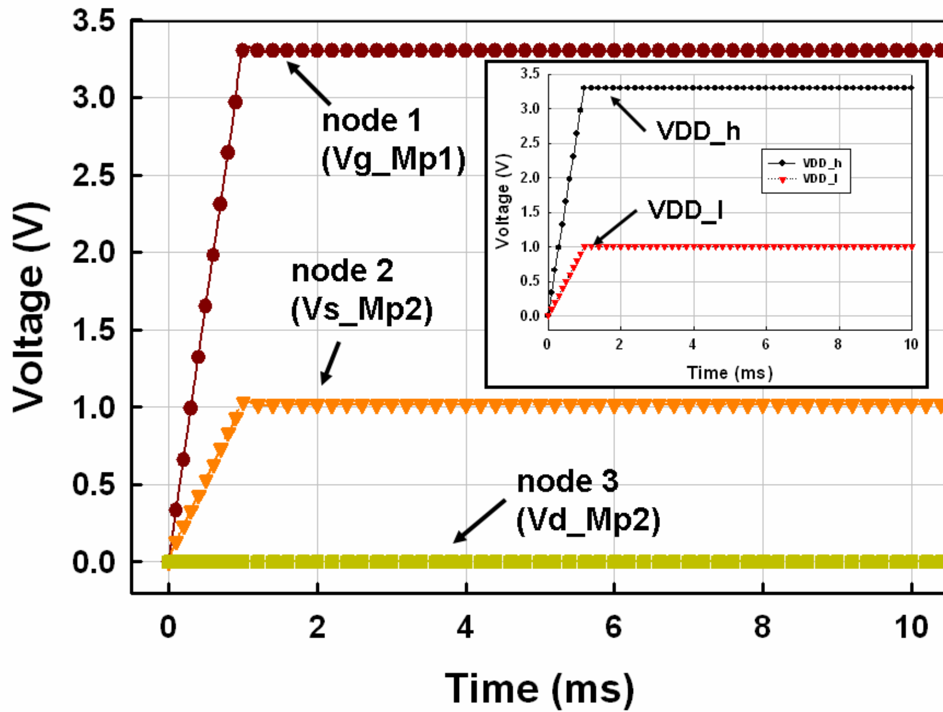

Fig. 4-4. Hspice-simulated voltages on nodes of the ESD detection circuit under normal power-on transition with a rise time of 1ms.

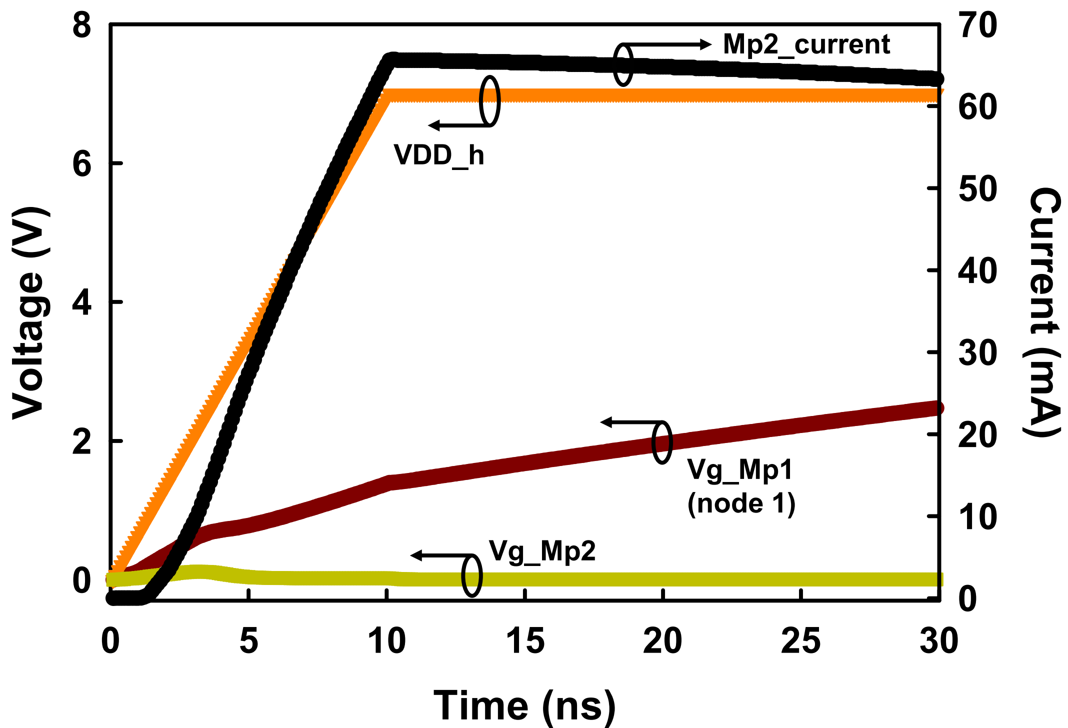

Fig. 4-5. Hspice-simulated voltages on nodes of the ESD detection circuit and the current of Mp2 under 0-to-7V ESD-like transition.

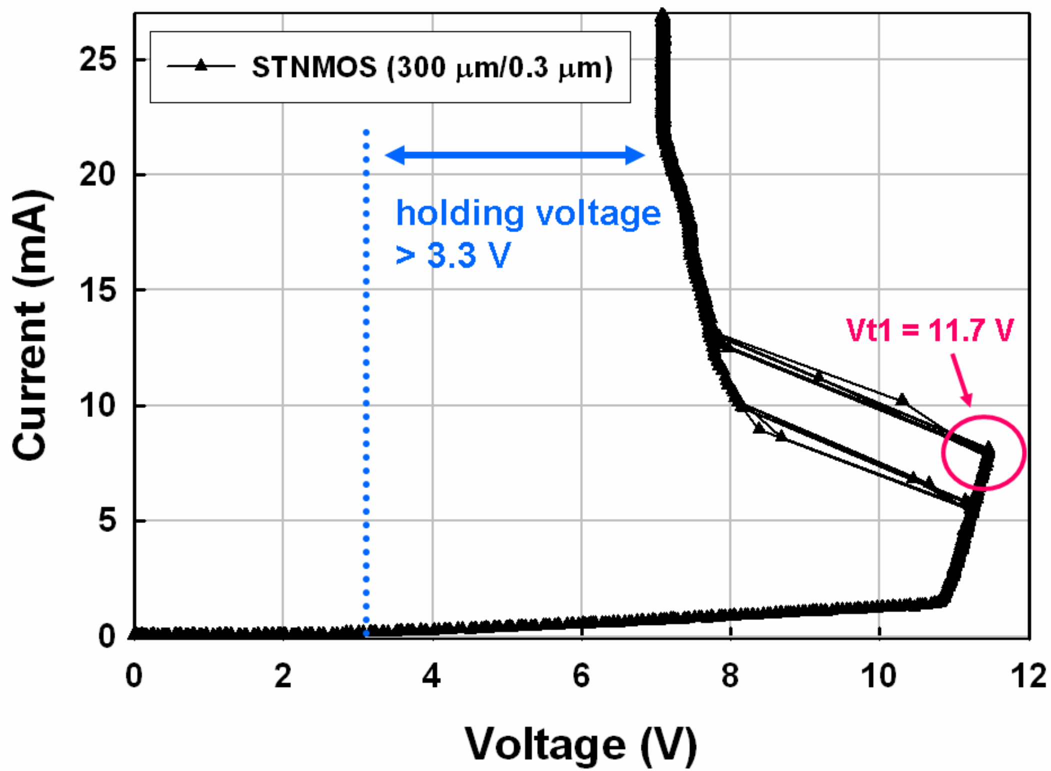

Fig. 4-6. The snapback I-V characteristic curve of a stand-alone STNMOS device.

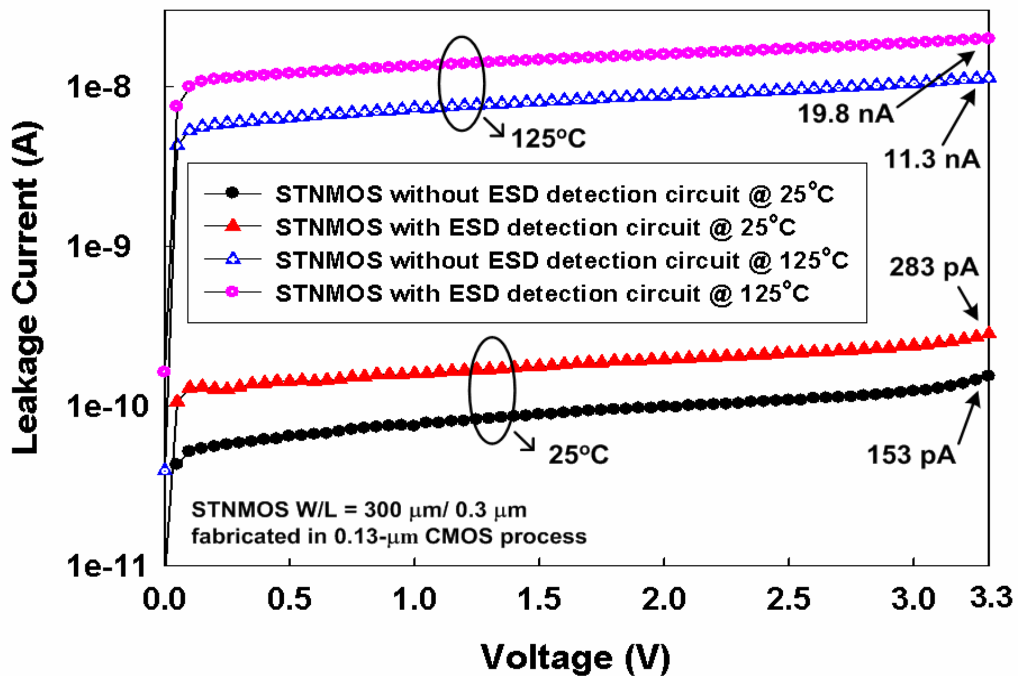

Fig. 4-7. The leakage currents of STNMOS with or without the ESD detection circuit under different temperatures.

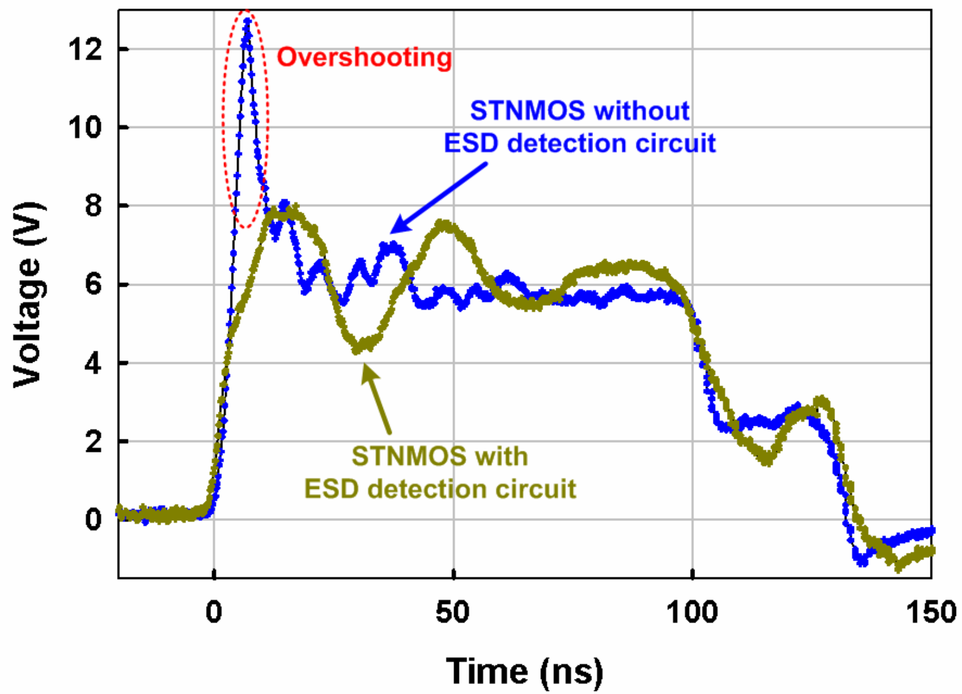

Fig. 4-8. The clamped voltage waveforms by STNMOS with or without the ESD detection circuit under the voltage pulse stress with the pulse height of 20V and the rise time of 10ns.

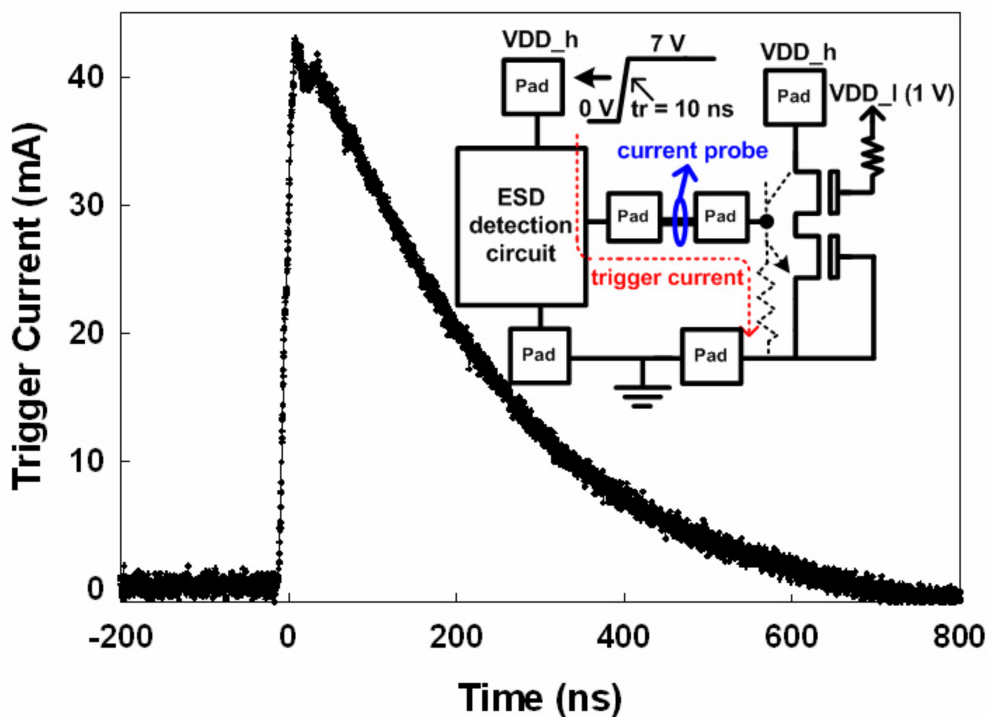

Fig. 4-9. The measured substrate-triggered current generated by the ESD detection circuit under 0-to-7V voltage pulse with a rise time of 10ns on the VDD_h pin.

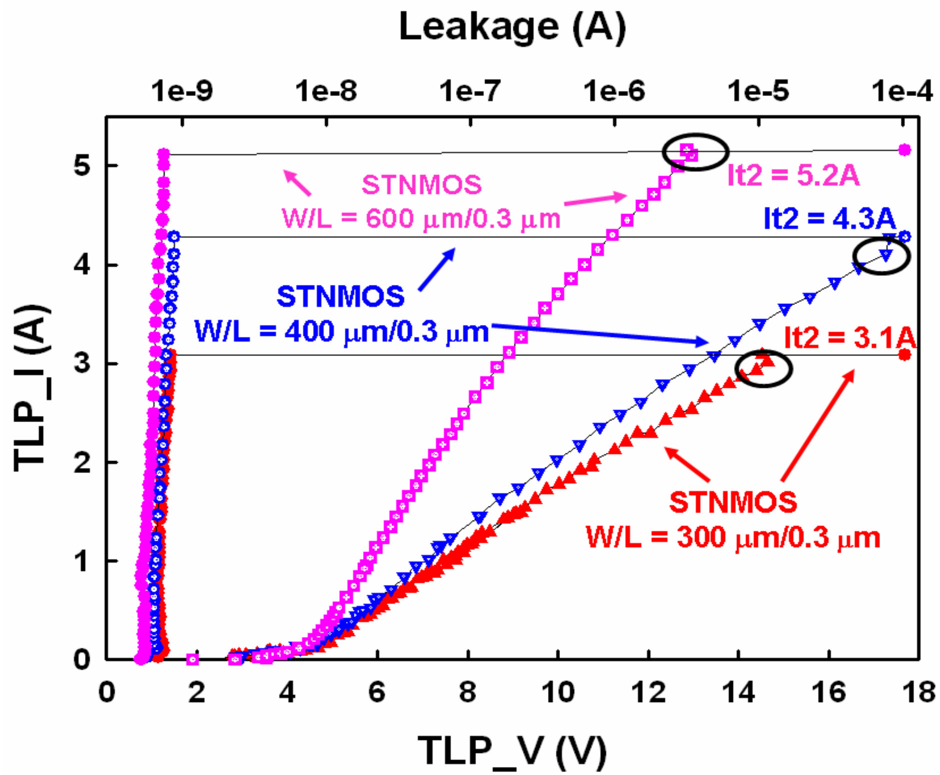

Fig. 4-10. TLP-measured I-V curves of STNMOS with ESD detection circuit under different device dimensions.

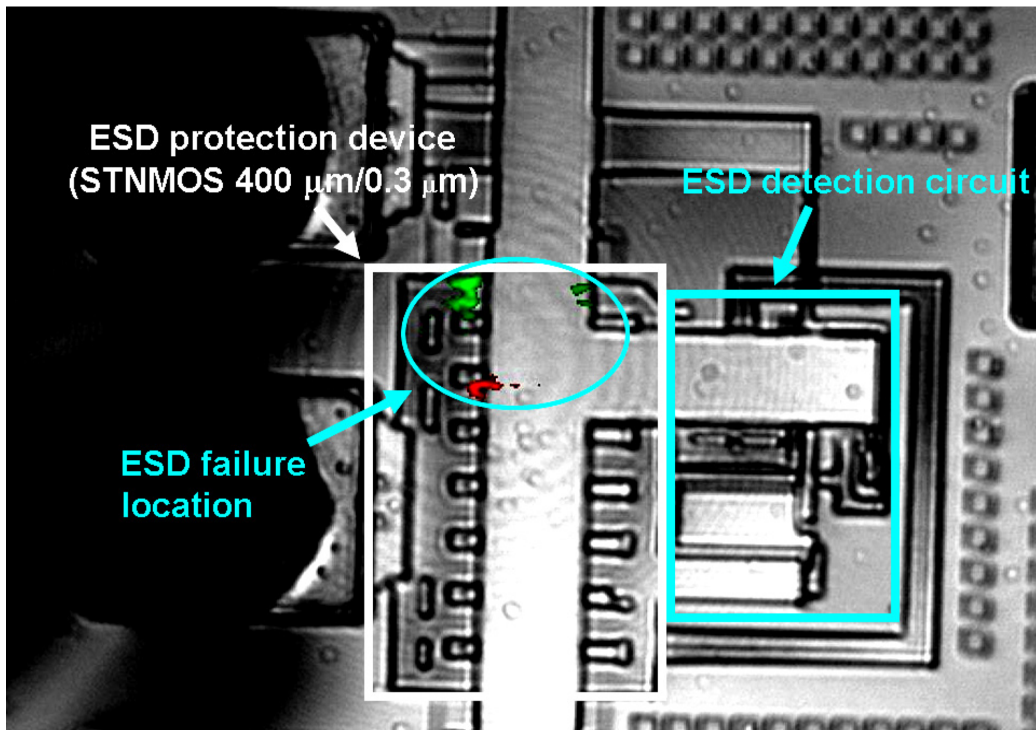

(a)

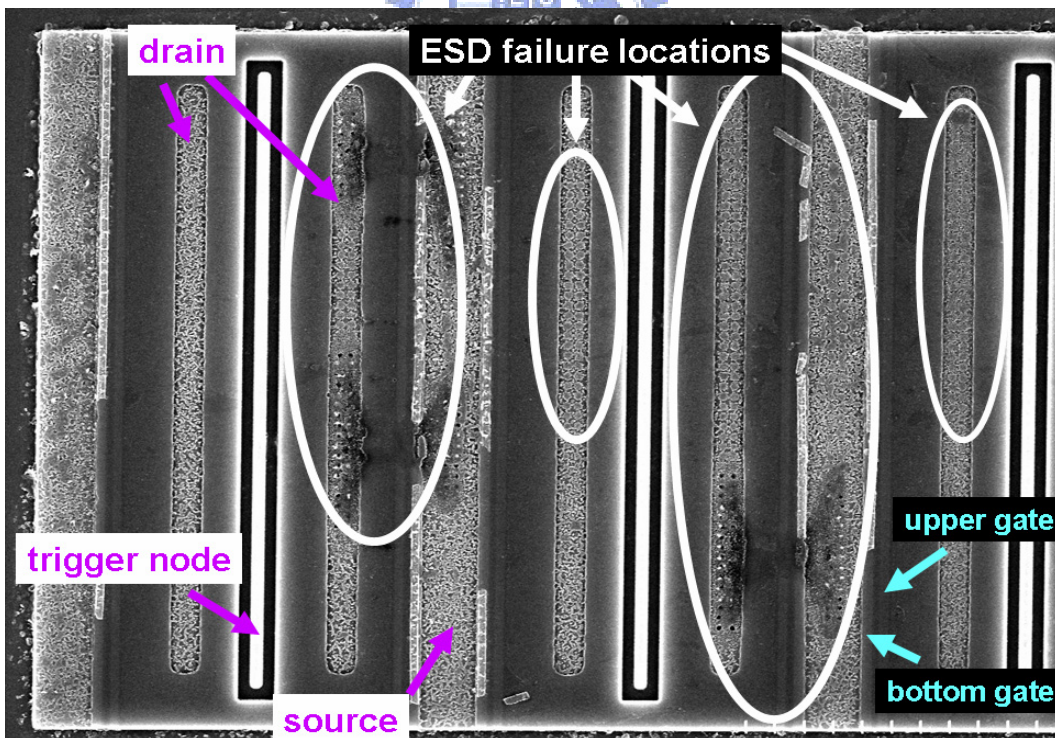

(b)

Fig. 4-11. The (a) OBIRCH, and (b) SEM, images of a 400μm/0.3μm STNMOS with ESD detection circuit after 325-V MM ESD stress.

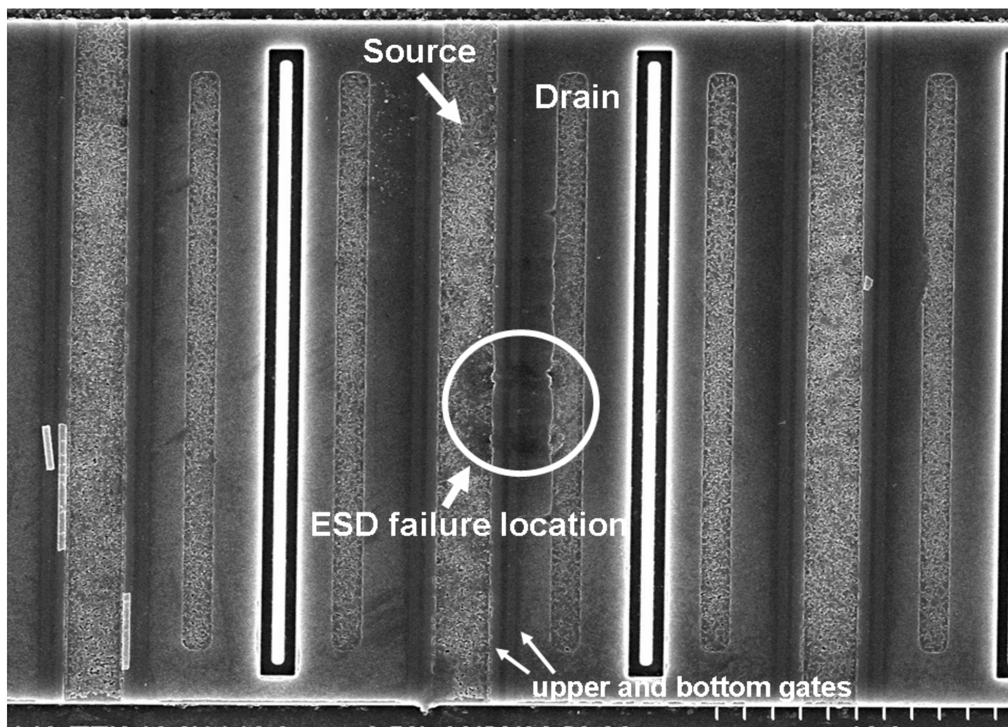

(a)

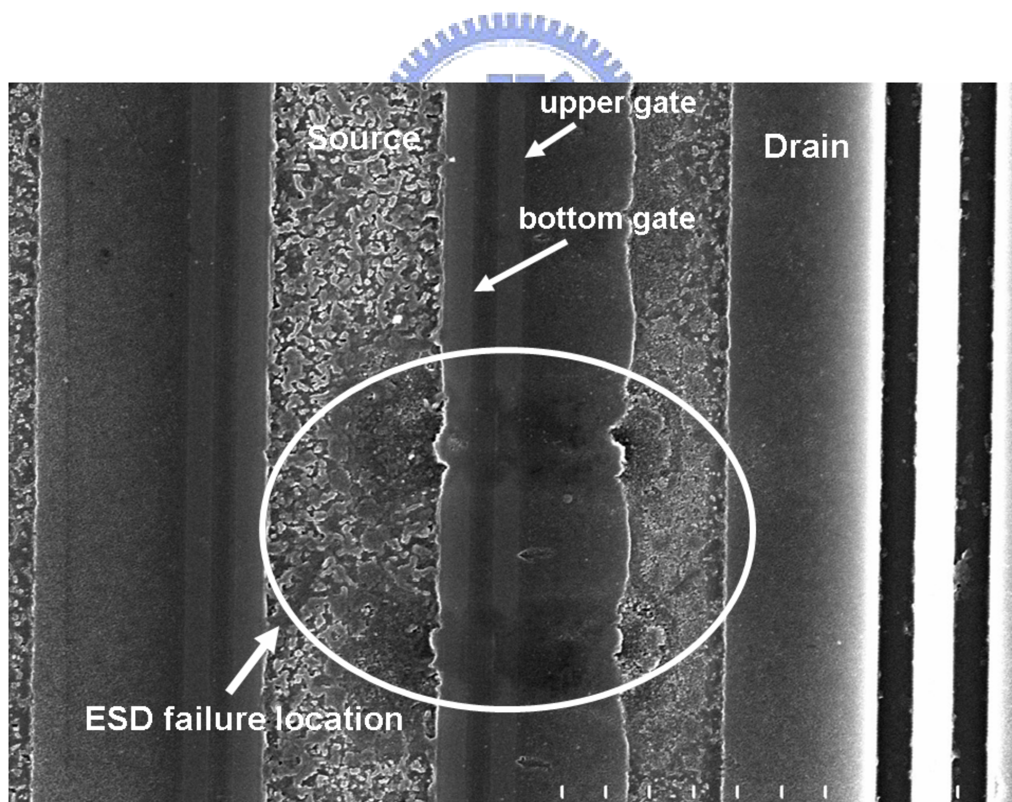

(b)

Fig. 4-12. SEM image of (a) a stand-alone 400μm/0.3μm STNMOS after 175-V MM ESD stress. (b) The enlarged image of its ESD failure location.

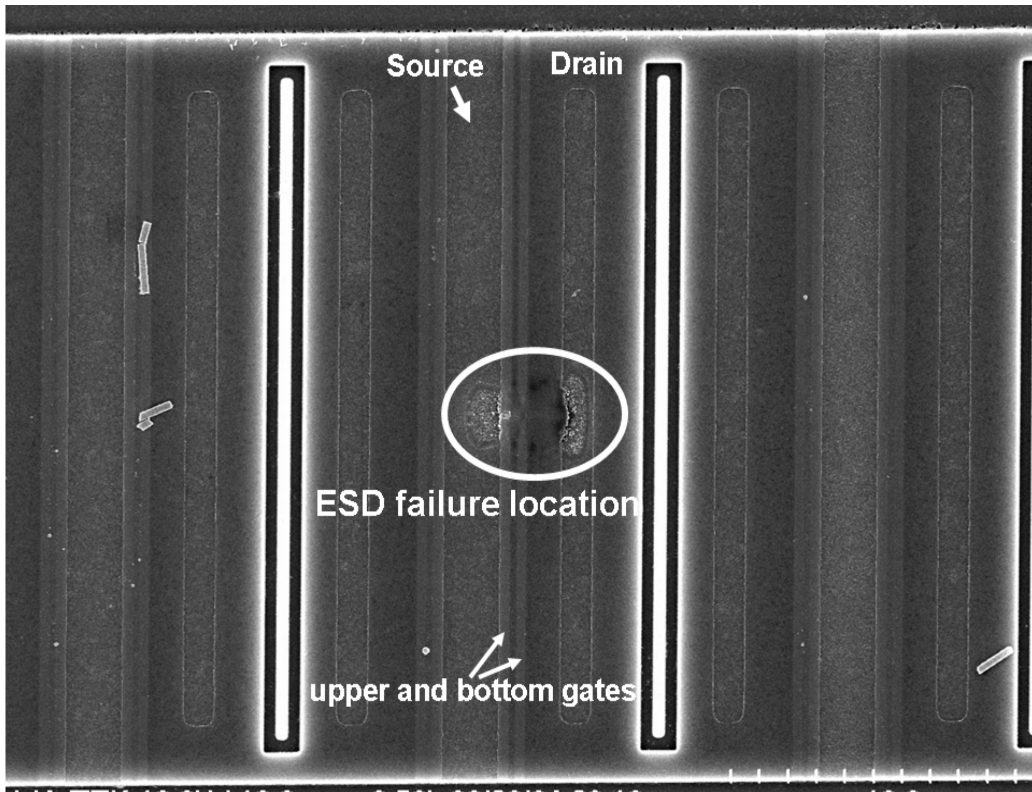

Fig. 4-13. SEM image of a stand-alone 400μm/0.3μm STNMOS after 1.5-kV HBM ESD stress.

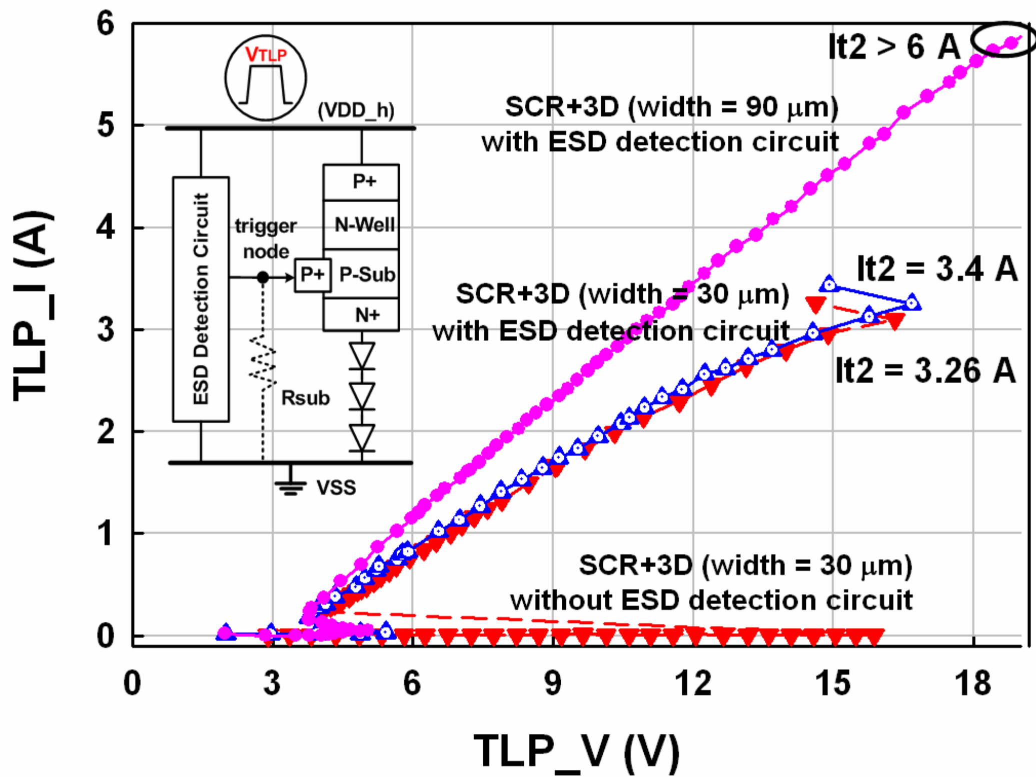

Fig. 4-14. TLP-measured I-V characteristics of both SCR with and without ESD detection circuit.

Chapter 5

Conclusion and Future Work

5.1 CONCLUSION

In this thesis, two practically verified ESD protection designs are proposed and verified. In the first design, the gate-voltage-limited circuit, proposes a solution to the over-gate-driven effect. This design is fabricated and verified in a 0.35-μm CMOS process. From the experimental results, the over-induced gate voltage during ESD transition can considerably lower the ESD robustness of the ESD protection NMOS. The proposed gate-voltage-limited circuit can substantially increase the ESD robustness of over-driven devices. The proposed design fits to different CMOS technologies and does not need to modify or increase the process steps or mask layers.

The second proposed design in this thesis, a power-rail ESD clamp circuit with only low-voltage devices that are specially design to be operated under 1-V/3.3-V mixed-voltage environments, is verified in a 130-nm 1-V/2.5-V CMOS process. The proposed power-rail ESD clamp circuit is fast responsive to ESD events, uniformly triggered during ESD transition, and tolerable to high-operating voltage without the gate-oxide reliability issue. Experimental results show extremely low standby leakage current of this power-rail ESD clamp circuit with high ESD robustness. This design provides a high-voltage tolerant solution to the mixed-voltage I/O applications.

5.2 FUTURE WORK

To further support the mixed-voltage I/O applications, an ESD protection designs with only 1-V or 1.2-V low-voltage devices that can stand 2.5-V or 3.3-V VDD power supply voltages is a work in need. It can further reduce the cost, increase the production yield, increase the circuit performance, etc. Furthermore, with the increasing complexity of chip functions, a high-voltage tolerant ESD protection circuit for mixed-voltage I/O application will be another work in necessary. As the process progresses, devices of internal circuits become more fragile, so that the high-voltage tolerant ESD protection circuit should have properties including fast turn-on speed, low turn-on resistance, and high noise immunity.

References

[1] S. H. Voldman, "The state of the art of electrostatic discharge protection: physics, technology, circuits, design, simulation, and scaling," *IEEE J. Solid-State Circuits*, vol. 34, pp. 1272–1282, Sep. 1999.

[2] C.-D. Lien, "Electostatic discharge protection circuit," U.S. Patent 5086365, Feb. 4, 1992.

[3] C. Duvvury, C. Diaz, and T. Haddock, "Achieving uniform NMOS device power distribution for submicron ESD reliability," *IEDM Tech. Dig.*, 1992, pp. 131–134.

[4] C. Duvvury and C. Diaz, "Dynamic gate coupling of nMOS for efficient output ESD protection," in *Proc. IEEE Int. Reliability Physics Symp.*, 1992, pp. 141–150.

[5] M.-D. Ker, C.-Y. Wu, T. Cheng, and H.-H. Chang, "Capacitor-couple ESD protection circuit for deep-submicron low-voltage CMOS ASIC," *IEEE Trans. VLSI Syst.*, vol. 4, pp. 307–321, Mar. 1996.

[6] J. Chen, A. Amerasekera, and C. Duvvury, "Design methodology and optimization of gate-driven NMOS ESD protection circuits in submicron CMOS processes," *IEEE Trans. Electron Devices*, vol. 45, pp. 2448–2456, Dec. 1998.

[7] M. Mergens, K. G. Verhaege, C. C. Russ, J. Armer, P. C. Jozwiak, G. Kolluri, and L. R. Avery, "Multi-finger turn-on circuits and design techniques for enhanced ESD performance and width-scaling," in *Proc. EOS/ESD symp.*, 2001, pp. 1–11.

[8] T.-Y. Chen, M.-D. Ker, and C.-Y. Wu, "Experimental investigation on the HBM ESD characteristics of CMOS devices in a 0.35-µm silicided process," in *Proc. Int. Symp. VLSI Technology, Systems, and Applications*, 1999, pp. 35–38.

[9] T.-Y. Chen and M.-D. Ker, "Investigation of the gate-driven effect and substrate-triggered effect on ESD robustness of CMOS devices," *IEEE Trans. Device and Materials Reliability*, vol. 1, pp. 190–203, Dec. 2001.

[10] K.-H. Oh, C. Duvvury, K. Banerjee, and R. W. Dutton, "Analysis of gate-bias-induced heating effects in deep-submicron ESD protection designs," *IEEE Trans. Device and Materials Reliability*, Vol. 2, pp. 36–42, June 2002.

[11] M.-D. Ker and W.-Y. Chen, "Design to avoid the over-gate-driven effect on ESD protection circuits in deep-submicron CMOS processes," in *Proc. IEEE Symp. Quality Electronic Design*, 2004, pp. 445–450.

[12] M.-D. Ker and W.-Y. Chen, "Design on power-rail ESD clamp circuit for 3.3-V I/O interface by using only 1-V/2.5-V low-voltage devices in a 130-nm CMOS process", in *Proc. IEEE Int. Reliability Physics Symp.*, 2005, in press.

[13] *Electrostatic discharge (ESD) sensitivity testing - human body model (HBM)*, EIA/JEDEC Standard Test Method A114-B, 2000.

[14] *Electrostatic discharge (ESD) sensitivity testing - machine model (MM)*, EIA/JEDEC Standard Test Method A115-A, 1997.

[15] *Field-induced charged-device model test method for electrostatic discharge withstand thresholds of microelectronic components*, EIA/JEDEC Standard Test Method C101-A, 2000.

[16] *ESD test standard for electrostatic discharge sensitivity testing: human body model (HBM) - component level*, ESD Association, ESD STM5.1, 2001.

[17] *ESD test standard for electrostatic discharge sensitivity testing: machine model (MM) - component level*, ESD Association, ESD STM5.2, 1999.

[18] C. Cook and S. Daniel, "Characterization of new failure mechanisms arising from power-pin ESD stressing," in *Proc. EOS/ESD Symp.*, 1993, pp. 149–156.

[19] M.-D. Ker, "Whole-chip ESD protection design with efficient VDD-to-VSS ESD clamp circuits for submicron CMOS VLSI," *IEEE Trans. Electron Devices*, vol. 46, pp. 173–183, 1999.

[20] P. Salome, C. Leroux, J. P. Chante, P. Crevel, and G. Reimbold, "Study of a 3D phenomenon during ESD stresses in deep submicron CMOS technologies using photon emission tool," in *Proc. IEEE Int. Reliability Physics Symp.*, 1997, pp. 325–332.

[21] C. Russ, K. Bock, M. Rasras, and I. D. Wolf, "Non-uniform triggering of gg-nMOST investigated by combined emission microscopy and transmission line pulsing," in *Proc. EOS/ESD Symp.*, 1998, pp. 177–186.

[22] K.-H. Oh, C. Duvvury, K. Banerjee, and R. W. Dutton, "Analysis of non-uniform ESD current distribution in deep submicron NMOS transistors," *IEEE Trans. Electron Devices*, vol. 49, pp. 2171–2182, Dec. 2002.

[23] T.-Y. Chen and M.-D. Ker, "Analysis on the dependence of layout parameters on ESD robustness of CMOS devices for manufacturing in deep-submicron CMOS process," *IEEE Trans. Semiconductor Manufacturing,* vol. 16, pp. 486–500, Aug. 2003.

[24] C. Jiang, E. Nowak, and M. Manley, "Process and design for ESD robustness in deep submicron CMOS technology," in *Proc. IEEE Int. Reliability Physics Symp.*, 1996, pp. 233–236.

[25] M.-D. Ker, H.-C. Hsu, and J.-J. Peng, "ESD implantation for sub-quarter-micron CMOS technology to enhance ESD robustness," *IEEE Trans. Electron Devices*, vol. 50, pp. 2126–2134, Oct. 2003.

[26] T. J. Maloney and N. Khurana, "Transmission line pulsing techniques for circuit modeling of ESD phenomena," in *Proc. EOS/ESD Symp*., 1985, pp. 49–54.

[27] J. Barth, K. Verhaege, L. G. Henry, and J. Richner, "TLP calibration, correlation, standards, and new techniques," in *Proc. EOS/ESD Symp.*, 2000, pp. 85–96.

[28] K. Verhaege and C. Russ, "Wafer cost reduction through design of high performance fully silicided ESD devices," in *Proc. EOS/ESD Symp.*, 2000, pp. 18-28.

[29] G. Notermans, "On the use of N-well resistors for uniform triggering of ESD protection elements," in *Proc. EOS/ESD Symp.*, 1997, pp. 221–229.

[30] C.-H. Chuang and M.-D. Ker, "Design on mixed-voltage tolerant I/O interface with novel tracking circuits in a 0.13-μm CMOS technology," in *Proc. IEEE Int. Symp. Circuits and Systems*, 2004, pp. 577–580.

[31] S.-L. Chen and M.-D. Ker, "A new output buffer for 3.3-V PCI-X application in a 0.13-μm 1/2.5-V CMOS process," in *Proc. IEEE Asia-Pacific Conf. Advanced System Integrated Circuits*, 2004, pp. 112–115.

[32] G. Singh and R. Salem, "High-voltage-tolerant I/O buffers with low voltage CMOS process," *IEEE J. Solid-State Circuits*, vol. 34, pp. 1512–1525, Nov. 1999.

[33] W. R. Anderson and D. B. Krakauer, "ESD protection for mixed-voltage I/O using NMOS transistors stacked in a cascode configuration," in *Proc. EOS/ESD Symp.*, 1998, pp. 54–62.

[34] M.-D. Ker and C.-H. Chuang, "ESD protection design for mixed-voltage CMOS I/O buffers," *IEEE J. Solid-State Circuits*, vol. 37, pp. 1046–1055, 2002.

[35] T. Maloney and W. Kan, "Stacked PMOS clamps for high-voltage power supply protection," in *Proc. EOS/ESD Symp.*, 1999, pp. 70–77.

[36] S. S. Poon and T. Maloney, "New considerations for MOSFET power clamps," in *Proc. EOS/ESD Symp.*, 2002, pp. 1–5.

[37] K. Yoshitake, "Integrated circuit having two circuit blocks therein independently energized through different power supply terminals," U.S. Patent 4855863, Aug. 1989.

[38] M.-D. Ker, H.-H. Chang, and T.-Y. Chen, "ESD buses for whole-chip ESD protection," in *Proc. IEEE Int. Symp. Circuits and Systems*, 1999, pp. 545–548.

[39] L. R. Avery, "ESD protection for overvoltage friendly input/output circuits," U.S. Patent 5708550, Jan. 1998.

[40] J. Watt, "Fast turn-on silicon controlled rectifier (SCR) for electrostatic discharge (ESD) protection," U.S. Patent 5825600, Oct. 1998.

[41] E. R. Worley, C. T. Nguyen, R. A. Kjar, and M. R. Tennyson, “Method and apparatus for coupling multiple independent on-chip VDD busses to an ESD core clamp,” U.S. Patent 5654862, Oct., 1996.

[42] S. Dabral, R. Aslett, and T. Maloney, “Designing on-chip power supply coupling diodes for ESD protection and noise immunity,” in *Proc. EOS/ESD Symp.*, 1993, pp. 239–249.

[43] T. Maloney and S. Dabral, ”Novel clamp circuits for IC power supply protection,” *IEEE Trans. Components, Packaging, and Manufacturing Technology*, vol 19, pp. 150–161, July 1996.

[44] T. Maloney, “Electrostatic discharge protection circuits using biased and terminated PNP transistor chains,” U.S. Patent 5530612, June 1996.

[45] S. Voldman and G. Gerosa, “Mixed-voltage interface ESD protection circuits for advanced microprocessors in shallow trench and LOCOS isolation CMOS technologies,” *IEDM Tech. Dig.*, 1994, pp. 277–280.

[46] M.-D. Ker and W.-Y. Lo, “Design on the low-leakage diode string for using in the power-rail ESD circuits in a 0.35-μm silicide CMOS process,” *IEEE J. Solid-State Circuits*, vol. 35, pp. 601–611, April 2000.

[47] M.-D. Ker, K.-H. Lin, and C.-H. Chuang, “On-chip ESD protection design with substrate-triggered technique for mixed-voltage I/O circuits in sub-quarter-micron CMOS process,” *IEEE Trans. Electron Devices*, vol. 51, pp. 1628–1635, Oct. 2004.

[48] M.-D. Ker and H.-C. Hsu, “ESD protection design for mixed-voltage-tolerant I/O buffers with substrate-triggered technique,” in *Proc. IEEE Int. SOC Conf.*, 2003, pp. 219–222.

[49] H. Gossner, “ESD protection for the deep sub micron regime – a challenge for design methodology,” in *Proc. IEEE Int. Conf. VLSI Design*, 2004, pp. 809–818.

[50] L. Soon, D. T. M. Ling, M. Kuan, K.-W. Yee, D. Cheong, and G. Zhang, “Application of IR-OBIRCH to the failure analysis of CMOS integrated circuits,” in *Proc. IEEE Int. Symp. Physical and Failure Analysis of Integrated Circuits*, 2003, pp. 86–91.

[51] M.-D. Ker and K.-C. Hsu, “Latch-up free ESD protection design with complementary substrate-triggered SCR devices,” *IEEE J. Solid-State Circuits*, vol. 38, pp. 1380–1392, Aug. 2003.

VITA

姓　名：陳穩義

學　歷：

台北市私立延平高級中學	(85年9月~88年7月)
國立交通大學電子工程系	(88年9月~92年7月)
國立交通大學電子研究所碩士班	(92年9月~94年4月)

Publication List

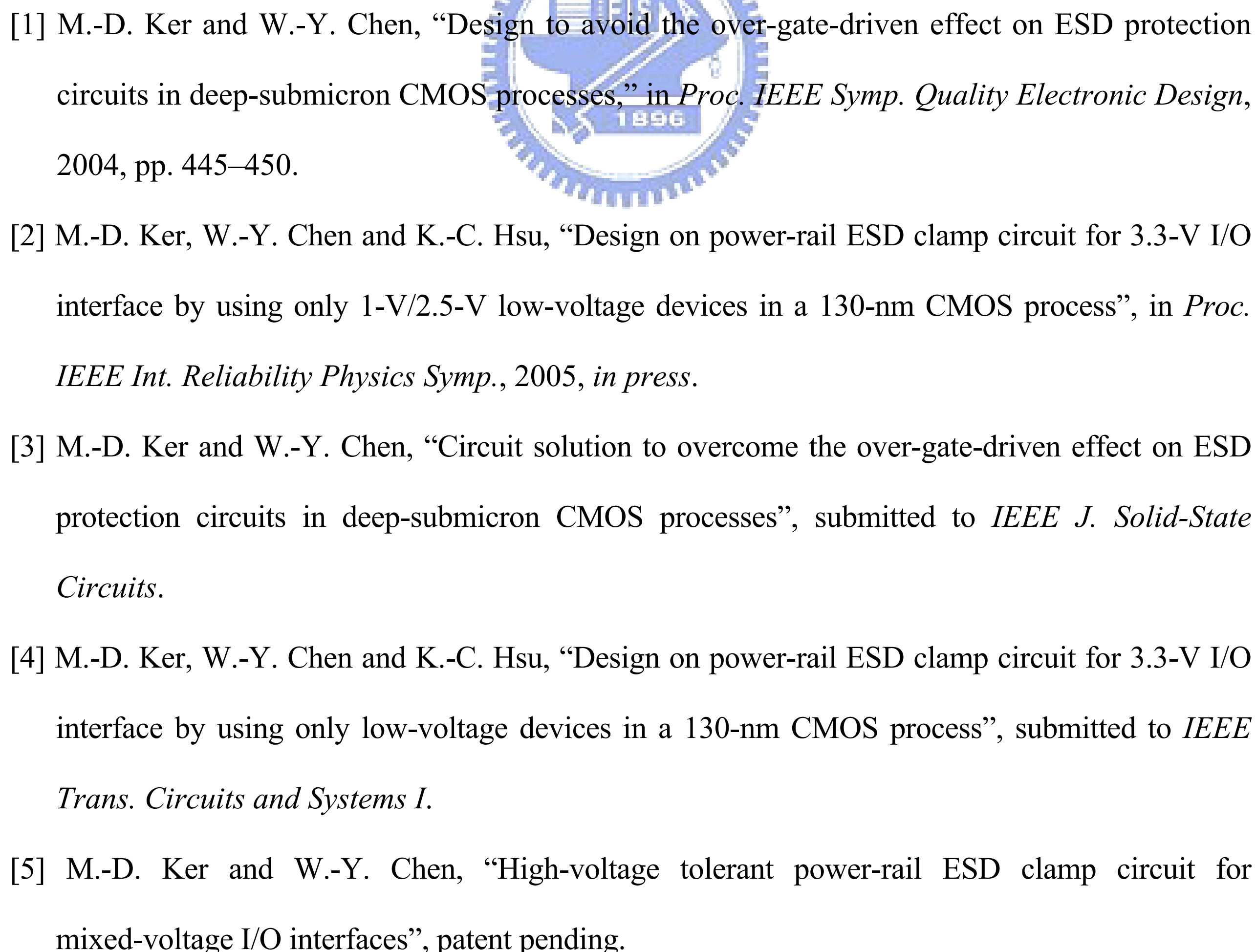

[1] M.-D. Ker and W.-Y. Chen, "Design to avoid the over-gate-driven effect on ESD protection circuits in deep-submicron CMOS processes," in *Proc. IEEE Symp. Quality Electronic Design*, 2004, pp. 445–450.

[2] M.-D. Ker, W.-Y. Chen and K.-C. Hsu, "Design on power-rail ESD clamp circuit for 3.3-V I/O interface by using only 1-V/2.5-V low-voltage devices in a 130-nm CMOS process", in *Proc. IEEE Int. Reliability Physics Symp.*, 2005, *in press*.

[3] M.-D. Ker and W.-Y. Chen, "Circuit solution to overcome the over-gate-driven effect on ESD protection circuits in deep-submicron CMOS processes", submitted to *IEEE J. Solid-State Circuits*.

[4] M.-D. Ker, W.-Y. Chen and K.-C. Hsu, "Design on power-rail ESD clamp circuit for 3.3-V I/O interface by using only low-voltage devices in a 130-nm CMOS process", submitted to *IEEE Trans. Circuits and Systems I*.

[5] M.-D. Ker and W.-Y. Chen, "High-voltage tolerant power-rail ESD clamp circuit for mixed-voltage I/O interfaces", patent pending.